Winter 12-15-2016

A Study on the Role and Regulation of the Na+-Leak Channel, Non-Selective (NALCN) in Myometrial Function

Erin Lynn Reinl
Washington University in St. Louis

WASHINGTON UNIVERSITY IN ST. LOUIS

Division of Biology and Biomedical Sciences
Molecular Cell Biology

Dissertation Examination Committee:
Sarah England, Chair
Thomas Baranski
Erik Herzog
Robert Mecham
Kelle Moley
Jeanne Nerbonne

A Study on the Role and Regulation of the Na^+-Leak Channel, Non-Selective (NALCN) in Myometrial Function

by
Erin L. Reinl

A dissertation presented to the
Graduate School of Arts & Sciences
of Washington University in
partial fulfillment of the
requirements for the degree
of Doctor of Philosophy

December 2016
St. Louis, Missouri

Table of Contents

List of Figures

List of Tables

.

Acknowledgments

I would like to thank my mentor, Dr. Sarah England, for her excellent mentorship, time investment in my work and development as a scientist, as well as the critical review of this document. I would also like to thank my committee chair, Jeanne Nerbonne, and committee members Kelle Moley, Thomas Baranski, Erik Herzog, and Robert Mecham for their guidance.

I also thank the Clinical Research Nurses in the Department of Obstetrics and Gynecology at Barnes Jewish Hospital for consenting patients and acquiring human myometrial biopsies, Dr. Dejian Ren for his gift of the NALCN$^{fx/fx}$ mouse, Dr. Arnaud Monteil for the gift of NALCN-targeting and overexpressing viral vectors and his helpful discussions, Dr. K. Joseph Hurt and Rachael Bok for mouse uterine tissue samples, Dr. Yong Wang and Wenjie Wu for development of a unique Matlab program to examine myometrial bursts, Dr. Andrew Blanks and Dr. Conor McCloskey for training in the technique of sharp electrode current clamp, and Dr. Ramon Lorca and Dr. Deborah Frank for critical review of chapter 2. I would also like to thank Dr. Alison Cahill for sharing her clinical perspectives with me.

Finally, I would like to thank Dr. England's and my funding sources; National Institute of Child Health & Human Development (NIH, HD076677) to SKE and AGC, and (F31 HD079148) to ER and the March of Dimes (FY15-147).

Erin Reinl

Washington University in St. Louis

December 2016

Dedicated to my parents.

ABSTRACT

A Study on the Role and Regulation of the Na^+-Leak Channel, Non-Selective (NALCN) in Myometrial Function

by

Erin L. Reinl

Doctor of Philosophy in Biology and Biomedical Sciences

(Molecular Cell Biology)

Washington University in St. Louis, 2016

Professor Sarah England, Chair

Uterine contractions are tightly regulated throughout pregnancy, remaining relatively quiescent for the majority of pregnancy to promote fetal development, while becoming highly activated at term to effectively expel the fetus. Contractions are coordinated through electrical and mechanical coupling of myometrial smooth muscle cells (MSMCs). Ion channel activity, which alters the electrical activity of MSMCs, can directly affect the contraction profile. Thus there is great interest in the field of reproduction to understand which ion channels regulate uterine excitability, and particularly how they may enable the transition from uterine quiescence to uterine activation for labor. The focus thus far has been primarily on Ca^{2+} and K^+ channels, however, in these studies, we identified the expression of a novel Na^+ leak channel (NALCN) in the human and mouse myometrium that has a direct effect on uterine excitability. In the human myometrium, NALCN contributes to a Gd^{3+}-sensitive, Na^+-dependent leak current. To study its role *in vivo*, we created a smooth muscle specific NALCN knockout mouse. These mice had

reduced myometrial excitability exemplified by shortening of action potential bursts, and an increased rate of prolonged and dysfunctional labor. Further implicating a role for NALCN in parturition, we found that NALCN protein levels were negatively regulated by progesterone, an important hormone in sustaining uterine quiescence, and that progesterone upregulates a novel, glycosylated isoform of NALCN. Our findings are significant in that we found NALCN contributes to the myometrial action potential, and that Na^+ channel contributions are important for successful labor outcomes.

Chapter 1: Introduction

1.1 Parturition

Pregnancy is one of the greatest physiological challenges that a woman's body endures. From conception to parturition, the female body undergoes a vast array of changes in order to adapt to and support the developing fetus. These changes range from metabolic reallocation, to suppression of the immune system toward the allogeneic fetus, to major cardiovascular adjustments, such as increased blood volume and cardiac output. The extreme physical demands of pregnancy culminate with the final step, parturition. Although parturition represents only a short period of time compared to the full duration of pregnancy and the future life of the offspring, it is crucial in determining the overall success of pregnancy and setting the stage for a healthy life. Despite knowing its clear importance in human survival, we still lack a complete understanding of the physiological and molecular mechanisms involved in successful parturition, including those which coordinate uterine contractions.

During normal pregnancy, the uterus undergoes rapid growth and functional modifications. The human uterus grows to be ~30 times its non-pregnant weight (1) and it does so by both increasing cell number (hyperplasia) and cell size (hypertrophy) (2). The uterus also changes in morphology, shifting from a small, pear-shaped organ, to a large balloon-like structure characterized by a thick-walled, contractile upper segment and thin-walled passive lower segment. Blood vessels stemming from the placenta penetrate the uterine wall, and the uterine artery increases its blood flow to provide nutrients to the fast growing fetus and uterine muscle. During pregnancy, the uterus also undergoes denervation, showing loss of cholinergic and adrenergic nerve terminals in uterine tissue (3-6). While all of these physiological

accommodations are occurring, this ordinarily contractile organ must remain quiescent throughout the majority of pregnancy but then rapidly transition to a state of activation at term. All of these transformations are mediated at the cell level by dynamic changes in gene expression, post-translational regulation, and cell-to-cell communication and migration. Since pregnancy and parturition rely heavily on the strict spatial and temporal regulation of a large and complex network of genes and interacting tissues, even small disruptions or environmental insults can result in adverse outcomes.

A number of adverse pregnancy outcomes center around dysfunctional uterine contractility. At one end of the spectrum, the uterus is overactive, contracting so forcefully or rapidly (tachysystole) during parturition that if left untreated endangers the fetus by causing ischemia and abnormal fetal heart rate. Although the uterine smooth muscle layer (myometrium) shows contractions at any point in pregnancy, these contractions tend to be weak and asynchronous and do not result in labor. Thus, another form of uterine 'hyperactivity' is when the uterus pathologically demonstrates spontaneous premature labor-quality contractions, and causes preterm birth. Preterm birth (birth before 37 weeks gestation) occurs in 10% of births in the Unites States (7), and is the leading cause of neonatal death and morbidity in the world (World Health Organization). About 30% of PTB is caused by preterm premature rupture of membranes (rupture of fetal membranes before 37 weeks gestation), ~20% are medically indicated and result from elective caesarean sections, and the remaining ~50% are considered idiopathic (8). Unfortunately, current contraction inhibiting drugs (tocolytics) used to prevent or halt preterm birth, such as the calcium channel blocker, nifedipine, or the beta-adrenergic receptor agonist, terbutaline, are ineffective at delaying labor for more than 48 hrs – 7 days (9). Treatment with vaginal progesterone or cervical cerclage have been effective in reducing preterm

birth rates in women with a prior preterm birth or short cervix (10-13), but this has only reduced the overall preterm birth rate in the US by 1.4% (14). Thus, preterm birth remains the highest motivating factor for better understanding uterine contractility and parturition.

At the other end of the spectrum is dystocia, when the uterus does not contract sufficiently during parturition. Dystocia can prolong labor and increase morbidity for both mother and child. Hypocontractility also contributes to post-term pregnancies. When a woman's uterus fails to initiate contractions at term, the pregnancy is at a greater risk of resulting in stillbirth, perinatal death, shoulder dystocia, fetal macrosomia, meconium aspiration syndrome, and severe perineal lacerations (15). Women are often given the contraction agonist oxytocin to induce labor or augment contractions in the case of dystocia, but this is not effective for many women and can have adverse outcomes (16, 17). Beyond oxytocin treatment, caesarean section is often the next line of treatment. Currently, caesarean sections account for 32% of births in the United States, a rate that is more than triple what is considered necessary for maintaining the lowest infant and maternal mortality rate (18). Many health agencies (ACOG, SMFM, CDC, WHO) are advocating to reduce the caesarean section rate, in part by encouraging further research into understanding normal labor progression (19). Thus, it is imperative for the health of women and babies that we better understand the dynamic regulation of uterine contractility so that we can improve pregnancy and parturition outcomes.

1.2 Uterine Contractions and Physiology

1.2.1 Uterine Anatomy

Uterine contractions are important in many stages of the female reproductive cycle, including menstruation, sperm transport, embryo implantation, and parturition. The main tissue of the uterus that drives these contractions is called the myometrium, and it performs its

contractile function through the work of individual myometrial smooth muscle cells (MSMCs). The bulk of MSMCs in the uterus are organized into a thick outer layer, that runs longitudinally, and this is the layer responsible for labor contractions (20). There is also evidence for a thin sub-endometrial layer, where MSMCs are organized in a transverse, circular orientation (21, 22). It is hypothesized that this layer may contribute more to the peristaltic like activity observed during the menstrual cycle (21, 23). In the rodent, the layers are subdivided into a luminal circular layer, and an outer longitudinal layer. The longitudinal muscle layer more closely mimics the longitudinally oriented fibers of the human myometrium, and because of ease of manipulation, is more widely used in tissue physiology experiments.

1.2.2 Mechanisms of MSMC Contractions

Uterine contractions are mediated by the molecular motors actin and myosin within MSMCs. The shortening the actomyosin filaments, through a process termed cross-bridge cycling (24), results in shortening of the smooth muscle cell and contraction of the tissue. Cross-bridge cycling is heavily dependent on the intracellular Ca^{2+} concentration ($[Ca^{2+}]_i$) (25). Ca^{2+} maintains a large chemical gradient in MSMCs where the extracellular Ca^{2+} concentration is near 1.5 mM and the $[Ca^{2+}]_i$ is closer to 130 nM (21, 26). When $[Ca^{2+}]_i$ increases, Ca^{2+} ions are bound up by the cytosolic protein calmodulin, which then activates myosin light chain kinase (MLCK) and initates the cross-bridge cycling cascade (27). Thus, increases in $[Ca^{2+}]_i$ directly coincide with increased contractility. *Therefore, mechanisms regulating MSMC $[Ca^{2+}]_i$ are key to the regulation of uterine contractions as a whole.* Increases in $[Ca^{2+}]_i$ are mediated by two primary pathways, influx from the extracellular space through voltage gated Ca^{2+} channels, and efflux from the intracellular stores through ligand gated Ca^{2+} channels (Figure 1.1).

Excitation-Contraction (EC) Coupling in MSMCs

The intracellular Ca^{2+} concentration of MSMCs (and therefore contractility) can be

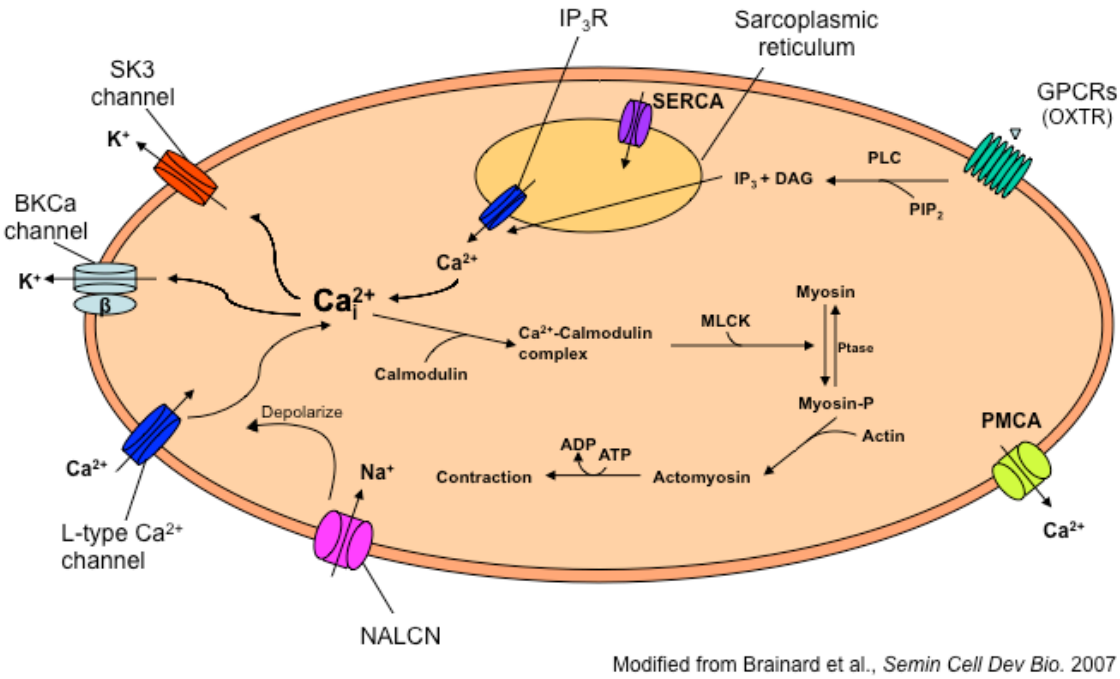

Figure 1.1 Abbreviated components of the excitation-contraction coupling pathway. Depolarization of the membrane potential through a Na^+ leak current (Na^+ Leak Channel, Non-Selective (NALCN)) activates L-type Ca^{2+} channels, and drives Ca^{2+} influx. Intracellular Ca^{2+} binds calmodulin to activate mysoin light chain kinase (MLCK), which phosphorylates myosin and initiates actomyosin cross-bridge cycling to initiate contraction. Intracellular Ca^{2+} can also increase through the activation of G-protein coupled receptors (GPCRs) like the oxytocin receptor (OXTR). Upon ligand binding, OXTR initiates a signaling cascade, which results in the production of IP_3 and activates the IP_3 receptor (IP_3R). IP_3R releases Ca^{2+} from the sarcoplasmic reticulum. Upon cell membrane depolarization and increased intracellular Ca^{2+}, voltage and Ca^{2+} activated K^+ channels, such as small conductance calcium activated channel 3 (SK3) and large conductance, calcium and voltage gated potassium channel (BKCa) open to repolarize the membrane potential. Simultaneously, plasma membrane calcium ATPase (PMCA), and sarcoendoplasmic reticulum calcium ATPase (SERCA) work to pump Ca^{2+} out of the cell and into the sarcoplasmic reticulum respectively, resulting in MSMC relaxation.

increased and decreased through modulation of the MSMC membrane potential. One of the main drivers of this process, termed excitation-contraction coupling (28), is the L-type Ca^{2+} channel (26, 29). Upon membrane depolarization, these channels open and conduct a large influx of Ca^{2+} into the cell. They are considered high-voltage activating channels, and in the myometrium their activation threshold is near -40 mV (30). These channels have a single channel conductance near 20 pS, and are slow to both activate and inactivate (31, 32). Their ability to remain open for an extended period of time (tens to hundreds of milliseconds (33), not only generates the increase in $[Ca^{2+}]_i$ necessary for contraction, but also gives rise to the characteristic slow bursting action potentials of the myometrium (Figure 1.2). Together Ca^{2+}-efflux from intracellular stores and Ca^{2+}-influx from the extracellular fluid work in a feed forward fashion to create strong and sustained contractions.

In order to relax, MSMCs reduce the $[Ca^{2+}]_i$ to resting conditions. Upon membrane depolarization, voltage-gated and Ca^{2+}-activated K^+ channels become activated (34). Because the $[K^+]$ is much higher inside of the cell (140 mM) than it is outside of the cell (5 mM), the opening of K^+ channels will result in K^+ flowing out of the cell to repolarize the cell membrane to more negative potentials (-55 mV). Repolarization of the membrane will then inactivate voltage-gated Ca^{2+} channels, thereby blocking the influx of Ca^{2+}. Simultaneously, the plasma membrane Ca^{2+}-ATPase (PMCA) and the sarcoendoplasmic reticulum Ca^{2+}-ATPase (SERCA) work to pump Ca^{2+} back out of the cell and into the sarcoplasmic reticulum (SR), respectively (35). The opposing actions of Ca^{2+} channels, Ca^{2+} pumps, K^+ channels, and other ion channels (both identified and remaining to be discovered) result in a bursting action potential (Figure 1.2) (36). Processes that alter Ca^{2+}-handling and membrane potential can alter the shape and duration of these bursts, and thereby also alter the strength and duration of myometrial contractions (37).

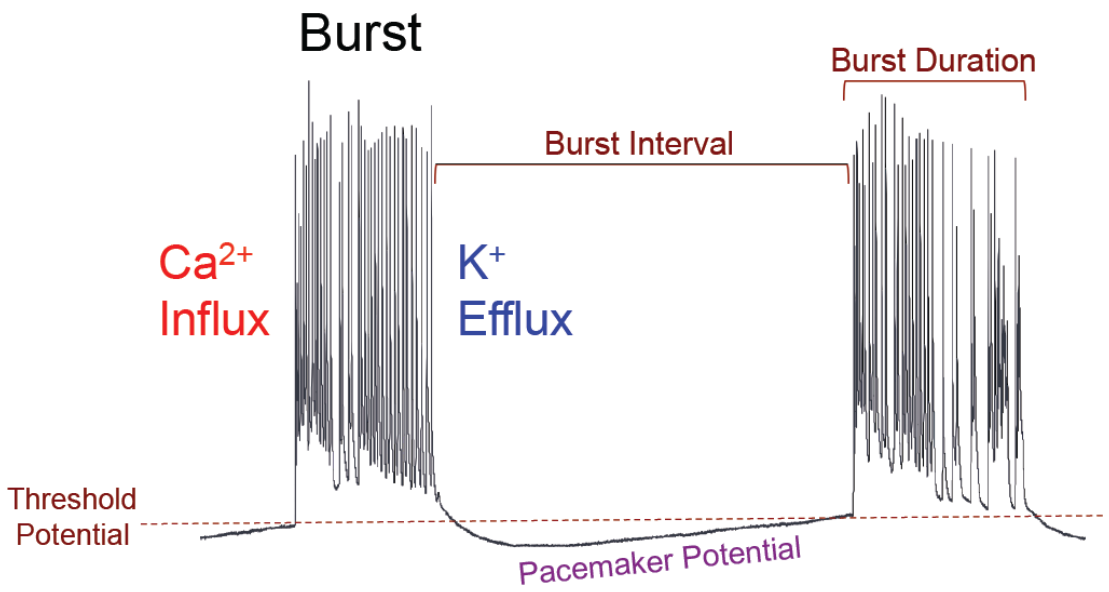

Figure 1.2 Schematic of myometrial action potentials (bursts).
Slow depolarization of the resting membrane potential produces a pacemaker potential that drives the cell to its threshold potential. At the threshold potential (~-40 mV), voltage-gated Ca^{2+}channels open leading to MSMC depolarization. A burst of depolarizing spikes develops as Ca^{2+} channels continue to activate and inactivate, and voltage-gated and Ca^{2+} activated K^+ channels activate to drive K^+-efflux and repolarization. The balance of depolarizing and repolarizing currents expressed by the cell can change the burst duration (from first spike to last spike) and burst interval (from last spike of previous burst to first spike of following burst).

Ligand-Mediated Excitation-Contraction Coupling

Ligands which increase uterine contractility are called uterotonins, and they primarily function by directly, or indirectly increasing $[Ca^{2+}]_i$. One of the most well studied uterotonins that functions through the Ca^{2+}-efflux pathway is oxytocin. Oxytocin is a nonapeptide hormone that initiates uterine contractility through its binding to the oxytocin receptor, a member of the G-protein coupled receptor family. Upon oxytocin binding, the OXTR undergoes a conformational change that activates its associated $G\alpha_{q/11}$ protein, leading to multiple downstream signaling pathways resulting in myometrial contraction (38). The primary pathway involves $G\alpha_{q/11}$ activation of phospholipase C-β and production of diacylglycerol and inositol triphosphate (IP_3) from phosphotidyl inositol. IP_3 activates the IP_3 receptor on the sarcoplasmic reticulum, which opens and releases Ca^{2+} from the SR into the cytosol. The increase in $[Ca^{2+}]_i$ induces Ca^{2+}-calmodulin binding and initiates the cross-bridge cycling cascade (reviewed in(39)).

Cross-Bridge Cycling

Upon the increased $[Ca^{2+}]_i$, calmodulin activates MLCK to phosphorylate myosin and initiate cross-bridge cycling with actin. Actin filaments, anchored to the dense bodies of the cytoskeleton, are juxtaposed to myosin thick filaments that are composed of two regulatory light chains, and two heavy chains. The heavy chains each contain a head region with an actin binding domain and an ATPase domain that produces the energy required for the force of contraction. To initiate contractions, the myosin light chains are phosphorylated by MLCK, inducing the ATPase activity of the heavy chains and increasing the angle of the myosin heads in relation to the actin filaments. This results in the myosin thick filaments pulling the actin filaments towards the center of the cell, thereby decreasing the length of the cell, and shortening the muscle. To finish the cycle, myosin thick filaments release their ADP, bind an ATP and are released from the actin filament, ready to start again (reviewed in (21)).

1.3 Uterine Activation

Throughout pregnancy the uterus remains quiescent, producing low amplitude, asynchronous contractions. At term, it undergoes a period of activation, in which it becomes 1) more sensitive to stimulation by agonists like oxytocin, 2) more sensitized to Ca^{2+}, 3) more electrically connected such that it can produce coordinated contractions, and 4) able to produce stronger contractions per unit area (40). In preparation for labor, human MSMCs increase the expression of the oxytocin receptor while simultaneously, the decidua increases local oxytocin production (39). In addition to increasing $[Ca^{2+}]_i$, oxytocin signaling also promotes greater force production in response to $[Ca^{2+}]_i$ than depolarization alone. This effect, known as calcium sensitization, occurs as the result of myosin light chain phosphatase (MLCP) inhibition. MLCP, which normally encourages muscle relaxation, is inhibited by the RhoA-associated kinase (ROCK) upon oxytocin receptor stimulation (41). This in turn gives oxytocin a two-pronged approach for enhancing uterine contractility at term. The effects of local $[Ca^{2+}]_i$ increases in the uterus are further amplified at term by the increased expression of the gap junction protein, connexin 43 (Cx43) (42, 43). Greater connectivity between MSMCs through gap junctions promotes whole-organ level, wave-like contractions that are necessary for parturition. Finally, contractions that occur during labor are more effective at expelling the fetus because they are stronger. Not only is there increased Ca^{2+} signaling (44), but it has been shown that force per unit of phosphorylated myosin light chain increases through an unknown mechanism (40).

1.4 Hormonal Coordination of Uterine Physiology

Uterine physiology is regulated throughout pregnancy in large part by the actions of the steroid hormones progesterone and estrogen. Progesterone, named for its pro-gestational effects, increases in serum concentration throughout pregnancy in both rodents and humans and serves to

block uterine contractions (45). The 'progesterone-block' is so essential that treatment with the progesterone receptor partial-antagonist, RU486, initiates labor at any point in pregnancy, and does so in both rodents and humans (46). Progesterone maintains uterine quiescence by inhibiting the expression of many pro-contractile, estrogen-mediated genes, such as the oxytocin receptor, the prostaglandin $F_{2\alpha}$ receptor, and connexin 43 in part by activating the repressive transcription factors ZEB1 and ZEB2 (47, 48). Additionally, progesterone maintains the PKA-mediated block of phospholipase C-β, thereby preventing the Ca^{2+}-efflux cascade initiated by oxytocin and prostaglandin $F_{2\alpha}$ (48, 49). Importantly, the mechanism of progesterone withdrawal at term differs between humans and rodents. Rodents experience a loss of circulating progesterone at term due to the break down of their primary progesterone producing organ, the corpus luteum, triggered by decidual prostaglandin synthesis. Conversely, in women high progesterone levels, produced by the placenta, are sustained until term (50, 51). This has lead to the hypothesis that in lieu of a drop in circulating progesterone, pregnant women experience a functional progesterone withdrawal to induce labor (52).

The human nuclear progesterone receptor has two main isoforms, PR-A and PR-B. PR-B encompasses the full length protein, whereas PR-A is a truncated form of the receptor resulting from the use of a downstream alternative promoter within the first exon (53). PR-A and PR-B share most of the same structural motifs including a DNA-binding motif, ligand binding domain, and hinge region (54). The two receptors only differ by the N-terminal regulatory domain, with PR-A being 164 amino acids shorter than PR-B. This structural alteration promotes differing activities between the two receptors. PR-A, thought to be less transcriptionally active, was shown to oppose the actions of PR-B especially when the PR-A:PR-B ratio is high (55). Sam Mesiano's laboratory has shown that PR-A expression increases in term laboring samples

compared to non-laboring samples, thereby increasing the PR-A:PR-B ratio and enhancing the block of PR-B target genes (56). Conversely, PR-A has been shown to transactivate the expression of its own unique subset of target genes, and like PR-B, often does so in coordination with other transcription factors in the absence of a progesterone response element (55, 57). Recently, Nadeem et al. demonstrated that PR-A can translocate to the nucleus and induce the expression of connexin 43, in an unliganded state (58). They showed that term MSMCs express high levels of 20α hydroxysteroid dehydrogenase, which breaks down progesterone, creating a low progesterone concentration within the local environment. Because PR-B remains inactive in the unliganded state, PR-A becomes the dominant form of the receptor at term. Together, these studies suggest that the effects of progesterone will differ depending on its levels, the PR-A:PR-B ratio, and the promoter elements of the target gene.

1.5 Phasic Activity of the Uterus

Despite the importance of hormones in regulating MSMC activity, uterine contractions are myogenic, and occur in the absence of nervous or hormonal stimuli. In fact, strips of dissected uterine tissue can produce spontaneous, rhythmic contractions in an *in vitro* setting. The observation that rhythmic uterine contractions occur spontaneously has lead researchers to hypothesize that there may be a uterine pacemaker stimulating rhythmic electrical activity. Typical biological pacemakers function by generating a current that slowly depolarizes the cell membrane to its threshold potential, thus culminating in an action potential. When this slow depolarization occurs at a constant rate, then action potentials, and therefore contractions, are produced in regularly spaced intervals. This electrical waveform is termed a 'pacemaker potential'. Sharp electrode recordings of human, mouse, and rat uterine tissue have all demonstrated the presence of a pacemaker potential in uterine tissue from different regions of the

uterus (59-61). Both *in vitro* and *in vivo* experiments have shown that electrical activity can initiate from any region in the uterus, further diminishing the notion that there is a central pacemaking node (62-64). Although cells similar to interstitital cells of Cajal (the cells which drive pacemaking in the gut) have been identified in the human and rodent myometrium, the evidence does not strongly support a role for these cells in uterine pacemaking (65-68). This has lead to the notion that all myometrial smooth muscle cells have the capacity to drive pacemaking activity. The identity of the proteins, presumably ion channels, involved remains to be identified.

1.6 Ion Channels in the Myometrium

There has long been interest in the specific mechanisms regulating uterine electrical activity. Studies in the late 1950s and 1960s assessed the shape, duration, ionic content, and endogenous agonists of uterine action potentials (59, 69-74). As pharmacology, electrophysiology, and molecular biology techniques advanced in the 1980s specific currents were identified. For example, in 1987 Boyle et al published a study in which patch-clamp experiments were performed on *Xenopus* oocytes injected with RNA extracts from estrus-staged or pregnancy-staged rat uterus (75). They found that in different hormonal milieus, the total mRNA pool contained different levels of K^+-channel transcripts, as measured by gain and loss of K^+-channel currents. A year later, Wilde and Marshall demonstrated that the broad K^+-channel blockers, tetraethylammonium chloride and 4-aminopyridine, could extend the duration of action potential bursts in rat uterine circular muscle (76). These types of studies lead to our broad understanding of how uterine excitability is regulated. In the 1990s, the genetic identities of many of the ion channels contributing to the currents in the myometrium and elsewhere were revealed by improved cloning techniques. This lead to candidate gene approaches, from which

uterine physiologists have gradually added to the list of ion channels present in the myometrium. More recently, RNAseq was applied to human uterine tissue to identify changes in the transcriptome between human myometrium samples of pregnant, non-laboring and laboring women (77). This study and others revealed that the myometrium expresses more than thirty different ion channels (77, 78). The wide variety of ion channels expressed in the myometrium likely provides functional redundancy, creates a more robust system, and allows fine-tuning of myometrial electrical signaling across regions of the uterus and throughout the reproductive life cycle.

1.7 The Role for Na^+ in MSMCs

Unlike many other excitable cells such as neurons where Na^+, conducted by fast, voltage-gated channels, is the main ion responsible for the the depolarizing upstroke of an action potential, the MSMC action potential upstroke is produced mainly by Ca^{2+} currents (29, 79). While there have been some reports of tetrodotoxin (TTX)-sensitive, fast Na^+ currents in rodent myometrial smooth muscle cells (80, 81), there have been additional reports citing no dampening of uterine excitability by TTX (82, 83). Although voltage-gated Na^+ channel transcripts have been observed (77), there have also been no observations of a TTX-sensitive current in human MSMCs. However, many studies have reported that the pattern of myometrial action potentials relies on Na^+ flux. Anderson et al. reported that the regenerative properties of estrogen-treated, non-pregnant rat myometrial action potentials relied on the presence of both Na^+ and Ca^{2+}, and that removal of Ca^{2+} from the extracellular solution increased the inward leak current in these cells (84, 85). Kleinhaus et al also demonstrated that in pregnant rabbit myometrium, bursting activity initially stopped when extracellular Na^+ was replaced by a non-permeable cation, and then recovered with sustained bursting (59). Anderson and Moore also demonstrated that Na^+-

free solution reduced a transient inward current in the estrogen treated rat myometrium. These studies along with others (86) suggest that there is a subtle role for Na^+ in regulating myometrial excitability. More recently Myoshi et al. reported the presence of a Na^+-dependent, Gd^{3+}-sensitive leak current in rat MSMCs that was hypothesized to contribute to uterine excitability (87). We identified the presence of a similar current in human MSMCs that was, in part, dependent on the expression of a Na^+-leak channel, called NALCN (See chapter 2).

1.8 Na^+-Leak Channel, Non-Selective (NALCN)

1.8.1 NALCN in Regulating Resting Membrane Potential

Most excitable cells maintain their resting membrane potential (RMP) between -80 mV and -50 mV, closer to the reversal potential of K^+ (-86 mV) than those of Na^+ or Ca^{2+} (+84 mV and +127 mV, respectively). Because of this, it has been well accepted that the background K^+ conductance is the primary regulator of the RMP. However, the reversal potential of K^+ (-86 mV based on a concentration of 5 mM $[K^+]_{out}$ and 140 mM $[K^+]_{in}$) is more negative than the typical resting membrane potential of MSMCs (-55 mV). This suggests that the RMP must also depend on other background currents, such as a Na^+ leak current. By letting small amounts of Na^+ into a cell, a Na^+-leak current can counteract the hyperpolarizing contribution of background K^+ currents. One particular ion channel that has been shown to function in this way is the Na^+-leak channel, non-selective (NALCN).

NALCN was named in 2007 by Boxun Lu in Dejian Ren's group after its ability to conduct a constitutively active, cationic leak current (88). This channel, which is a member of the 4x6 transmembrane domain (TMD) family of channels that includes voltage gated Na^+ (Na_v) and Ca^{2+} (Ca_v) channels, was found to be voltage insensitive (88). Voltage sensitivity is conferred by the charged residues of the S4 segment of each domain, which in NALCN are

reduced from 21 to 14 (88). Also in 4x6 TMD channels, ion selectivity is determined by an amino acid motif composed of one amino acid contributed from the pore-forming loop of each transmembrane domain. While Na_v channels have a DEKA motif, and Ca_v channels have a EEEE motif, NALCN's selectivity filter motif is EEKE, a unique fusion of the other two, which gives it a non-selective pore (Fig 1.3) (88). NALCN conducts Na^+ (relative permeability (P) = 1.3), K^+ (P = 1.2), Cs^+ (P = 1.0) and, to a lesser extent, Ca^{2+} (P = 0.5) (88). The NALCN current (I_{NALCN}) was found to be constitutively active, insensitive to inhibition by tetrodotoxin, and sensitive to inhibition by Gd^{3+}, Cd^{2+}, Co^{2+}, and verapamil (88). Although NALCN can conduct both Na^+ and K^+, at the RMP the driving force for Na^+ into the cell is greater than that for K^+, making NALCN primarily a Na^+-conducting channel. As was hypothesized based on its constitutive Na^+ conductance, NALCN has been shown to be an important modulator of RMP in cell types including neurons and pancreatic beta cells (88-93).

1.8.2 NALCN Discovery

NALCN, originally called Vgcnl1, was cloned from the rat in 1999, by J.H. Lee et al (94, 95). Based on analysis of its hydropathy plot and protein sequence homology to other ion channels NALCN was hypothesized to be a cation channel (95). Homologs of this channel have been identified in vertebrates and invertebrates, including yeast (96). As such, some of the first studies of NALCN were done in the invertebrate nematode, *C. elegans*, and the fruit fly, *D. melanogaster*. Since its original discovery, studies of NALCN have gone on to reveal a widespread role for this channel in biological rhythms, ranging from the rapid respiratory rhythm of a mouse (seconds) (88), to the slower circadian rhythms of the fly (~24 hrs) (97). Additionally, researchers have found that this channel does not work in isolation, but that it associates with a complex of proteins including UNC79, UNC80, and NLF-1, and can be

regulated by several G-protein coupled receptors.

1.8.3 NALCN in Regulating Neuronal Excitability

Much of the early research done on NALCN has been in the context of the nervous system and NALCN's role in regulating spontaneous and rhythmic neuronal firing. Learning the function of NALCN in the nervous system provides a useful framework for understanding its function in other excitable tissues, like the myometrium. The foundational works that have established NALCN's role in excitability were done in three different animal models: *Mus musculus*, *Caenorhabditis elegans, and Drosophila melanogaster*.

Studies in *C. elegans* identified the *NALCN* homologs *nca-1* and *nca-2* through forward genetic screens assessing important genes for the characteristic sinusoidal locomotion pattern of the worm. *Nca* loss-of-function (*nca(lf)*) mutants display a 'fainter' phenotype in which the worm repeatedly paused as it attempted to move across the petri plate (98). Conversely, *nca-1* or *nca-2* gain of function mutants (*nca(gf)*) displayed a 'coiler' phenotype in which they showed uncoordinated and exaggerated bending behavior that resulted in a coiling motion (98). *In vivo* Ca^{2+}-imaging experiments of the hermaphrodite specific neurons (HSN) in *nca(lf)* worms showed normal Ca^{2+}-spikes at the neuron cell body, but reduced spike frequency and amplitude in the pre-synaptic area (98). The *nca(gf)* mutants similarly showed normal Ca^{2+}-spikes at the cell body, but had increased spike amplitude at the presynaptic area (98). In the *C. elegans* nervous system, which lacks voltage-gated Na^{+} channels, *nca* seems to be playing an important role in transmitting the depolarization signal from the cell body, down the length of the synapse. Supporting this hypothesis, *nca(lf)* mutants had decreased miniature post-synaptic currents at the neuromuscular junction (90).

In the initial reverse genetics studies in the fly, mutations of *NALCN* or *NA* as its called in

D. melanogaster, caused a narrow abdomen (NA) phenotype and hypersensitivity to the volatile anesthetic halothane (99, 100). Beyond a narrow abdomen phenotype, they also had disrupted circadian regulation of their locomotion behavior. Specifically, *na* mutant flies had lost the increase in activity at dawn, and the light-dark transition anticipation behavior characteristic of WT flies (95). Immunofluorescent staining of fly brains showed that NA was expressed in circadian pacemaker neurons (97). Normal circadian behavior was rescued by the reintroduction of *na* to these select neurons, and it was suggested that NA mediated this activity through conducting an inward cation current. Importantly, the mutation of NA did not disrupt normal cycling of clock genes like PERIOD, suggesting that NA may be a downstream target of the clock genes (97). Greatly expanding on this work, Flourakis et al showed that NA is indeed working through modulation of the RMP of circadian pacemaker neurons, and mutations of NA result in a significantly reduced firing rate of these neurons (91). They found that while *na* levels remained constant across the 24 hr light:dark period, its activity was being rhythmically altered by a chaperone protein of NA called NLF-1 (see section on NALCN complex partners). In fact, NLF-1 mRNA levels were increased during the day, thereby allowing greater activity of NA at the cell membrane. They expanded upon their findings by creating an NALCN forebrain specific knockout mouse, and found that the neurons of the suprachiasmatic nucleus (the central clock) showed a similar dependence on NALCN for regulating spontaneous firing and RMP. They proposed a 'bicycle model' in which depolarizing NA currents drive excitability of circadian pacemaker neurons during the day, and hyperpolarizing K^+ currents silence firing at night. This work was important in demonstrating how an ion channel like NALCN which can stimulate rapid firing in neurons, can also affect slower biological rhythms by regulation of its cell surface expression.

Finally, key studies in the murine model have begun to establish the role of NALCN in mammalian neurophysiology and played an important part in garnering interest in the study of NALCN. Boxun Lu and colleagues described the phenotype of the global NALCN knockout mouse in 2007 (88). These mice were found to die within 24 hours of birth due to disrupted respiratory rhythm wherein they experienced repeated episodes of apnea (arrested breathing for more than 3 seconds). This phenotype was linked to reduced spontaneous firing of the fourth cervical nerve root, which innervates the diaphragm, indicating a role for NALCN in spontaneous neuronal firing. NALCN was also found to be expressed in the hippocampus, and comparisons between membrane potential of neonatal hippocampal neurons showed that NALCN KO mice had a more hyperpolarized RMP (-70 mV) compared to WT (-60 mV). Hyperpolarization of the membrane potential reduced the spontaneous firing rate of these neurons, such that +50 pA of exogenous current needed to be injected into the cells to achieve similar firing rates as WT neurons. This landmark paper demonstrated the significant role for NALCN in modulating RMP and excitability of mammalian neurons, and the profound effect that this could have on physiology. More recently, Gary Yellen's group expanded on this work by showing that NALCN contributes to the firing rate of substantia nigra pars reticulata neurons (92). Together, studies by these labs and others have shown that NALCN can contribute to basal firing rates as well as agonist enhanced firing rates (discussed below).

1.8.4 NALCN Complex

Shortly after its discovery, researchers discovered that NALCN does not work in isolation, but rather interacts with a complex of proteins that help it carry out its function. In studying the *C. elegans nca-1/2* mutants, Yeh et al. recognized that two previously described *C. elegans* mutants, called *unc80* and *unc79*, had the same fainter phenotype as the *nca-1/2* double

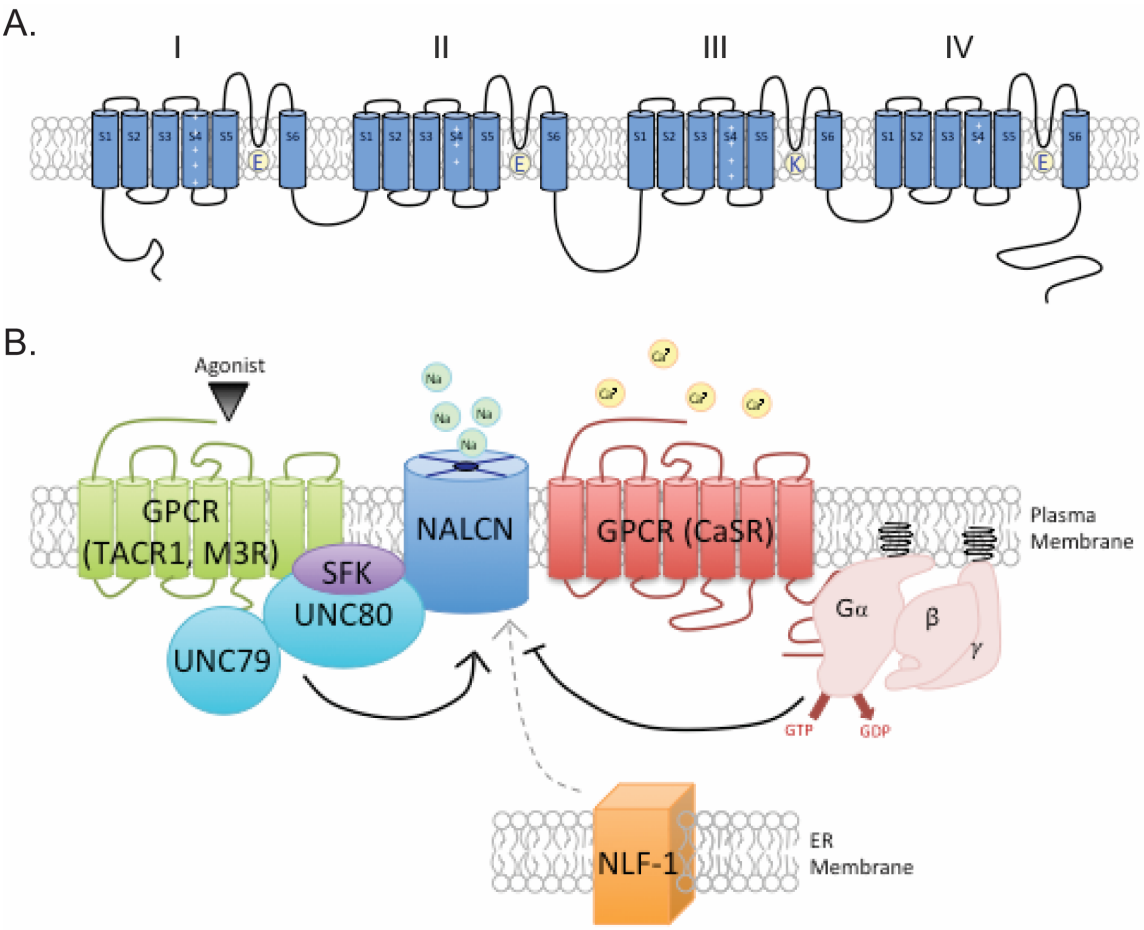

Figure 1.3 The NALCN complex.
A) NALCN has four homologous repeats (I – IV) each containing six transmembrane domains (S1 – S6). The S4 domains contain 14 positively charged residues compared to the 21 charged residues in Ca_v and Na_v channels. The pore motif in NALCN is EEKE, with residues interacting from the in the S5-S6 loop regions of each repeat. B) NALCN is transported to the plasma membrane with the help of the ER-resident protein, NCA localizatin factor 1 (NLF-1). At the plasma membrane, NALCN can interact with G-protein coupled receptors (GPCRs) including Tachykinin receptor 1 (TACR1) and Muscarinic receptor 3 (M3R). When stimulated by their agonists, substance P and acetylcholine, respectively, they can enhance NALCN currents through a Src-family kinase (SFK) dependent pathway. These processes require the presence of the scaffolding proteins UNC80 and UNC79. NALCN can also be inhibited by the calcium sensing receptor (CaSR), another GPCR. CaSR signals through its G-protein to inhibit NALCN under normal (2 mM) Ca^{2+} concentrations.

mutant (98). Crossing *unc80* and *nca(lf)* resulted in worms with the same fainter phenotype as the single mutants, and crossing *unc80* with the *nca(gf)* coiler mutant eliminated the coiler phenotype and produced only worms with the loss of function 'fainter' phenotype, indicating a dependence of NCA on UNC80. Through further study they found that UNC79 and UNC80 co-localized with NCA-1, and that each of the three proteins is required for the localization of the others to the axon. Later work by Dejian Ren's lab showed that NALCN drives the substance P (SP) induced current (I_{SP}) in mouse hippocampal neurons, and that in HEK293T cells, this stimulated current requires the expression of UNC80 and the tachykinin receptor (TACR1) (101). Interestingly, though TACR1 is a Gq G-protein coupled receptor (GPCR), I_{SP} was unaffected by the presence of the non-hydrolyzable forms of GTP (GTP-γ-S) and GDP (GDP-β-S), indicating a signaling mechanism independent of classic GPCR signaling. However, I_{SP} was inactivated by Src-family kinase inhibitors PP1 and genistein, implicating SFK-dependent phosphorylation of NALCN and UNC80 as the mechanism of I_{SP} activation. Additional studies in the Ren lab suggest that UNC80 serves as a scaffolding protein for NALCN, recruiting Src to the channel complex (102).

In addition to TACR1, other GPCRs have been shown to modulate the NALCN current (I_{NALCN}). The neurotensin receptor and the muscarinic receptor 3 (M3R) were found to activate I_{NALCN} upon binding of their ligands, neurotensin and acetylcholine, in a manner similar to TACR1 and SP (89). Conversely, the calcium sensing receptor (CaSR) was found to have an inhibitory effect on I_{NALCN} under normal extracellular calcium concentrations (103). Upon reduction of extracellular calcium from 2 mM to 0.1 mM, NALCN currents more than tripled in size, and this effect was synergistic with the activation caused by SP. The low calcium

activation of NALCN was found to be the result of removal of a constant inhibition of NALCN by the CASR, and this was found to be G-protein dependent as was evidenced by loss of the current under low calcium conditions when CASR activity was sustained by GTP-γ-S (103).

One last component of the NALCN complex was again originally identified in *C. elegans*, and because it was shown to be essential for the proper localization of NALCN to the plasma membrane, it was given the name NCA localization factor-1 (NLF-1) (104). *NLF-1* mutants have the same fainter phenotype as the *unc80*, *unc79*, and *nca(lf)* mutants. However, unlike UNC79 and UNC80, NLF-1 contains an ER-retention motif and does not co-localize with the rest of the complex at the cell surface, but is nonetheless essential for the trafficking of the complex. As previously mentioned, NLF-1 plays an important role in the SCN in regulating the day/night trafficking of NALCN to the plasma membrane of the pacemaker neurons (91). This novel mechanism of temporally regulating NALCN activity could play an important role in other tissues where excitability is strategically modulated over time or upon environmental changes.

1.8.5 Human Mutations of NALCN

Since 2013, several mutations of NALCN have been found as driver mutations in children with differing arrays of neurologic and developmental defects. Four recessive mutations of NALCN have been found in children of different consanguineous families. Three of the recessive mutations result in truncated proteins by creating premature stop codons at different locations in the NALCN protein: 1) between S3 and S4 of domain II, 2) between II-III linker region, and 3) within the pore region of homologous repeat III. The remaining recessive NALCN mutation results in a missense mutation (W1287L) in S3 of domain IV (105). Although it is expected that these truncating mutations cause loss of function of the channel, the effect of the W1287L mutation has not been studied in further detail. The children with these mutations

have many overlapping traits including facial dysmorphisms, intellectual disability, and hypotonia. Some of the children also present with speech impairment, chronic constipation, cachexia, strabismus, and abnormal respiratory rhythm (106-108). As a group these children are classified as having infantile hypotonia with psychomotor retardation and characteristic facies (IHPRF). Additionally, many *de novo* NALCN mutations have been discovered in children with some similar traits including hypotonia, facial dysmorphisms, and developmental delay. However, many of the patients with heterozygous, *de novo* mutations also presented with arthrogryposis (contractures of the joints) as well as congenital contractures of the face, and individual patients presented with ataxia, hyperthermia, and central hypertonia (105, 109-111). These patients are classified as having congenital contractures of the limbs and face with hypotonia and developmental delay (CLIFHADD). All of the *de novo* mutations discovered have been missense mutations and are primarily located in the pore forming regions of the channel. Only three of the mutations have been studied *in vitro*. Y587S (S6 of domain II) and L509S (S4-S5 linker of domain II) were found to inhibit expression of the WT channel when cotransfected in HEK293T cells. Additionally, R1181Q, found in two separate studies, when introduced into *C. elegans* produced a coiler phenotype, indicating that it may create a gain of function mutation. A recent study examined the effect of several of the *de novo*, autosomal dominant mutations on *C. elegans* locomotion (112). Many of these mutations produced the gain-of-function coiler phenotype, while others appeared to function as dominant negative 'fainters.' Although it is confusing that patients with dominant negative and gain-of-function mutations have similar features, the authors argue that this could be the result of differential effects in inhibitory and excitatory neuronal circuits. Importantly, these mutations demonstrate the crucial role of NALCN at neuromuscular junctions, and in normal neurologic function and

development. Interestingly, the good health of parents with one copy of the NALCN recessive mutations (primarily truncating), suggests that only one normal copy of NALCN is needed. However, the effect of the *de novo* heterozygous mutations suggests that particular mutations can negate the presence of a normal copy.

Recently, several UNC80 mutations have also been discovered (113-115). All of these mutations are recessive, and include both truncating and missense mutations. These patients have some similar traits to those with NALCN mutations, including hypotonia and intellectual disability, and also have unique traits including encephalopathy, growth failure, and one experienced intrauterine growth restriction. Again, the function of these mutations has not been studied in great detail.

1.8.6 Other Functions of NALCN

In addition to the extensive work examining the function of NALCN in the nervous system, there have been a few studies linking NALCN to other excitable tissues, such as the pancreas and interstitial cells of cajal (ICCs), and in osmoregulation. In the murine pancreatic beta cell line, MIN6 cells, NALCN was found to associate with M3R and be activated by acetylcholine through an SFK-dependent pathway (89). Further studies assessing the importance of NALCN in pancreatic function and insulin release have not been published, but it is hypothesized that NALCN would be an important factor in depolarizing beta cells to initiate insulin release. Additionally, NALCN was found to be expressed in cultured murine ICCs, cells that are important for stimulating the rhythmic peristalsis of the intestinal smooth muscle (116). These cells show increased firing and the induction of an inward leak current upon the addition of substance P. ICCs from NALCN knockout mice showed a reduction in the SP-induced leak current and a dampened SP-induced firing rate, indicating that NALCN may play an important

role in enteric responses. Finally, NALCN has been linked to osmoregulation in mice (117). In fact, heterozygous NALCN knockout mice have significantly higher serum Na^+ concentrations (149 mM in NALCN KO compared to 146 mM in WT). These studies point to the broad importance of NALCN as a modulator of membrane excitability, and the likely possibility for new discoveries of NALCN functioning in many different tissue types.

1.9 The Role of NALCN in Uterine Physiology

In my thesis work, I examined the presence and role of NALCN in MSMC excitability and in parturition outcomes. First, I demonstrated that NALCN is expressed in human MSMCs, and that it conducts a Na^+-dependent, Gd^{3+}-sensitive leak current in these cells. I went on to show that NALCN is also expressed in the mouse myometrium, and that it is essential for successful parturition. I created an NALCN smooth muscle specific knockout mouse line ($smNALCN^{-/-}$), which within the reproductive tract, primarily deletes NALCN from the myometrium. These mice show an increased prevalence of prolonged or dysfunctional labor, and reduced uterine excitability exemplified by a shortened myometrial burst duration. Finally, I have found that NALCN is regulated by progesterone and shows regional expression differences. The protein levels of NALCN inversely correlate with circulating progesterone levels in the mouse, and the addition of exogenous progesterone at term keeps NALCN levels low. Progesterone also enhances the expression of a potential novel isoform of NALCN. This work has identified NALCN as an important player in uterine physiology and builds the foundation for further study of the mechanism of NALCN function in parturition.

1.10 References

1. Mesiano S, Wang Y, and Norwitz ER. Progesterone receptors in the human pregnancy uterus: do they hold the key to birth timing? *Reprod Sci.* 2011;18(1):6-19.

2. Shynlova O, Lee YH, Srikhajon K, and Lye SJ. Physiologic uterine inflammation and labor onset: integration of endocrine and mechanical signals. *Reprod Sci.* 2013;20(2):154-67.

3. Latini C, Frontini A, Morroni M, Marzioni D, Castellucci M, and Smith PG. Remodeling of uterine innervation. *Cell Tissue Res.* 2008;334(1):1-6.

4. Haase EB, Buchman J, Tietz AE, and Schramm LP. Pregnancy-induced uterine neuronal degeneration in the rat. *Cell Tissue Res.* 1997;288(2):293-306.

5. Wikland M, Lindblom B, Dahlstrom A, and Haglid KG. Structural and functional evidence for the denervation of human myometrium during pregnancy. *Obstet Gynecol.* 1984;64(4):503-9.

6. Marshall JM. Effects of ovarian steroids and pregnancy on adrenergic nerves of uterus and oviduct. *Am J Physiol.* 1981;240(5):C165-74.

7. Hamilton BE, Martin JA, Osterman MJ, Curtin SC, and Matthews TJ. Births: Final Data for 2014. *Natl Vital Stat Rep.* 2015;64(12):1-64.

8. Menon R. Spontaneous preterm birth, a clinical dilemma: etiologic, pathophysiologic and genetic heterogeneities and racial disparity. *Acta Obstet Gynecol Scand.* 2008;87(6):590-600.

9. Simhan HN, and Caritis SN. Prevention of preterm delivery. *N Engl J Med.* 2007;357(5):477-87.

10. Romero R, Dey SK, and Fisher SJ. Preterm labor: one syndrome, many causes. *Science.* 2014;345(6198):760-5.

11. Romero R, Nicolaides K, Conde-Agudelo A, Tabor A, O'Brien JM, Cetingoz E, Da Fonseca E, Creasy GW, Klein K, Rode L, et al. Vaginal progesterone in women with an asymptomatic sonographic short cervix in the midtrimester decreases preterm delivery and neonatal morbidity: a systematic review and metaanalysis of individual patient data. *Am J Obstet Gynecol.* 2012;206(2):124 e1-19.

12. Romero R, Yeo L, Miranda J, Hassan SS, Conde-Agudelo A, and Chaiworapongsa T. A blueprint for the prevention of preterm birth: vaginal progesterone in women with a short cervix. *J Perinat Med.* 2013;41(1):27-44.

13. Meis PJ, Klebanoff M, Thom E, Dombrowski MP, Sibai B, Moawad AH, Spong CY, Hauth JC, Miodovnik M, Varner MW, et al. Prevention of recurrent preterm delivery by 17 alpha-hydroxyprogesterone caproate. *N Engl J Med.* 2003;348(24):2379-85.

14. Schoen CN, Tabbah S, Iams JD, Caughey AB, and Berghella V. Why the United States preterm birth rate is declining. *Am J Obstet Gynecol.* 2015;213(2):175-80.

15. Galal M, Symonds I, Murray H, Petraglia F, and Smith R. Postterm pregnancy. *Facts Views Vis Obgyn.* 2012;4(3):175-87.

16. Simpson KR, and Knox GE. Oxytocin as a high-alert medication: implications for perinatal patient safety. *MCN Am J Matern Child Nurs.* 2009;34(1):8-15; quiz 6-7.

17. Frey HA, Tuuli MG, England SK, Roehl KA, Odibo AO, Macones GA, and Cahill AG. Factors associated with higher oxytocin requirements in labor. *J Matern Fetal Neonatal Med.* 2015;28(13):1614-9.

18. World Health Organization and Human Reproduction Programme. (2015). *WHO statement of caesarean section rates.* (WHO ref. no. WHO/RHR/15.02). Retrieved from: http://www.who.int/reproductivehealth/publications/maternal_perinatal_health/cs-statement/en/

19. American College of O, Gynecologists, Society for Maternal-Fetal M, Caughey AB, Cahill AG, Guise JM, and Rouse DJ. Safe prevention of the primary cesarean delivery. *Am J Obstet Gynecol.* 2014;210(3):179-93.

20. Huszar G, and Naftolin F. The myometrium and uterine cervix in normal and preterm labor. *N Engl J Med.* 1984;311(9):571-81.

21. Aguilar HN, and Mitchell BF. Physiological pathways and molecular mechanisms regulating uterine contractility. *Hum Reprod Update.* 2010;16(6):725-44.

22. Hricak H, Alpers C, Crooks LE, and Sheldon PE. Magnetic resonance imaging of the female pelvis: initial experience. *AJR Am J Roentgenol.* 1983;141(6):1119-28.

23. van Gestel I, MM IJ, Hoogland HJ, and Evers JL. Endometrial wave-like activity in the non-pregnant uterus. *Hum Reprod Update.* 2003;9(2):131-8.

24. Lymn RW, and Taylor EW. Mechanism of adenosine triphosphate hydrolysis by actomyosin. *Biochemistry.* 1971;10(25):4617-24.

25. Chacko S, Conti MA, and Adelstein RS. Effect of phosphorylation of smooth muscle myosin on actin activation and Ca2+ regulation. *Proc Natl Acad Sci U S A.* 1977;74(1):129-33.

26. Sanborn BM. Relationship of ion channel activity to control of myometrial calcium. *J Soc Gynecol Investig.* 2000;7(1):4-11.

27. Walsh MP, Vallet B, Cavadore JC, and Demaille JG. Homologous calcium-binding proteins in the activation of skeletal, cardiac, and smooth muscle myosin light chain kinases. *J Biol Chem.* 1980;255(2):335-7.

28. Sandow A. Excitation-contraction coupling in muscular response. *Yale J Biol Med.* 1952;25(3):176-201.

29. Granger SE, Hollingsworth M, and Weston AH. Effects of calcium entry blockers on tension development and calcium influx in rat uterus. *Br J Pharmacol.* 1986;87(1):147-56.

30. Amedee T, Mironneau C, and Mironneau J. The calcium channel current of pregnant rat single myometrial cells in short-term primary culture. *J Physiol.* 1987;392(253-72.

31. Lipscombe D, Helton TD, and Xu W. L-type calcium channels: the low down. *J Neurophysiol.* 2004;92(5):2633-41.

32. Snutch TP PJ, Mathews E, et al. *Madame Curie Bioscience Database.* Austin, TX: Landes Bioscience; 2000 - 2013.

33. Lacinova L, and Hofmann F. Ca2+- and voltage-dependent inactivation of the expressed L-type Ca(v)1.2 calcium channel. *Arch Biochem Biophys.* 2005;437(1):42-50.

34. Brainard AM, Korovkina VP, and England SK. Potassium channels and uterine function. *Semin Cell Dev Biol.* 2007;18(3):332-9.

35. Tribe RM, Moriarty P, and Poston L. Calcium Homeostatic Pathways Change with Gestation in Human Myometrium. *Biol Reprod.* 2000;63(3):748-55.

36. Parkington HC, and Coleman HA. Ionic mechanisms underlying action potentials in myometrium. *Clin Exp Pharmacol Physiol.* 1988;15(9):657-65.

37. Wray S, Burdyga T, and Noble K. Calcium signalling in smooth muscle. *Cell Calcium.* 2005;38(3-4):397-407.

38. Arrowsmith S, and Wray S. Oxytocin: its mechanism of action and receptor signalling in the myometrium. *J Neuroendocrinol.* 2014;26(6):356-69.

39. Arthur P, Taggart MJ, and Mitchell BF. Oxytocin and parturition: a role for increased myometrial calcium and calcium sensitization? *Frontiers in bioscience : a journal and virtual library.* 2007;12(619-33.

40. Word RA, Stull JT, Casey ML, and Kamm KE. Contractile elements and myosin light chain phosphorylation in myometrial tissue from nonpregnant and pregnant women. *J Clin Invest.* 1993;92(1):29-37.

41. Hudson CA, Heesom KJ, and Lopez Bernal A. Phasic contractions of isolated human myometrium are associated with Rho-kinase (ROCK)-dependent phosphorylation of myosin phosphatase-targeting subunit (MYPT1). *Mol Hum Reprod.* 2012;18(5):265-79.

42. Ambrus G, and Rao CV. Novel regulation of pregnant human myometrial smooth muscle cell gap junctions by human chorionic gonadotropin. *Endocrinology.* 1994;135(6):2772-9.

43. Sakai N, Tabb T, and Garfield RE. Studies of connexin 43 and cell-to-cell coupling in cultured human uterine smooth muscle. *Am J Obstet Gynecol.* 1992;167(5):1267-77.

44. Collins PL, Moore JJ, Lundgren DW, Choobineh E, Chang SM, and Chang AS. Gestational changes in uterine L-type calcium channel function and expression in guinea pig. *Biol Reprod.* 2000;63(5):1262-70.

45. Csapo A. Progesterone block. *Am J Anat.* 1956;98(2):273-91.

46. Chwalisz K, and Garfield RE. Antiprogestins in the induction of labor. *Ann N Y Acad Sci.* 1994;734(387-413.

47. Williams KC, Renthal NE, Gerard RD, and Mendelson CR. The microRNA (miR)-199a/214 cluster mediates opposing effects of progesterone and estrogen on uterine contractility during pregnancy and labor. *Mol Endocrinol.* 2012;26(11):1857-67.

48. Mesiano S, and Welsh TN. Steroid hormone control of myometrial contractility and parturition. *Semin Cell Dev Biol.* 2007;18(3):321-31.

49. Ku CY, and Sanborn BM. Progesterone prevents the pregnancy-related decline in protein kinase A association with rat myometrial plasma membrane and A-kinase anchoring protein. *Biol Reprod.* 2002;67(2):605-9.

50. Boroditsky RS, Reyes FI, Winter JS, and Faiman C. Maternal serum estrogen and progesterone concentrations preceding normal labor. *Obstet Gynecol.* 1978;51(6):686-91.

51. Tulchinsky D, Hobel CJ, Yeager E, and Marshall JR. Plasma estrone, estradiol, estriol, progesterone, and 17-hydroxyprogesterone in human pregnancy. I. Normal pregnancy. *Am J Obstet Gynecol.* 1972;112(8):1095-100.

52. Csapo AI, and Pinto-Dantas CA. The effect of progesterone on the human uterus. *Proc Natl Acad Sci U S A.* 1965;54(4):1069-76.

53. Kastner P, Krust A, Turcotte B, Stropp U, Tora L, Gronemeyer H, and Chambon P. Two distinct estrogen-regulated promoters generate transcripts encoding the two functionally different human progesterone receptor forms A and B. *EMBO J.* 1990;9(5):1603-14.

54. Patel B, Elguero S, Thakore S, Dahoud W, Bedaiwy M, and Mesiano S. Role of nuclear progesterone receptor isoforms in uterine pathophysiology. *Hum Reprod Update.* 2015;21(2):155-73.

55. Tan H, Yi L, Rote NS, Hurd WW, and Mesiano S. Progesterone receptor-A and -B have opposite effects on proinflammatory gene expression in human myometrial cells: implications for progesterone actions in human pregnancy and parturition. *J Clin Endocrinol Metab.* 2012;97(5):E719-30.

56. Merlino AA, Welsh TN, Tan H, Yi LJ, Cannon V, Mercer BM, and Mesiano S. Nuclear progesterone receptors in the human pregnancy myometrium: evidence that parturition

involves functional progesterone withdrawal mediated by increased expression of progesterone receptor-A. *J Clin Endocrinol Metab.* 2007;92(5):1927-33.

57. Dong X, Yu C, Shynlova O, Challis JR, Rennie PS, and Lye SJ. p54nrb is a transcriptional corepressor of the progesterone receptor that modulates transcription of the labor-associated gene, connexin 43 (Gja1). *Mol Endocrinol.* 2009;23(8):1147-60.

58. Nadeem L, Shynlova O, Matysiak-Zablocki E, Mesiano S, Dong X, and Lye S. Molecular evidence of functional progesterone withdrawal in human myometrium. *Nat Commun.* 2016;7(11565.

59. Kleinhaus AL, and Kao CY. Electrophysiological actions of oxytocin on the rabbit myometrium. *J Gen Physiol.* 1969;53(6):758-80.

60. Parkington HC, Tonta MA, Davies NK, Brennecke SP, and Coleman HA. Hyperpolarization and slowing of the rate of contraction in human uterus in pregnancy by prostaglandins E2 and f2alpha: involvement of the Na+ pump. *J Physiol.* 1999;514 (Pt 1)(229-43.

61. Kuriyama H, and Suzuki H. Changes in electrical properties of rat myometrium during gestation and following hormonal treatments. *J Physiol.* 1976;260(2):315-33.

62. Lammers WJ, Mirghani H, Stephen B, Dhanasekaran S, Wahab A, Al Sultan MA, and Abazer F. Patterns of electrical propagation in the intact pregnant guinea pig uterus. *Am J Physiol Regul Integr Comp Physiol.* 2008;294(3):R919-28.

63. Lammers WJ, Stephen B, Al-Sultan MA, Subramanya SB, and Blanks AM. The location of pacemakers in the uteri of pregnant guinea pigs and rats. *Am J Physiol Regul Integr Comp Physiol.* 2015;309(11):R1439-46.

64. Ramon C, Preissl H, Murphy P, Wilson JD, Lowery C, and Eswaran H. Synchronization analysis of the uterine magnetic activity during contractions. *Biomed Eng Online.* 2005;4(55.

65. Duquette RA, Shmygol A, Vaillant C, Mobasheri A, Pope M, Burdyga T, and Wray S. Vimentin-positive, c-kit-negative interstitial cells in human and rat uterus: a role in pacemaking? *Biol Reprod.* 2005;72(2):276-83.

66. Ciontea SM, Radu E, Regalia T, Ceafalan L, Cretoiu D, Gherghiceanu M, Braga RI, Malincenco M, Zagrean L, Hinescu ME, et al. C-kit immunopositive interstitial cells (Cajal-type) in human myometrium. *J Cell Mol Med.* 2005;9(2):407-20.

67. Cretoiu D, Ciontea SM, Popescu LM, Ceafalan L, and Ardeleanu C. Interstitial Cajal-like cells (ICLC) as steroid hormone sensors in human myometrium: immunocytochemical approach. *J Cell Mol Med.* 2006;10(3):789-95.

68. Hutchings G, Williams O, Cretoiu D, and Ciontea SM. Myometrial interstitial cells and the coordination of myometrial contractility. *J Cell Mol Med.* 2009;13(10):4268-82.

69. Marshall JM. Regulation of activity in uterine smooth muscle. *Physiol Rev Suppl.* 1962;5(213-27.

70. Casteels R, and Kuriyama H. Membrane Potential and Ionic Content in Pregnant and Non-Pregnant Rat Myometrium. *J Physiol.* 1965;177(263-87.

71. Inoue Y, Nakao K, Okabe K, Izumi H, Kanda S, Kitamura K, and Kuriyama H. Some electrical properties of human pregnant myometrium. *Am J Obstet Gynecol.* 1990;162(4):1090-8.

72. Kao CY. Long-term observations of spontaneous electrical activity of the uterine smooth muscle. *Am J Physiol.* 1959;196(2):343-50.

73. Grosset A, and Mironneau J. An analysis of the actions of prostaglandin E1 on membrane currents and contraction in uterine smooth muscle. *J Physiol.* 1977;270(3):765-84.

74. Mollard P, Mironneau J, Amedee T, and Mironneau C. Electrophysiological characterization of single pregnant rat myometrial cells in short-term primary culture. *Am J Physiol.* 1986;250(1 Pt 1):C47-54.

75. Boyle MB, MacLusky NJ, Naftolin F, and Kaczmarek LK. Hormonal regulation of K+-channel messenger RNA in rat myometrium during oestrus cycle and in pregnancy. *Nature.* 1987;330(6146):373-5.

76. Wilde DW, and Marshall JM. Effects of tetraethylammonium and 4-aminopyridine on the plateau potential of circular myometrium from the pregnant rat. *Biol Reprod.* 1988;38(4):836-45.

77. Chan YW, van den Berg HA, Moore JD, Quenby S, and Blanks AM. Assessment of myometrial transcriptome changes associated with spontaneous human labour by high-throughput RNA-seq. *Experimental physiology.* 2014;99(3):510-24.

78. Atia J, McCloskey C, Shmygol AS, Rand DA, van den Berg HA, and Blanks AM. Reconstruction of Cell Surface Densities of Ion Pumps, Exchangers, and Channels from mRNA Expression, Conductance Kinetics, Whole-Cell Calcium, and Current-Clamp Voltage Recordings, with an Application to Human Uterine Smooth Muscle Cells. *PLoS Comput Biol.* 2016;12(4):e1004828.

79. Wray S, Jones K, Kupittayanant S, Li Y, Matthew A, Monir-Bishty E, Noble K, Pierce SJ, Quenby S, and Shmygol AV. Calcium signaling and uterine contractility. *J Soc Gynecol Investig.* 2003;10(5):252-64.

80. Ohya Y, and Sperelakis N. Fast Na+ and slow Ca2+ channels in single uterine muscle cells from pregnant rats. *Am J Physiol.* 1989;257(2 Pt 1):C408-12.

81. Amedee T, Renaud JF, Jmari K, Lombet A, Mironneau J, and Lazdunski M. The presence of Na^+ channels in myometrial smooth muscle cells is revealed by specific neurotoxins. *Biochem Biophys Res Commun.* 1986;137(2):675-81.

82. Miller SM, Garfield RE, and Daniel EE. Improved propagation in myometrium associated with gap junctions during parturition. *Am J Physiol.* 1989;256(1 Pt 1):C130-41.

83. Phillippe M, and Basa A. Effects of sodium and calcium channel blockade on cytosolic calcium oscillations and phasic contractions of myometrial tissue. *J Soc Gynecol Investig.* 1997;4(2):72-7.

84. Anderson NC, Ramon F, and Snyder A. Studies on Calcium and Sodium in Uterine Smooth Muscle Excitation under Current-Clamp and Voltage-Clamp Conditions. *J Gen Physiol.* 1971;58(3):322-39.

85. Anderson NC, Jr. Voltage-clamp studies on uterine smooth muscle. *J Gen Physiol.* 1969;54(2):145-65.

86. Kao CY, Zakim D, and Bronner F. Sodium influx and excitation in uterine smooth muscle. *Nature.* 1961;192(1189-90.

87. Miyoshi H, Yamaoka K, Garfield RE, and Ohama K. Identification of a non-selective cation channel current in myometrial cells isolated from pregnant rats. *Pflugers Arch.* 2004;447(4):457-64.

88. Lu B, Su Y, Das S, Liu J, Xia J, and Ren D. The Neuronal Channel NALCN Contributes Resting Sodium Permeability and Is Required for Normal Respiratory Rhythm. *Cell.* 2007;129(2):371-83.

89. Swayne LA, Mezghrani A, Varrault A, Chemin J, Bertrand G, Dalle S, Bourinet E, Lory P, Miller RJ, Nargeot J, et al. The NALCN ion channel is activated by M3 muscarinic receptors in a pancreatic beta-cell line. *EMBO Rep.* 2009;10(8):873-80.

90. Gao S, Xie L, Kawano T, Po MD, Guan S, Zhen M, Pirri JK, and Alkema MJ. The NCA sodium leak channel is required for persistent motor circuit activity that sustains locomotion. *Nat Commun.* 2015;6(6323).

91. Flourakis M, Kula-Eversole E, Hutchison AL, Han TH, Aranda K, Moose DL, White KP, Dinner AR, Lear BC, Ren D, et al. A Conserved Bicycle Model for Circadian Clock Control of Membrane Excitability. *Cell.* 2015;162(4):836-48.

92. Lutas A, Lahmann C, Soumillon M, and Yellen G. The leak channel NALCN controls tonic firing and glycolytic sensitivity of substantia nigra pars reticulata neurons. *Elife.* 2016;5(13):e15271.

93. Reinl EL, Cabeza R, Gregory IA, Cahill AG, and England SK. Sodium leak channel, non-selective contributes to the leak current in human myometrial smooth muscle cells from pregnant women. *Mol Hum Reprod.* 2015;21(10):816-24.

94. Lee JH, Cribbs LL, and Perez-Reyes E. Cloning of a novel four repeat protein related to voltage-gated sodium and calcium channels. *FEBS Lett.* 1999;445(2-3):231-6.

95. Nash HA, Scott RL, Lear BC, and Allada R. An unusual cation channel mediates photic control of locomotion in Drosophila. *Curr Biol.* 2002;12(24):2152-8.

96. Ghezzi A, Liebeskind BJ, Thompson A, Atkinson NS, and Zakon HH. Ancient association between cation leak channels and Mid1 proteins is conserved in fungi and animals. *Front Mol Neurosci.* 2014;7(15).

97. Lear BC, Lin JM, Keath JR, McGill JJ, Raman IM, and Allada R. The ion channel narrow abdomen is critical for neural output of the Drosophila circadian pacemaker. *Neuron.* 2005;48(6):965-76.

98. Yeh E, Ng S, Zhang M, Bouhours M, Wang Y, Wang M, Hung W, Aoyagi K, Melnik-Martinez K, Li M, et al. A putative cation channel, NCA-1, and a novel protein, UNC-80, transmit neuronal activity in C. elegans. *PLoS Biol.* 2008;6(3):e55.

99. Krishnan KS, and Nash HA. A genetic study of the anesthetic response: mutants of Drosophila melanogaster altered in sensitivity to halothane. *Proc Natl Acad Sci U S A.* 1990;87(21):8632-6.

100. Leibovitch BA, Campbell DB, Krishnan KS, and Nash HA. Mutations that affect ion channels change the sensitivity of Drosophila melanogaster to volatile anesthetics. *J Neurogenet.* 1995;10(1):1-13.

101. Lu B, Su Y, Das S, Wang H, Wang Y, Liu J, and Ren D. Peptide neurotransmitters activate a cation channel complex of NALCN and UNC-80. *Nature.* 2009;457(7230):741-4.

102. Wang H, and Ren D. UNC80 functions as a scaffold for Src kinases in NALCN channel function. *Channels (Austin).* 2009;3(3):161-3.

103. Lu B, Zhang Q, Wang H, Wang Y, Nakayama M, and Ren D. Extracellular calcium controls background current and neuronal excitability via an UNC79-UNC80-NALCN cation channel complex. *Neuron.* 2010;68(3):488-99.

104. Xie L, Gao S, Alcaire Salvador M, Aoyagi K, Wang Y, Griffin Jennifer K, Stagljar I, Nagamatsu S, and Zhen M. NLF-1 Delivers a Sodium Leak Channel to Regulate Neuronal Excitability and Modulate Rhythmic Locomotion. *Neuron.* 2013;77(6):1069-82.

105. Karakaya M, Heller R, Kunde V, Zimmer KP, Chao CM, Nurnberg P, and Cirak S. Novel Mutations in the Nonselective Sodium Leak Channel (NALCN) Lead to Distal Arthrogryposis with Increased Muscle Tone. *Neuropediatrics.* 2016;47(4):273-7.

106. Al-Sayed MD, Al-Zaidan H, Albakheet A, Hakami H, Kenana R, Al-Yafee Y, Al-Dosary M, Qari A, Al-Sheddi T, Al-Muheiza M, et al. Mutations in NALCN cause an autosomal-recessive syndrome with severe hypotonia, speech impairment, and cognitive delay. *Am J Hum Genet.* 2013;93(4):721-6.

107. Koroglu C, Seven M, and Tolun A. Recessive truncating NALCN mutation in infantile neuroaxonal dystrophy with facial dysmorphism. *J Med Genet.* 2013;50(8):515-20.

108. Gal M, Magen D, Zahran Y, Ravid S, Eran A, Khayat M, Gafni C, Levanon EY, and Mandel H. A novel homozygous splice site mutation in NALCN identified in siblings with cachexia, strabismus, severe intellectual disability, epilepsy and abnormal respiratory rhythm. *Eur J Med Genet.* 2016;59(4):204-9.

109. Fukai R, Saitsu H, Okamoto N, Sakai Y, Fattal-Valevski A, Masaaki S, Kitai Y, Torio M, Kojima-Ishii K, Ihara K, et al. De novo missense mutations in NALCN cause developmental and intellectual impairment with hypotonia. *J Hum Genet.* 2016;61(5):451-5.

110. Aoyagi K, Rossignol E, Hamdan FF, Mulcahy B, Xie L, Nagamatsu S, Rouleau GA, Zhen M, and Michaud JL. A Gain-of-Function Mutation in NALCN in a Child with Intellectual Disability, Ataxia, and Arthrogryposis. *Hum Mutat.* 2015;36(8):753-7.

111. Chong JX, McMillin MJ, Shively KM, Beck AE, Marvin CT, Armenteros JR, Buckingham KJ, Nkinsi NT, Boyle EA, Berry MN, et al. De novo mutations in NALCN cause a syndrome characterized by congenital contractures of the limbs and face, hypotonia, and developmental delay. *Am J Hum Genet.* 2015;96(3):462-73.

112. Bend EG, Si Y, Stevenson DA, Bayrak-Toydemir P, Newcomb TM, Jorgensen EM, and Swoboda KJ. NALCN channelopathies: Distinguishing gain-of-function and loss-of-function mutations. *Neurology.* 2016.

113. Shamseldin HE, Faqeih E, Alasmari A, Zaki MS, Gleeson JG, and Alkuraya FS. Mutations in UNC80, Encoding Part of the UNC79-UNC80-NALCN Channel Complex, Cause Autosomal-Recessive Severe Infantile Encephalopathy. *Am J Hum Genet.* 2016;98(1):210-5.

114. Stray-Pedersen A, Cobben JM, Prescott TE, Lee S, Cang C, Aranda K, Ahmed S, Alders M, Gerstner T, Aslaksen K, et al. Biallelic Mutations in UNC80 Cause Persistent Hypotonia, Encephalopathy, Growth Retardation, and Severe Intellectual Disability. *Am J Hum Genet.* 2016;98(1):202-9.

115. Perez Y, Kadir R, Volodarsky M, Noyman I, Flusser H, Shorer Z, Gradstein L, Birnbaum RY, and Birk OS. UNC80 mutation causes a syndrome of hypotonia, severe intellectual disability, dyskinesia and dysmorphism, similar to that caused by mutations in its interacting cation channel NALCN. *J Med Genet.* 2016;53(6):397-402.

116. Kim BJ, Chang IY, Choi S, Jun JY, Jeon JH, Xu WX, Kwon YK, Ren D, and So I. Involvement of Na(+)-leak channel in substance P-induced depolarization of pacemaking activity in interstitial cells of Cajal. *Cell Physiol Biochem.* 2012;29(3-4):501-10.

117. Sinke AP, Caputo C, Tsaih SW, Yuan R, Ren D, Deen PM, and Korstanje R. Genetic analysis of mouse strains with variable serum sodium concentrations identifies the Nalcn

sodium channel as a novel player in osmoregulation. *Physiol Genomics.* 2011;43(5):265-70.

Chapter 2: Sodium Leak Channel, Non-selective (NALCN) Contributes to the Leak Current in Human Myometrial Smooth Muscle Cells from Pregnant Women.

Erin L. Reinl[1], Rafael Cabeza[2], Ismail A. Gregory[1], Alison G. Cahill[1], and Sarah K. England[1]*

[1]Department of Obstetrics and Gynecology, Basic Science Division, Washington University in St. Louis School of Medicine, St. Louis, MO 63110

[2]Department of Molecular Physiology and Biophysics, University of Iowa, Iowa City, IA 52442

The majority of this chapter was published in *Molecular Human Reproduction*, 2015 Oct;21(10):816-24.

2.1 Introduction

Regulation of uterine contractile frequency and intensity is essential for several functions of the female reproductive tract, including implantation of the embryo, transport of sperm for fertilization, and formation of contractile waves associated with the menstrual cycle (1). Most notably, the contractile state of the uterus must be tightly regulated throughout pregnancy; the uterus must remain quiescent during pregnancy to foster growth of the fetus, become activated at term to produce forceful, coordinated, and rhythmic contractions to deliver the infant, and finally involute to return to its pre-pregnancy state.

The myometrial smooth muscle cell (MSMC) action potential underlies control of uterine contractions, with the phasic and regenerative depolarization and repolarization of the MSMC membrane resulting in rhythmic, spontaneous contractions. The depolarizing upstroke is predominantly due to Ca^{2+} influx, which is modulated, in large part, by activation of L-type calcium channels. The roles of Ca^{2+} in mediating the membrane potential and providing a contractile signal for electromechanical coupling have been well characterized (2). Recent evidence has revealed that a large milieu of ion channels underlie the electrical activity of MSMCs (3), indicating the complexity of signals that must function coordinately to keep MSMCs in a pro- or anti-contractile state. However, the currents that depolarize the membrane to the extent required for L-type calcium channel activation have not been fully elucidated.

An important contributor to cell excitability is the action of a non-selective cationic leak current, defined as a non-gated, or constitutively active, flow of cations across the cell membrane with a reversal potential nearing 0 mV under physiological ion concentrations. For example, in the sinoatrial node of the heart, the inwardly rectifying K^+ channels and the hyperpolarization-activated 'funny' current provide a coordinated leak of cations into cardiomyocytes to produce pacemaker activity (4-6). Similarly, the rhythmic firing of dopaminergic neurons of the ventral tegmental area of the brain is modulated by a tetrodotoxin-insensitive Na^+-leak current (7).

Working with rat MSMCs, Miyoshi *et al.* (8) observed a leak current that displayed a Na^+-dependent conductance and was sensitive to inhibition by the trivalent cation gadolinium (Gd^{3+}) (IC_{50} of 3.0 μM). No such leak current has yet been identified in the human myometrium. Furthermore, the specific ion channels that drive this current remain to be identified. RNA sequencing data from human myometrial tissue revealed the expression of a channel with leak-distinctive features, the Na^+ leak channel, non-selective (NALCN) (3). This channel is a

member of the 4x6 transmembrane domain family, which includes voltage-gated Ca^{2+} and voltage-gated Na^{+} channels (9-11). Studies of NALCN in heterologous expression systems, mice, *C. elegans*, *L. stagnalis,* and *D. melanogaster* nervous systems have demonstrated that, unlike other members of its family, NALCN is voltage-insensitive and contains a non-selective pore domain, allowing it to conduct Na^{+}, Ca^{2+}, K^{+}, and Cs^{+} (9, 12-15). In addition to its canonical form, NALCN has several alternatively spliced isoforms with undescribed functions (15, 16). NALCN is sensitive to inhibition by Gd^{3+} (IC_{50} of 1.4 μM) (9, 17, 18) and has properties similar to the current described in the rat myometrium (8).

By conducting a leak current, NALCN has a profound effect on excitable cells. NALCN mediates the slow influx of Na^{+} into the cell, bringing the resting membrane potential closer to the threshold for action potential generation (9, 12, 14). This characteristic allows it to drive rhythmic processes including respiratory rhythm, gastro-intestinal contractility, and circadian behavior (9, 13, 19), making it a strong candidate for the regulation of uterine activity. On the basis of evidence that NALCN mRNA is expressed in the human myometrium and its role in conducting an excitatory leak current in multiple rhythmic cell types, we hypothesized that the NALCN channel is expressed in the human myometrium and contributes to a cationic leak current in MSMCs. We addressed our hypothesis by using electrophysiology and RNAi technology in freshly isolated and cultured MSMCs from pregnant women at term. We report that human MSMCs have a Na^{+}-dependent, Gd^{3+}-sensitive leak current that is dependent on NALCN expression. The discovery of NALCN expression and activity in the myometrium has implications for the modulation of uterine contractility and reproductive function in women.

2.2 Materials and Methods

2.2.1 Ethical Approval and Acquisition of Human Samples

Human myometrial tissue from the lower uterine segment was obtained from 23 non-laboring women who underwent Cesarean hysterotomy under regional anesthesia in late pregnancy (term non-labor [TNL]; 37-40 weeks of gestation). The indications for Cesarean were placenta previa (1 woman), non-reassuring fetal status (1), breech presentation (1), previous delivery with shoulder dystocia (2), hip replacement (1), and previous Cesarean section (17). None of the women reported having contractions, and no contraction-altering drugs were given. Before the procedure, a clinical research nurse coordinator in the Department of Obstetrics and Gynecology at Washington University School of Medicine explained details of the biopsy procedure to the subjects and obtained signed written consent forms approved by the Washington University in St. Louis Human Research Protection Office (IRB 201108143). The subject population was approximately 50% African American and 50% Caucasian. Nine of the 23 women reported an underlying health problem(s), including mental illness (3 women, 1 of whom was taking medication), hypotension (1), gestational hypertension (1), history of syncopal episode (1), Bell's Palsy (1), morbid obesity (1), rheumatoid arthritis (1), and an ovarian cyst (1). Additionally, one woman's fetus was large for gestational age, and another woman's fetus presented with intrauterine growth restriction. None of the data acquired from samples from women with underlying disease was outside the normal range, and analysis was done blinded to underlying conditions. Samples were stored in ice-cold phosphate buffered saline (PBS) and processed for explant expansion and smooth muscle cell isolation within 90 min of acquisition. Samples used for RNA extraction were collected in RNA*later*® (Ambion, Austin, TX, USA) and stored at -20°C within 30 min of acquisition. Samples used for membrane preparations were flash frozen in liquid nitrogen and stored at -80°C within 90 minutes of acquisition. Samples

obtained from at least three women were used for each experiment.

2.2.2 Cell Isolation

Freshly isolated human myometrial smooth muscle cells (hMSMCs) were isolated from myometrial samples according to previously described methods (20) with minor modifications. Briefly, samples were cut into pieces ~2 – 4 mm^2 and digested with 1 mg/ml collagenase IA (Sigma, St. Louis, MO, USA) and 1 mg/ml collagenase XI (Sigma) in DMEM F-12 media (Ref. 11039, Gibco, Grand Island, NY, USA) containing 0.1% BSA (Sigma) and 25 μg/ml gentamicin (Gibco) for 40 min at 37°C. Digested tissue was strained through a 40-μm cell strainer, washed twice with DMEM F-12 containing 10% FBS (Ref. 26140, Gibco) and 25 μg/ml gentamicin (standard media), and then plated onto a six-well plate in DMEM F-12 containing 5% FBS and 25 μg/ml gentamicin. Freshly isolated cells were used within 3 and 22 hours after tissue biopsy.

Cultured hMSMCs from TNL explants were expanded within 2 h of biopsy in DMEM F-12 medium supplemented with 5% FBS, 2 ng/ml basic fibroblast growth factor (Lonza, Allendale, NJ, USA), 3 ng/ml epithelial growth factor (Lonza), 25 μg/ml gentamicin, 5 μg/ml fungizone (Gibco), and 5 μg/ml insulin (Sigma). Cells were maintained in standard media and used at passage four. Immunoblotting confirmed that NALCN expression was maintained through this passage. Quantitative RT-PCR showed that NALCN expression was higher in passage four than in passage one.

2.2.3 Electrophysiology

Cells were plated directly or trypsinized and transferred to glass coverslips, and electrophysiological measurements were made within 4 h. Cultured hMSMCs were serum starved in 0.5% FBS-containing media for 20 – 24 h before electrophysiology experiments were performed. Glass pipettes were pulled and polished to 2.5 – 5 MΩ and filled with a pipette

solution containing 125 mM Cs-Aspartate, 20 mM tetraethylammonium (TEA)-Cl, 5 mM Mg-ATP, 5 mM EGTA, 100 nM free Ca^{2+} (calculated with Maxchelator software [Stanford University]), and 10 mM HEPES, pH 7.2. Currents were measured in an extracellular bath solution containing: 125 mM NaCl or N-methyl-D-glucamine (NMDG), 20 mM TEA-Cl, 0.1 mM $MgCl_2$, 5 mM HEPES, 11 mM glucose, 1 μM $CaCl_2$, and 5 μM nifedipine, pH 7.4. K^+ was replaced with Cs^+. TEA-Cl and nifedipine were added to the bath solution to isolate the leak current by blocking voltage-gated K^+ and Ca^{2+} channels, respectively. Leak currents were recorded at a sampling rate of 10 kHz and filtered at 1 kHz by using an Axopatch 200B amplifier (Molecular Devices, Sunnyvale, CA, USA). Cells were held at 0 mV and currents were elicited by stepping from -55 mV (50 ms) to +40 mV for 100 ms (to inactivate voltage-gated Ca^{2+} and K^+ channels) followed by 20 mV steps (500 ms) from -100 mV to +100 mV using the pClamp 10 software (Molecular Devices). Currents were normalized to cell capacitance, and the mean and standard error of the mean (SEM) of the current density were calculated for each group of samples. Normalized conductance was determined by calculating the slope of the linear regression for currents elicited by voltages between -100 mV and -20 mV, as this was the most linear part of the currents. Reversal potentials were similarly determined by calculating the X-intercept of the linear regressions and calculating the mean ± SEM.

2.2.4 RNA Isolation and RT-PCR

Total RNA was isolated from myometrial biopsies by using the Aurum Total RNA Fatty and Fibrous Tissue Pack Kit (BioRad, Hercules, CA, USA) and reverse transcribed to generate cDNA by using the iScript cDNA Synthesis Kit (BioRad) according to the manufacturer's instructions. cDNA was stored at -20°C until PCR was performed. Forty-cycle PCR was performed on cDNA by using Taq PCR Master Mix (2X) (Affymetrix, Santa Clara, CA, USA)

and primers (Table I) specific to NALCN, UNC80, UNC79, or NLF-1 (Integrated DNA Technologies, Coralville, IA, USA). Products were electrophoresed on a 1.5% agarose gel.

2.2.5 RNAi Lentiviral Transduction

Replication-deficient lentiviruses were packaged by the England lab or by the HOPE Center Viral Vectors Core at Washington University in St. Louis. The lentiviral vector, pLVTHM, was a gift from Arnaud Monteil (18). The encoded shRNA target sequences were designed by an Ambion algorithm to be specific to NALCN and have no more than 70% coverage with any other part of the human transcriptome. The target sequences are reported in Table I. hMSMCs were incubated with half the normal flask volume (6 ml for a T-75, 1 ml for a 6-well plate) of standard media containing 8 μg/ml polybrene for 10-15 min before adding viral particles. Transductions took place over 16 h, after which media was replaced with standard media. Only cells expressing GFP (co-expressed by the viral vector and confirmed by fluorescence microscopy) were used for electrophysiological measurements. For analysis of knockdown, an MOI that generated 85% – 95% GFP-positive cells (confirmed by flow cytometry 48 h after transduction) was used. Cells were used 6-8 days post-transduction for electrophysiology and 6-20 days post-transduction for qRT-PCR and western blot analyses.

Table 2.1 DNA Primer and shRNA Target Sequences.

Primer Name	Sequence
NALCN_F	ACCATGGGTTCACTCTTTGC
NALCN_R	TGCTATCATCTCTGCCGTGT
UNC80_F	TCAGTCTGGTCAGTGCGTTC
UNC80_R	ACCTCACCATCCTCCATCAG
UNC79_F	TGGACCACAATTAGCAACCA
UNC79_R	CCAGGTAGGCCAGAGTGAAG
NLF-1a_F	CACAGGACATCGCTCACAGT
NLF-1a_R	TTTCTTCCAGCGTGTTGAT
SDHA_F	CAAACAGGAACCCGAGGTTTT
SDHA_R	ATACAGCATGTGTTACCAAGCTG
TOP1_F	CCAGACGGAAGCTCGGAAAC
TOP1_R	TTCAAGATAGAGCCTCCTGGAC
shRNA Name	**Target Sequence**
shNALCN*	AATGTATGACATAACCCAGCA
shScrambled*	GCTCAGTACGATCATACTCAC

*Previously published in Swayne *et al.* (2009)

2.2.6 Quantitative RT-PCR

RNA was extracted from stored human myometrial tissue, or hMSMCs 6-9 days after transduction with lentiviral vectors. RNA quality was ensured by gel electrophoresis analysis and 260/280 nm and 260/230 nm absorbance ratios above 1.8 and 2.0, respectively. qRT-PCR reactions (20 μl) contained 5 pmol of each forward and reverse primer (Table I), cDNA produced from 50 ng of RNA, and iQ SYBR Green Supermix (BioRad). Gene targets were amplified and quantified by the CFX96 BioRad Real-Time PCR Detection System. The temperature cycles were as follows: 95°C for 3 min (1X), and 95°C for 10s followed by 57°C for 30s (40X), ending with a 0.5°C increment melt curve from 65°C to 95°C. Primer efficiencies were ≥ 77% with human brain cDNA, and the calculated efficiency values were used in Pfaffl analysis of relative gene expression (21). Target gene expression was normalized to the reference genes topoisomerase I (TOP1) and succinate dehydrogenase complex, subunit A (SDHA), chosen because of their consistency of expression in the myometrium across pregnancy (22).

2.2.7 Immunoblot

For lysis of cultured hMSMCs, media was aspirated from the cells, and they were washed with cold DPBS. Cells were then scraped into ice-cold lysis buffer containing: 10 mM Tris-Cl, 150 mM NaCl, 1% Triton X-100, and a Complete Mini Protease Inhibitor Cocktail pellet (EDTA-free, Roche Molecular Biochemicals, Indianapolis, IN, USA), pH 8.0. Cells were then homogenized with 0.1-mm glass beads by using the Next Advance Bullet Blender (Averill Park, NY, USA). Homogenates were separated by centrifugation at 9,000 *g* for 20 min at 4°C. For preparation of human myometrium cell membranes, flash frozen tissue was finely chopped and then homogenized by a Tekmar Tissumizer (Cincinnati, OH) in membrane preparation solution containing: 250 mM sucrose, 50 mM MOPS, 2 mM EDTA, 2 mM EGTA, pH7.4, 1 mM PMSF,

and a Complete Mini Protease Inhibitor Cocktail pellet (EDTA-free). Non-homogenized tissue was removed by centrifugation at 14,000 *g* for 15 min. Cell membranes were isolated from the supernatant by ultracentrifugation at 100,000 *g* for 1 h. Membrane pellets were dissolved in lysis buffer for 2 h. Any remaining insoluble components were removed by centrifugation at 9,000 *g* for 20 min. All steps were performed at 4°C with ice-cold buffers to prevent proteins from degrading.

Protein concentrations of whole cell lysates and membrane preparations were measured by using a bicinchoninic acid protein assay kit (Pierce, Rockford, IL, USA). Protein samples were mixed with Laemmli sample buffer, heated to 65°C for 15 min, and stored at -20°C. Protein samples (40 μg for myometrium, and 10 μg for mouse brain) were separated by SDS-PAGE and transferred to a nitrocellulose membrane. After blocking in PBS containing 0.075% Tween-20 (PBST) and 5% milk, membranes were probed with the following primary antibodies: anti-NALCN N-20 (1:500; Santa Cruz Biotechnologies, Inc., Santa Cruz, CA, USA) in the presence or absence of the NALCN N20 antigenic peptide (1 μg/ml), anti-GAPDH (1:1000; Millipore, Billerica, MA, USA), or anti-transferrin receptor (1:500; Invitrogen, Camarillo, CA, USA). Blots were then probed with HRP-conjugated secondary antibodies (1:4000; Jackson ImmunoResearch Laboratory Inc., West Grove, PA, USA) in PBST containing 3% milk. Signal was detected with Clarity ECL Western chemiluminescence (BioRad). NALCN expression was normalized to GAPDH by using ImageJ densitometry, and values from shNALCN-treated cells were compared to those from shScr-treated cells.

2.2.8 Statistical Analysis

All data are presented as mean ± SEM. Statistical significance was determined by one-tailed Student's t-test (two groups), one- or two-way ANOVA (three or more groups) correcting

for multiple comparisons by using GraphPad Prism 6 (San Diego, CA, USA), and $P < 0.05$ was considered significant. N refers to number of cells, and n refers to the number of patient samples tested.

2.3 Results

2.3.1 The Na^+-dependent, Gd^{3+}-sensitive Leak Current in hMSMCs

To determine whether a leak current is expressed in the human myometrium, whole-cell voltage clamp experiments were performed on freshly isolated human myometrial smooth muscle cells (hMSMCs) from uterine samples from non-laboring women who had Cesarean sections at full term. An ohmic leak current with a reversal potential of 21.8 ± 9.2 mV was identified (Fig. 2.1.A, C, and Table 2.2). Adding 10 μM Gd^{3+} (a concentration known to inhibit NALCN currents by ~80%)(Lu, et al., 2007) to the bath solution significantly reduced the average conductance of this current by 75% and shifted the reversal potential to +88 mV (Table 2.2), indicating the presence of a Gd^{3+}-sensitive current in freshly isolated cells. Although freshly isolated hMSMCs are optimal for characterizing myometrial cell biology, they cannot be used for repeated and longer-term experiments. The same whole-cell voltage clamp experiments revealed that, qualitatively, cultured hMSMCs behaved like freshly isolated hMSMCs (Fig. 2.1.B, D, and F). As in freshly isolated hMSMCs, currents elicited in cultured cells at -60 mV, near the resting membrane potential, were significantly inhibited by addition of Gd^{3+} (Fig. 2.1.E).

To elucidate the predominant cation contributing to the current in cultured hMSMCs, Na^+ in the bath solution was replaced with the channel-impermeable monovalent cation, NMDG. This reduced the conductance (Fig. 2.2.A, B, Table 2.2) to a similar extent as addition of Gd^{3+} (Fig. 2.1.D). As anticipated, the reversal potential with NMDG was similar to control (unlike the

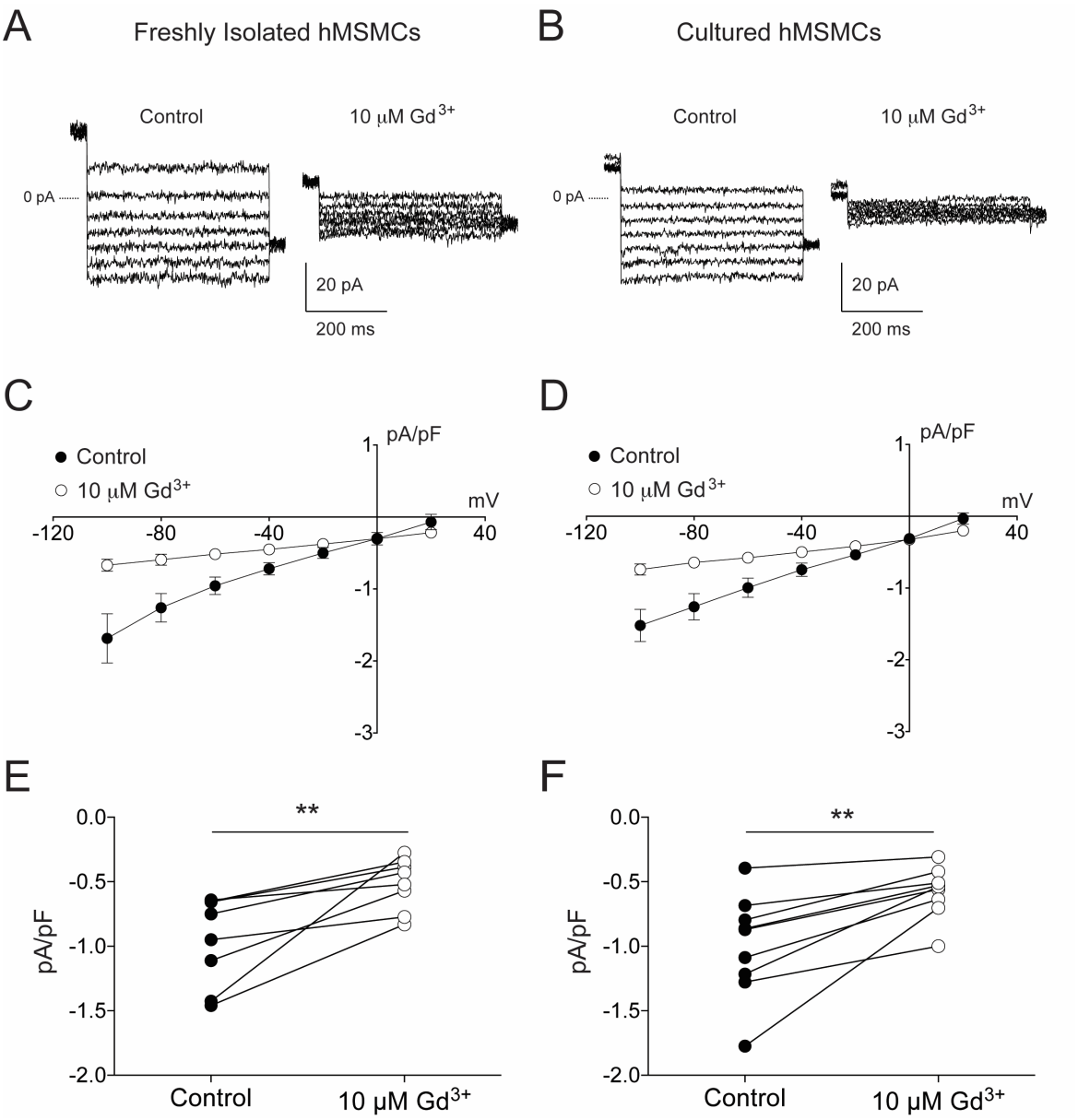

Figure 2.1 The Gd^{3+}-sensitive leak current in freshly isolated and cultured hMSMCs.
A and B) Representative traces of leak current evoked from a freshly isolated hMSMC (A) and a cultured hMSMC (B) by using a voltage step protocol with 20 mV increments from -100 mV to +20 mV, before and after treatment with 10 μM Gd^{3+}. Capacitive currents were removed from these traces. C and D) Current-voltage relationships obtained from freshly isolated (C, N = 7) and cultured (D, N = 7) hMSMCs before (closed circles) and after (open circles) treatment with 10 μM Gd^{3+}. Data is presented as mean values ± SEM. E and F) Current density analysis from freshly isolated (E) and cultured (F) hMSMCs at -60 mV before and after treatment with 10 μM Gd^{3+}. Symbols represent individual cells, and connecting lines link values in the same cell before and after treatment with Gd^{3+}. ** $P = 0.0039$ (E) and $P = 0.0020$ (F).

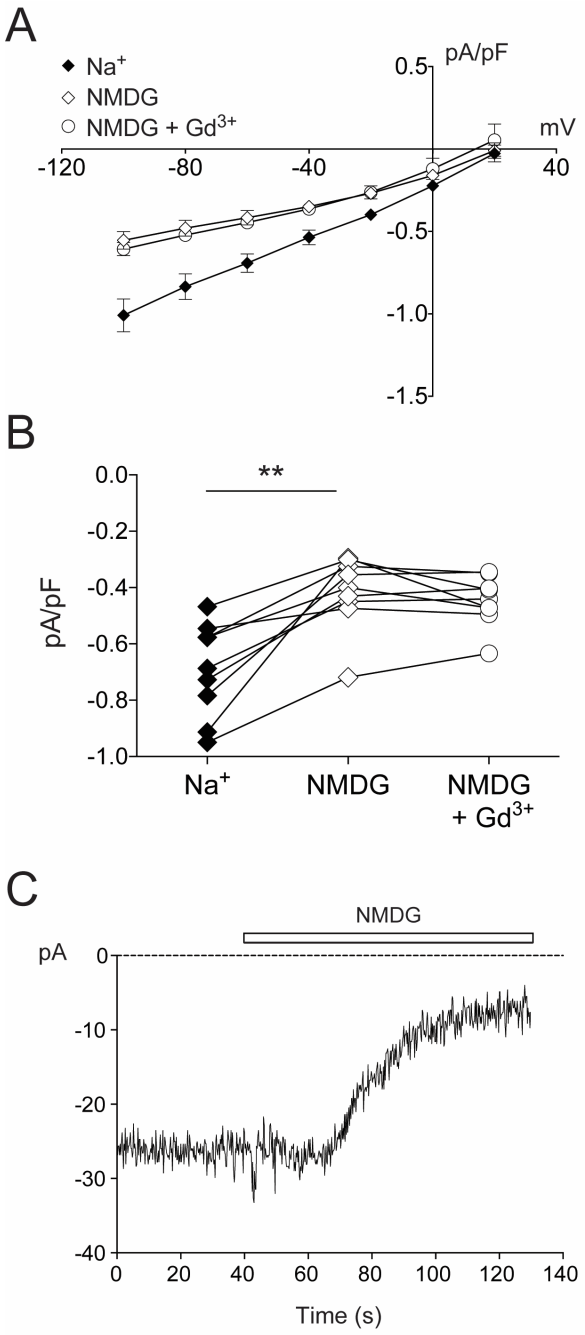

Figure 2.2 The Na^+-dependent leak current in cultured hMSMCs.
A) Current-voltage relationship observed in cultured hMSMCs superfused with bath solution containing 125 mM Na^+ (closed diamonds) and replaced with 125 mM NMDG (open diamonds) and 125 mM NMDG + 10 μM Gd^{3+} (open circles) (N = 9). Data is presented as mean values ± SEM. B) Current density analysis at -60 mV from voltage step protocol in *A* before (Na^+, closed diamonds) and after perfusion with NMDG (open diamonds) and NMDG + Gd^{3+} (open circles) (N = 9). Symbols represent individual cells, and connecting lines link values before and after each treatment. ** $P = 0.0020$. C) Representative current from a cultured hMSMC clamped at -60 mV. Na^+-containing bath solution was replaced with NMDG-containing solution at the indicated time.

Table 2.2. Summary of Leak Current Parameters in hMSMCs.

Treatment (n)	Calculated Reversal Potential (mV)	Normalized Conductance (pS/pF)	Current Density[#] (pA/pF)
Freshly Isolated Cells (11)	21.8 ± 9.2	14.6 ± 4.0	-0.96 ± 0.12
+ 10 μM Gd^{3+}	88.0 ± 17.1**	3.6 ± 0.5**	-0.52 ± 0.07**
Cultured Cells (18)	31.7 ± 4.3	10.0 ± 1.3	-0.84 ± 0.08
+ 10 μM Gd^{3+} (9)	86.1 ± 6.5**	4.0 ± 0.5**	-0.56 ± 0.04**
NMDG (9)	66.6 ± 12.9**	3.5 ± 0.4**	-0.42 ± 0.04**
shScr (11)	16.8 ± 5.1	9.4 ± 1.6	-0.64 ± 0.07
+ 10 μM Gd^{3+}	57.7 ± 11.8[b]	2.7 ± 0.5[b]	-0.28 ± 0.03[b]
shNALCN (9)	28.9 ± 5.2	5.9 ± 0.8[a]	-0.51 ± 0.04
+ 10 μM Gd^{3+}	75.6 ±13.0[b]	2.6 ± 0.5[b]	-0.30 ± 0.03[b]

Mean values ± SEM. [#] Calculated at -60 mV.

* P <0.05 and ** P < 0.01 from paired Student's t-Test comparing before and after treatment with Gd^{3+} or NMDG-containing solution.
[a] P < 0.05 from multiple-comparisons two-way ANOVA between shScr and shNALCN groups.
[b] P < 0.01 from matched, multiple-comparisons two-way ANOVA between before and after treatment with Gd^{3+}.

large positive shift seen with Gd^{3+} treatment [Fig. 1D]), indicating that Na^+ replacement significantly inhibited the inward portion of the leak current (Fig. 2.2.A). To determine the extent to which the leak current was active at a physiologically relevant membrane potential, currents were recorded while holding cultured hMSMCs at -60 mV (Fig. 2.2.C) (23). Although Na^+-dependent current density varied noticeably between individual hMSMCs, replacement with NMDG resulted in a significant reduction of the average current density elicited at -60 mV (Fig. 2.2.B and Table 2.2). Finally, to determine the extent to which Na^+ drives the Gd^{3+}-sensitive current, 10 μM Gd^{3+} was added to the NMDG superperfusate, and any further reduction in the current density was analyzed (Figs. 2.2.B). Gd^{3+} did not significantly inhibit the leak current any further, indicating that Na^+ is the major cation driving the Gd^{3+}-sensitive inward current. Overall, these data suggest that the Gd^{3+}-sensitive current in cultured hMSMCs is largely driven by Na^+ conductance.

2.3.2 NALCN Expression in the Human Myometrium

Given that NALCN conducts a Na^+-dependent, Gd^{3+}-sensitive leak current and, like the myometrial leak current, can be modulated by G-protein coupled receptor (GPCR)-mediated signaling (17, 18, 24-26), NALCN was a prime candidate for the specific ion channel that conducts the myometrial leak current. To assess this possibility, NALCN expression was assessed in the human myometrium. NALCN mRNA expression was detected in uterine tissue from pregnant term non-laboring (TNL) women by using non-quantitative RT-PCR (Fig. 2.3.A). Protein expression of NALCN was confirmed in TNL myometrial tissue by immunoblot (Fig. 2.3.B). In hippocampal and ventral tegmental area neurons in the mouse and premotor interneurons in nematodes, modulation of NALCN by GPCRs requires the presence of two

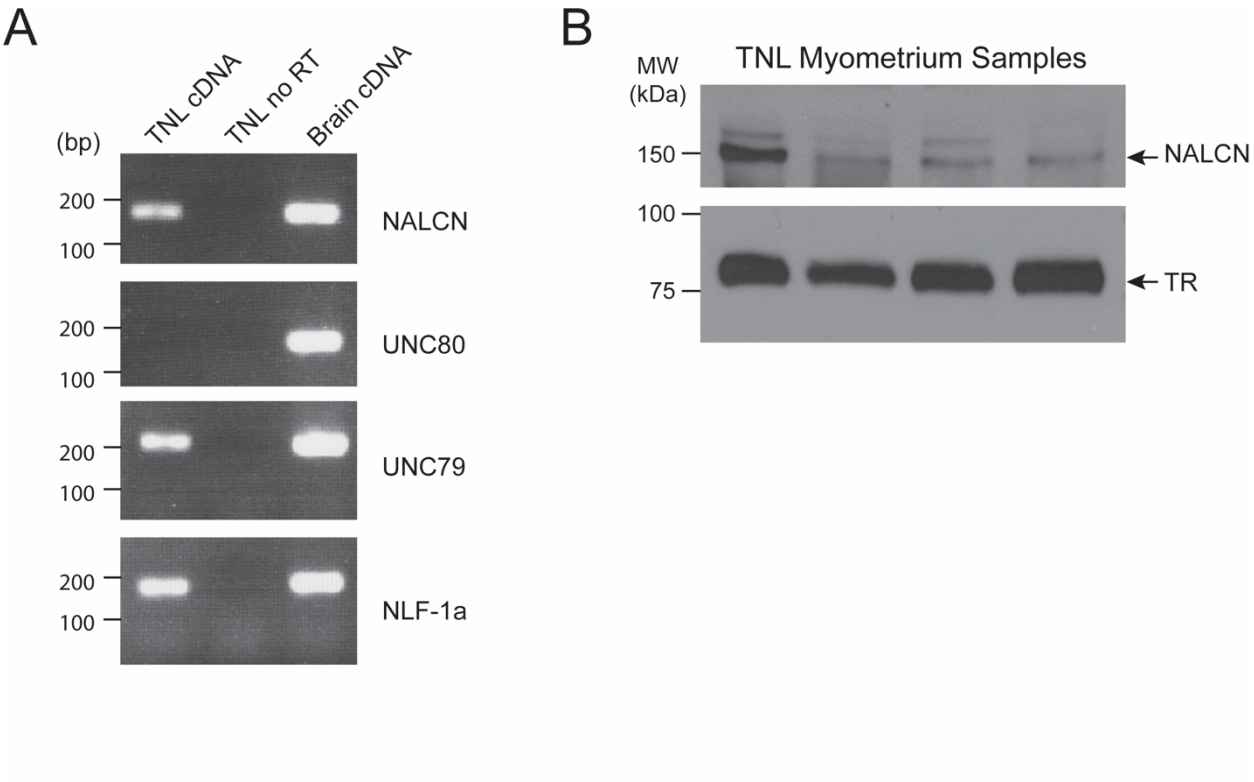

Figure 2.3 mRNA and protein expression of NALCN in human myometrium.
A) Representative RT-PCR of NALCN complex subunits (UNC79, UNC80, and NLF-1a) from human myometrial samples from four pregnant term non-labor (TNL) women. Negative (no reverse transcriptase [RT]) and positive (human brain cDNA) controls are also shown. B) Representative immunoblot of NALCN from TNL human myometrial sample membrane preparations from four different women. A mouse brain (msBr) membrane preparation served as a positive control. Transferrin receptor (TR) served as a loading control.

putative scaffolding proteins, UNC80 and UNC79, and a localization factor (NLF-1) (14, 17, 25, 27) (Fig. 2.3.B). Non-quantitative RT-PCR showed that whereas UNC79 and NLF-1a were expressed in TNL human myometrial tissue, UNC80 was not (Fig. 2.3.A). However, UNC80 expression was detected in uterine tissue from non-pregnant women (data not shown).

Many genes are regulated with the onset of labor, thus it was hypothesized that as an excitatory protein, NALCN expression would be upregulated with labor. Quantitative RT-PCR of NALCN from human myometrium samples from preterm, not in labor (PTNL), preterm, in labor (PTL), term, not in labor (TNL), and term, in labor (TL) women revealed a range of variability, but no significant change in NALCN mRNA levels at any stage (Fig. 2.4).

2.3.3 The Effect of NALCN Knockdown

Importantly, Gd^{3+} has many ion channel targets (28, 29) and, to date, no specific blockers of NALCN exist. Thus, to assess the contribution of NALCN to the leak current in hMSMCs, shRNAs were used to knock down its expression. Cultured hMSMCs were transduced with lentiviral vectors expressing shRNAs that target all isoforms of NALCN. NALCN mRNA was decreased by 50%, and protein expression was reduced by 80%-90% (Figs. 2.5.A and B); the level of transcript knockdown matches that previously observed by Swayne *et al*. (2009). NALCN levels did not notably differ between cells treated with transduction additive, polybrene, alone and those transduced with shScr (Fig. 2.5.B). Cells in which NALCN expression was reduced with shRNAs had 37% lower average leak current conductance and 20% lower average leak current density at -60 mV than control cells (Fig. 2.5.C and Table II). However, knockdown by shNALCN did not reduce the current to the same extent as 10 μM Gd^{3+}. Importantly, Gd^{3+} does not completely abolish the leak current, likely because Gd^{3+}-insensitive channels contribute to the current or inherent leak exists in the patch clamp seal. Therefore, the contribution of

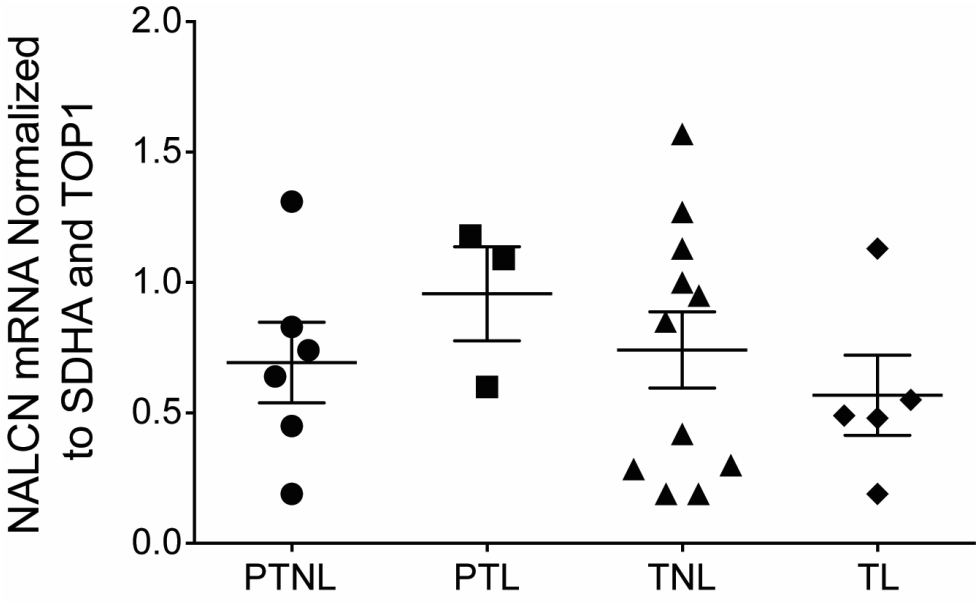

Figure 2.4 Normalized NALCN mRNA levels in the human myometrium.
Analyzed by qRT-PCR. Preterm, non-labor (PTNL), preterm, in labor (PTL), term, non-labor (TNL), and term, in labor (TL). SDHA and TOP1 were used as the reference genes.

NALCN to the Gd^{3+}-sensitive leak current alone can be calculated by subtracting the Gd^{3+}-insensitive current. Doing this revealed that NALCN knockdown reduced the Gd^{3+}-sensitive current density at -60 mV by an average of 42% (Fig. 2.5.D). Taken together, these data are consistent with the notion that NALCN significantly contributes to the Na^{+}-dependent, Gd^{3+}-sensitive leak current in cultured hMSMCs.

2.4 Discussion

Uterine contractions are regulated by the coordination of depolarizing and repolarizing currents mediated by ion channel activity. Here, we present the identification of a likely source of myometrial excitation – a cationic leak current. This current was Gd^{3+}-sensitive, Na^{+}-dependent, and present in both freshly isolated and cultured hMSMCs. This is the first demonstration that NALCN is expressed in the human myometrium and that its expression significantly contributes to the leak current. Notably, knockdown of NALCN expression significantly reduced the leak current at a physiologically relevant membrane potential of -60 mV.

We found that NALCN-targeting shRNAs were able to reduce the Gd^{3+}-sensitive conductance by 42% in hMSMCs. This substantial reduction indicates a significant contribution by NALCN to the leak current. Nonetheless, NALCN knockdown did not abolish the leak current in hMSMCs. Although it is possible that the remaining ~10 - 20% of NALCN channels were capable of carrying 58% of the cell's leak current, it is more likely that the remaining Gd^{3+}-sensitive (and also Na^{+}-dependent) current is driven by additional channels that contribute to the leak current in MSMCs. For example, several transient receptor potential channels, which are sensitive to inhibition by Gd^{3+}, have been described to contribute to MSMC currents (30-33). Additionally, Gd^{3+} and NMDG have recently been shown to block non-specific leak currents in

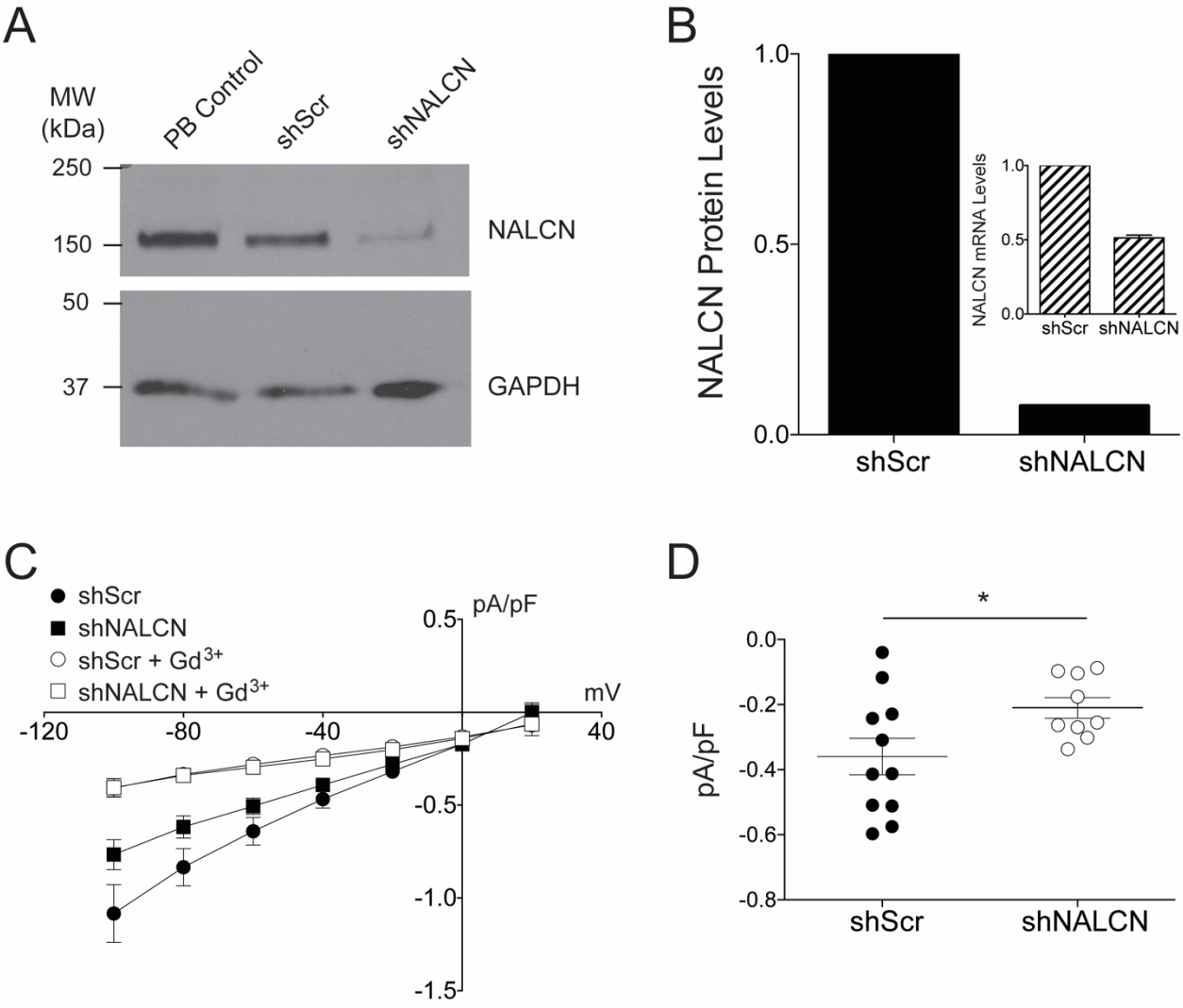

Figure 2.5 The contribution of NALCN to the Gd^{3+}-sensitive leak current in hMSMCs.
A) qRT-PCR analysis of NALCN mRNA levels after transduction with shRNAs. Bars represent the mean values ± SEM. Levels were normalized to SDHA and TOP1 and compared to scrambled shRNA (shScr) levels (n = 3). B) Quantification of NALCN protein expression from immunoblots of cultured hMSMCs treated with polybrene alone or transduced with lentiviruses expressing shScr or NALCN-targeting shRNA (shNALCN). Bars represent the mean values ± SEM, normalized to shScr levels (n = 4). Inset shows a representative immunoblot. GAPDH served as loading control. C) Current-voltage relationships obtained from cultured hMSMCs transduced with shRNAs before and after treatment with 10 μM Gd^{3+}. Symbols represent mean values ± SEM (N = 9-11). D) Gd^{3+}-sensitive current density analysis at -60 mV. Symbols represent individual cells. Lines represent mean values ± SEM. * $P = 0.0401$.

whole-cell recordings with poor seal quality of less than 1 GΩ (34). However, we assured membrane seals of ≥ 1 GΩ in our experiments and therefore conclude that the inhibition observed by treatment with Gd^{3+} and removal of Na^{+} from the bath solution is channel specific.

The low level of NALCN activity observed in hMSMCs could also be due to the fact that the uterine tissue we used was biopsied from the lower uterine segment. This segment of the uterus has been shown to be less contractile than the uterine fundus (35, 36) and may express fewer excitatory ion channels such as NALCN. Furthermore, we did not detect mRNA expression in TNL myometrium of an important NALCN complex subunit, UNC80. This finding is consistent with an observation that HEK293 cells have NALCN leak activity in the absence of UNC80 co-expression (9). Therefore, although GPCR-mediated modulation of NALCN activity requires UNC80 expression, baseline NALCN leak activity appears to function independent of canonical UNC80. Controversy exists in the field as to whether NALCN is a true leak channel or is an agonist-induced (through GPCRs) non-selective, voltage-insensitive channel. Although our work indicates that NALCN functions as a leak channel in MSMCs, MSMCs may express low-level constitutive GPCR activity that keeps NALCN active in these cells, as discussed by Swayne *et al.* (18). Acetylcholine and substance P, two agonists that increase uterine contractility, have been shown to activate NALCN in neurons, pancreatic β cells, and interstitial cells of Cajal (18, 19, 24-26, 37-39). Thus, the involvement of NALCN in agonist-induced contractility is an important subject for future research.

Establishing the source of a non-selective leak current in the human myometrium fills an important knowledge gap in the field of myometrial physiology. Clues to the existence of this current have been reported over the last several decades. Miyoshi *et al.* described a Na^{+}-dependent Gd^{3+}-sensitive leak current in the rat myometrium in 2003, but the channel conducting

this current had not yet been identified. In 1971, Anderson *et al*. described a transient Na^+- and Ca^{2+}-conducting current in the rat myometrium that they hypothesized to be due to a single channel (40). They found that a low concentration of extracellular Ca^{2+} enhanced the leak current and that the membrane potential was reduced by nearly 10 mV in a Na^+-free solution. NALCN is a good candidate to generate this current as this channel is activated by low extracellular Ca^{2+} through its regulation by the Ca^{2+}-sensing receptor (17) and drives Na^+-dependent membrane depolarization (9). Studies also suggest that uterotonins such as acetylcholine increase the rate of membrane depolarization and increase the frequency of action potentials in the myometrium (24, 26). Given that NALCN can be activated by acetylcholine through muscarinic receptor 3 in pancreatic beta cells (18), NALCN may play roles not only in spontaneous MSMC activity, but also in agonist-induced myometrial excitability.

Through its effect on resting membrane potential, NALCN has been linked to the regulation of rhythmic activity and overall membrane excitability in a variety of biological systems (9, 12-14, 19). The discovery of its activity in the myometrium could have implications for all stages of reproduction, including sperm transport, embryo implantation, embryonic gestation, and parturition. These processes require a range of activity, including complete quiescence, subtle directional peristalsis, and rhythmic, maximal force contractions of the uterus. Considering NALCN's effect on excitability, it is reasonable to hypothesize that altering NALCN expression or activity could significantly alter the contractile state of the uterus. In fact, the resting membrane potential of the human uterus changes throughout gestation (23) and likely drives the unique contraction phenotype of each phase. Thus, an important next step will be to measure NALCN's contribution to the resting membrane potential and overall uterine excitability.

2.5 Acknowledgements

We thank Dr. Arnaud Monteil for the gift of the viral vectors, critical review of the manuscript, and helpful discussions. We also thank Dr. Ramon Lorca and Dr. Deborah Frank for critical review of the manuscript and the Clinical Research Nurses in the Department of Obstetrics and Gynecology for consenting patients and acquiring myometrial biopsies.

2.6 References

1. Fanchin R, and Ayoubi JM. Uterine dynamics: impact on the human reproduction process. *Reproductive biomedicine online.* 2009;18 Suppl 2(57-62).

2. Berridge MJ. Smooth muscle cell calcium activation mechanisms. *J Physiol.* 2008;586(Pt 21):5047-61.

3. Chan YW, van den Berg HA, Moore JD, Quenby S, and Blanks AM. Assessment of myometrial transcriptome changes associated with spontaneous human labour by high‐throughput RNA‐seq. *Experimental physiology.* 2014;99(3):510-24.

4. DiFrancesco D. The role of the funny current in pacemaker activity. *Circulation research.* 2010;106(3):434-46.

5. DiFrancesco D. A new interpretation of the pace-maker current in calf Purkinje fibres. *J Physiol.* 1981;314(359-76).

6. Nichols CG, Makhina EN, Pearson WL, Sha Q, and Lopatin AN. Inward rectification and implications for cardiac excitability. *Circulation research.* 1996;78(1):1-7.

7. Khaliq ZM, and Bean BP. Pacemaking in Dopaminergic Ventral Tegmental Area Neurons: Depolarizing Drive from Background and Voltage-Dependent Sodium Conductances. *The Journal of Neuroscience.* 2010;30(21):7401-13.

8. Miyoshi H, Yamaoka K, Garfield RE, and Ohama K. Identification of a non-selective cation channel current in myometrial cells isolated from pregnant rats. *Pflugers Arch.* 2004;447(4):457-64.

9. Lu B, Su Y, Das S, Liu J, Xia J, and Ren D. The Neuronal Channel NALCN Contributes Resting Sodium Permeability and Is Required for Normal Respiratory Rhythm. *Cell.* 2007;129(2):371-83.

10. Yu FH, and Catterall WA. The VGL-chanome: a protein superfamily specialized for electrical signaling and ionic homeostasis. *Science's STKE : signal transduction knowledge environment.* 2004;2004(253):re15.

11. Lee JH, Cribbs LL, and Perez-Reyes E. Cloning of a novel four repeat protein related to voltage-gated sodium and calcium channels. *FEBS Lett.* 1999;445(2-3):231-6.

12. Lu TZ, and Feng Z-P. A Sodium Leak Current Regulates Pacemaker Activity of Adult Central Pattern Generator Neurons in *Lymnaea Stagnalis*. *PLoS ONE.* 2011;6(4):e18745.

13. Lear BC, Lin JM, Keath JR, McGill JJ, Raman IM, and Allada R. The ion channel narrow abdomen is critical for neural output of the Drosophila circadian pacemaker. *Neuron.* 2005;48(6):965-76.

14. Yeh E, Ng S, Zhang M, Bouhours M, Wang Y, Wang M, Hung W, Aoyagi K, Melnik-Martinez K, Li M, et al. A putative cation channel, NCA-1, and a novel protein, UNC-80, transmit neuronal activity in C. elegans. *PLoS Biol.* 2008;6(3):e55.

15. Senatore A, Monteil A, van Minnen J, Smit AB, and Spafford JD. NALCN Ion Channels Have Alternative Selectivity Filters Resembling Calcium Channels or Sodium Channels. *PLoS One.* 2013;8(1):e55088.

16. Cochet-Bissuel M, Lory P, and Monteil A. The sodium leak channel, NALCN, in health and disease. *Frontiers in cellular neuroscience.* 2014;8(132).

17. Lu B, Zhang Q, Wang H, Wang Y, Nakayama M, and Ren D. Extracellular calcium controls background current and neuronal excitability via an UNC79-UNC80-NALCN cation channel complex. *Neuron.* 2010;68(3):488-99.

18. Swayne LA, Mezghrani A, Varrault A, Chemin J, Bertrand G, Dalle S, Bourinet E, Lory P, Miller RJ, Nargeot J, et al. The NALCN ion channel is activated by M3 muscarinic receptors in a pancreatic beta-cell line. *EMBO Rep.* 2009;10(8):873-80.

19. Kim BJ, Chang IY, Choi S, Jun JY, Jeon JH, Xu WX, Kwon YK, Ren D, and So I. Involvement of Na(+)-leak channel in substance P-induced depolarization of pacemaking activity in interstitial cells of Cajal. *Cell Physiol Biochem.* 2012;29(3-4):501-10.

20. Tribe RM, Moriarty P, and Poston L. Calcium Homeostatic Pathways Change with Gestation in Human Myometrium. *Biol Reprod.* 2000;63(3):748-55.

21. Pfaffl MW. A new mathematical model for relative quantification in real-time RT-PCR. *Nucleic acids research.* 2001;29(9):e45.

22. Rosenbaum ST, Svalo J, Nielsen K, Larsen T, Jorgensen JC, and Bouchelouche P. Immunolocalization and expression of small-conductance calcium-activated potassium channels in human myometrium. *J Cell Mol Med.* 2012.

23. Parkington HC, Tonta MA, Brennecke SP, and Coleman HA. Contractile activity, membrane potential, and cytoplasmic calcium in human uterine smooth muscle in the third trimester of pregnancy and during labor. *Am J Obstet Gynecol.* 1999;181(6):1445-51.

24. Lodge S, and Sproat JE. Resting membrane potentials of pacemaker and non pacemaker areas in rat uterus. *Life Sci.* 1981;28(20):2251-6.

25. Lu B, Su Y, Das S, Wang H, Wang Y, Liu J, and Ren D. Peptide neurotransmitters activate a cation channel complex of NALCN and UNC-80. *Nature.* 2009;457(7230):741-4.

26. Marshall JM. Effects of estrogen and progesterone on single uterine muscle fibers in the rat. *Am J Physiol.* 1959;197(935-42).

27. Xie L, Gao S, Alcaire Salvador M, Aoyagi K, Wang Y, Griffin Jennifer K, Stagljar I, Nagamatsu S, and Zhen M. NLF-1 Delivers a Sodium Leak Channel to Regulate Neuronal Excitability and Modulate Rhythmic Locomotion. *Neuron.* 2013;77(6):1069-82.

28. Lacampagne A, Gannier F, Argibay J, Garnier D, and Le Guennec JY. The stretch-activated ion channel blocker gadolinium also blocks L-type calcium channels in isolated ventricular myocytes of the guinea-pig. *Biochimica et biophysica acta.* 1994;1191(1):205-8.

29. Yang XC, and Sachs F. Block of stretch-activated ion channels in Xenopus oocytes by gadolinium and calcium ions. *Science.* 1989;243(4894 Pt 1):1068-71.

30. Murtazina DA, Chung D, Ulloa A, Bryan E, Galan HL, and Sanborn BM. TRPC1, STIM1, and ORAI influence signal-regulated intracellular and endoplasmic reticulum calcium dynamics in human myometrial cells. *Biol Reprod.* 2011;85(2):315-26.

31. Shlykov SG, Yang M, Alcorn JL, and Sanborn BM. Capacitative cation entry in human myometrial cells and augmentation by hTrpC3 overexpression. *Biol Reprod.* 2003;69(2):647-55.

32. Dalrymple A, Slater DM, Beech D, Poston L, and Tribe RM. Molecular identification and localization of Trp homologues, putative calcium channels, in pregnant human uterus. *Mol Hum Reprod.* 2002;8(10):946-51.

33. Dalrymple A, Mahn K, Poston L, Songu-Mize E, and Tribe RM. Mechanical stretch regulates TRPC expression and calcium entry in human myometrial smooth muscle cells. *Mol Hum Reprod.* 2007;13(3):171-9.

34. Boone AN, Senatore A, Chemin J, Monteil A, and Spafford JD. Gd3+ and Calcium Sensitive, Sodium Leak Currents Are Features of Weak Membrane-Glass Seals in Patch Clamp Recordings. *PLoS One.* 2014;9(6):e98808.

35. Crane LH, and Martin L. In vivo myometrial activity during early pregnancy and pseudopregnancy in the rat. *Reproduction, fertility, and development.* 1991;3(3):233-44.

36. Fuchs AR. Uterine activity in late pregnancy and during parturition in the rat. *Biol Reprod.* 1969;1(4):344-53.

37. Patak EN, Ziccone S, Story ME, Fleming AJ, Lilley A, and Pennefather JN. Activation of neurokinin NK(2) receptors by tachykinin peptides causes contraction of uterus in pregnant women near term. *Mol Hum Reprod.* 2000;6(6):549-54.

38. Kitazawa T, Hirama R, Masunaga K, Nakamura T, Asakawa K, Cao J, Teraoka H, Unno T, Komori S, Yamada M, et al. Muscarinic receptor subtypes involved in carbachol-induced contraction of mouse uterine smooth muscle. *Naunyn Schmiedebergs Arch Pharmacol.* 2008;377(4-6):503-13.

39. Kitazawa T, Uchiyama F, Hirose K, and Taneike T. Characterization of the muscarinic receptor subtype that mediates the contractile response of acetylcholine in the swine myometrium. *European journal of pharmacology.* 1999;367(2-3):325-34.

40. Anderson NC, Ramon F, and Snyder A. Studies on Calcium and Sodium in Uterine Smooth Muscle Excitation under Current-Clamp and Voltage-Clamp Conditions. *J Gen Physiol.* 1971;58(3):322-39.

Chapter 3: Na^+-Leak Channel, Non-Selective Modulates Uterine Excitability and Labor Efficiency

Erin L. Reinl[1], Xiaofeng Ma[1], Wenjie Wu[1], Chinwendu Amazu[1], Rachael Bok[2], K. Joseph Hurt[2], Yong Wang[1], and Sarah K. England[1]

[1] Department of Obstetrics and Gynecology, Center for Reproductive Health Sciences, Washington University in St. Louis School of Medicine, St. Louis, MO 63110

[2] Department of Obstetrics and Gynecology, Basic Reproductive Sciences and Maternal Fetal Medicine, University of Colorado School of Medicine, Aurora, CO 80045

3.1 Introduction

Uterine contractility is tightly regulated during pregnancy to ensure an appropriate length (>37 weeks) gestation and successful parturition. Throughout pregnancy, the uterus remains quiescent producing only asynchronous, regional contractions that permit development of the growing fetus. During parturition, uterine contractions increase in force, frequency, and synchrony to enable effective expulsion of the infant. The force and frequency of these contractions is an important feature monitored during labor, as measured by Montevideo units in humans. Excessive contractility or tachysystole, endangers both mother and fetus by increasing the risk for uterine rupture and insufficient placental perfusion. Conversely, dystocia or failure to progress through labor are some of the principal indications for caesarean sections (1, 2), which increase the incidence of severe maternal morbidity and the likelihood of placental

abnormalities in future pregnancies (3-5). As the caesarean section rate in the US (32%) (6) is nearly triple the recommended rate by the World Health Organization (10 – 15%) , it is imperative that we understand normal labor progress as a component of our effort to reduce the caesarean section rate. As part of that effort, there is also a need to better understand the basic molecular mechanisms behind normal labor, and specifically those that regulate contraction force and frequency.

Uterine contractions are myogenic and arise due to the underlying electrical activity of the MSMC. Although myogenic in nature, this electrical activity can be modulated by hormonal stimuli, and can occur, albeit with limited synchrony, at all stages of pregnancy (7-9). The electrical activity of the myometrium occurs through recurrent depolarization of the membrane potential that manifests as bursts of high frequency spikes, and this activity closely couples with the contractile activity. Over 50 years ago, Marshall demonstrated that the amplitude, frequency, and contraction duration correlates to the number of cells that are simultaneously active, their electrical burst frequency, and the duration of the bursts (10). Both Ca^{2+} and Na^{+} have been reported to contribute to the initiation of excitatory activity, although the role of Ca^{2+} has been better defined. Upon spontaneous or agonist-mediated depolarization of the plasma membrane, voltage-gated Ca^{2+} channels activate and mediate an influx of Ca^{2+}. The increase in intracellular Ca^{2+} results in Ca^{2+}-calmodulin binding and activates myosin light chain kinases to phosphorylate myosin, initiating actomyosin cross-bridge cycling and subsequent cell shortening. Bursts are terminated and muscle relaxation occurs when voltage-gated and Ca^{2+}-activated K^{+} channels become activated to repolarize the plasma membrane, and when Ca^{2+} is pumped out of the cell or into the intracellular stores via ATPase-mediated transport (11). To date, the bursting activity of MSMCs has been primarily attributed to the function of these Ca^{2+}

and K^+ channels. However, focusing on these channels alone leaves us with an incomplete understanding of the mechanisms which fine tune spike density and burst frequency, and therefore overall uterine contraction patterns.

We previously identified the expression and activity of a novel Na^+ leak channel in human MSMCs, called NALCN, that may contribute to fine tuning uterine excitability (12). NALCN is a tetrodotoxin-insensitive member of the 4x6 transmembrane domain family of voltage gated Ca^{2+} (Ca_v) and and Na^+ (Na_v) channels. Because NALCN lacks some of the charged residues in the would-be voltage sensing domain, NALCN is voltage insensitive (13). Additionally, NALCN's selectivity filter is a fusion of that found in Na_vs and Ca_vs, making NALCN a non-selective channel, allowing it to conduct $Na^+ > K^+ > Cs^+ > Ca^{2+}$ with decreasing permeability (13). Under physiological conditions, the driving force and greater Na^+ permeability pushes NALCN toward conducting a constitutive Na^+ leak current. Through its Na^+ leak activity, NALCN has been shown to be essential in depolarizing the membrane potential, promoting spontaneous firing, and sustaining rhythmic burst activity in other spontaneously active cells (13-16). Previously, Na^+ conductance in the myometrium had been hypothesized to play a limited role in MSMC excitability, as the presence and identity of tetrodotoxin (a blocker of fast Na^+ currents) -sensitive currents have not been clearly established in MSMCs (17, 18). However, historically Na^+ has been implicated as an important ion in regulating myometrial excitability (19-21). We hypothesized that the Na^+ leak activity of NALCN plays a critical role in regulating myometrial excitability throughout pregnancy, and therefore is an important factor in pregnancy and parturition outcomes.

To gain a better understanding of the role of myometrial NALCN across pregnancy and *in vivo*, we transitioned to the mouse model. We created a smooth muscle specific knockout

mouse model of NALCN (smNALCN$^{-/-}$) by crossing NALCN floxed mice with a myosin heavy chain 11 promoter driven Cre line (22). With these mice, we tested the function of NALCN in the myometrium on gestational length, labor efficiency, and uterine excitability.

3.2 Materials and Methods

3.2.1 Mice

All animal procedures complied with guidelines for the care and use of animals set forth by the National Institutes of Health. All protocols were approved by the Animal Studies Committee at Washington University in St. Louis. Wild type C57BL/6J mice were obtained from the Jackson Laboratory and bred in house. *NALCN$^{fx/fx}$* mice were a kind gift from Dr. Dejian Ren at the University of Pennsylvania. These mice, bred on a C57BL/6J background, contain loxP sites surrounding the fourth and fifth exons of NALCN, which when excised results in an early termination codon before the fourth transmembrane domain of the first homologous repeat (15). Female NALCN$^{fx/fx}$ mice were crossed with male myosin heavy chain 11 promoter driven Cre-eGFP mice (*smMHC$^{eGFP/Cre}$*) (22). The male *NALCN$^{fx/WT}$ smMHC$^{eGFP/Cre+/-}$* F1 offspring were crossed *NALCN$^{fx/fx}$* females to produce *NALCN$^{fx/fx}$ smMHC$^{eGFP/Cre+/-}$* (smNALCN$^{-/-}$), *NALCN$^{fx/WT}$ smMHC$^{eGFP/Cre+/-}$* (smNALCN$^{+/-}$), and *NALCN$^{fx/fx}$ smMHC$^{eGFP/Cre-/-}$* (flox control) F2 females that were used for parturition phenotyping. This breeding scheme was chosen to avoid the creation of global NALCN knockouts, as *smMHC$^{eGFP/Cre}$* females show aberrant Cre expression up to the early embryo stage. Male *smMHC$^{eGFP/Cre}$* gametes also express Cre during early spermatogenesis but it is lost before fertilization. However, for this reason, the flox control and smNALCN$^{-/-}$ females are also globally heterozygous for NALCN. Cre control mice used in parturition phenotyping were either F1 littermates, or were the offspring of *smMHC$^{eGFP/Cre}$* males crossed with wild type females.

K. Joseph Hurt generously gifted us with uterine tissue from pregnancy day 19.5 non-labor and laboring, and post-partum C57BL/6 mice. All protocols were approved by the University of Colorado Institutional Animal Care and Use Committee. These mice were obtained from Charles River Laboratories.

3.2.2 RNA Isolation and RT-PCR

Total RNA was extracted from flash frozen whole mouse uterine or brain tissue using the Aurum Total RNA Fatty and Fibrous Tissue Pack Kit (BioRad, Hercules, CA), and copy DNA was created using the iScript cDNA Synthesis Kit (BioRad), both according to manufacturer's instructions. PCR was performed to determine the presence of *NALCN* and other proteins with which it complexes, *UNC79, UNC80,* and *NLF-1* in mouse uterine tissue at different stages of pregnancy. PCR reactions included Taq PCR Master Mix (2X) (Affymetrix, Santa Clara, CA), gene specific primers (20 nM) (Table 3.1) (Integrated DNA Technologies, Coralville, IA), 0.5 μl DMSO and 2 μl cDNA per 25 μl reaction. Reverse transcriptase-free reactions were also performed to confirm the absence of genomic DNA contamination (data not shown). Reactions were run for one 5 min cycle at 95 °C, 40 cycles of one min at 95 °C / one min at 55 °C / one min at 72 °C, and one 5 min cycle at 72 °C. Results were electrophoresed on 1.5% agarose gels and visualized using GelRed Nucleic Acid Stain (Phenix Research Products, Candler, NC).

3.2.3 Quantitative Real Time PCR (qRT-PCR)

After dissection, mouse uterine tissue was immediately transferred into a vial of RNA*later*® (Thermo Fisher Scientific, Waltham, MA) and stored at -20 °C until ready for RNA extraction. RNA was extracted as detailed above, and quality was confirmed by 28S to 18S rRNA analysis via gel electrophoresis, and 260/280 nm and 260/230 nm absorbance ratios above 1.8 and 2.0, respectively. qRT-PCR reactions were performed in the same way as written in

chapter two. qRT-PCR reactions (20 µl) contained 5 pmol of each forward and reverse primer (Table 3.1), cDNA produced from 50 ng of RNA, and iQ SYBR Green Supermix (BioRad). Gene targets were amplified and quantified by the CFX96 BioRad Real-Time PCR Detection System. The temperature cycles were as follows: 95°C for 3 min (1X), and 95°C for 10s followed by 57°C for 30s (40X), ending with a 0.5°C increment melt curve from 65°C to 95°C. Primer efficiencies were ≥ 77% with mouse brain cDNA, and the calculated efficiency values were used in Pfaffl analysis of relative gene expression (23). Target gene expression was normalized to the reference genes topoisomerase I (TOP1) and succinate dehydrogenase complex, subunit A (SDHA), chosen because of their stable expression in the myometrium across pregnancy (24).

Table 3.1 DNA Primer Sequences.

Primer Name	Sequence
mNALCN_F	TTTCCCCGCTGGCGCTCCTA
mNALCN_R	ACCAGCTGCCAACCACCAGC
mUNC80_F	TGTCGAAGCTTCATGTCTGG
mUNC80_R	GCTGTGGTACATTCCGAGGT
mUNC79_F	GAGCGTTCACAAAGGAGAGG
mUNC79_R	GCTAGCTTGGTTCCAGCATC
mNLF-1a_F	TTGAAAGCGTGCTGCATAAG
mNLF-1a_R	GGGCAATATGAATGGACACC
mSDHA_F	GGAACACTCCAAAAACAGACCT
mSDHA_R	CCACCACTGGGTATTGAGTAGAA
mTOP1_F	AAGATCGAGAACACCGGCATA
mTOP1_R	CTTTTCCTCCTTCGGTCTTTCC

3.2.4 Membrane Preparations

Flash frozen mouse uterine or brain tissue was minced over ice, and transferred to ice cold membrane prep solution (250 mM sucrose, 50 mM MOPS, 2 mM EDTA, 2 mM EGTA, 1 mM PMSF, pH 7.4) containing cOmplete, Mini, EDTA-free Protease Inhibitor Cocktail (Roche, Indianapolis, IN). Tissue was homogenized using the BioGen PRO200 homogenizer (ProScientific, Oxford CT) at 4 °C. Lysate was spun at 14,000 ×*g* for 15 min, and supernatants were transferred to ice cold ultracentrifuge tubes. Samples were centrifuged at 100,000 ×*g* for one hour. Pellets were resuspended in 1% Triton lysis buffer (150 mM NaCl, 10 mM Tris, 1% Triton X-100, pH 8.0), and rotated for two hours or overnight (no noticeable difference) at 4 °C. Non-solubilized protein was removed via centrifugation at 9000 ×*g* for 20 min at 4 °C. Membrane prep protein concentration was quantified via Bicinchoninic Acid Kit for Protein Determination (Thermo Scientific).

3.2.5 Immunoblot

Immunoblots were performed in a similar fashion as in chapter 2. Protein samples were mixed with Laemmli sample buffer, heated to 65°C for 15 min, and stored at -20°C. Protein samples (40 μg for myometrium) were separated by 6% SDS-PAGE and transferred to a nitrocellulose membrane. After blocking in PBS containing 0.075% Tween-20 (PBST) and 5% milk, membranes were probed with the following primary antibodies: anti-NALCN N-20 (1:500; Santa Cruz Biotechnologies, Inc., Santa Cruz, CA, USA), anti-PDI (C81H6, Cell Signaling Technology, Danvers, MA), anti-GAPDH (1:1000; Millipore, Billerica, MA, USA), or anti-transferrin receptor (1:1000; 84036 Abcam, Cambridge, UK). Blots were then probed with HRP-conjugated secondary antibodies (1:4000; Jackson ImmunoResearch Laboratory Inc., West Grove, PA, USA) in PBST containing 3% milk. Signal was detected with Clarity ECL Western chemiluminescence (BioRad) and exposed onto film or viewed through a ChemiDoc MP

Imaging System (BioRad). NALCN expression was quantified and normalized to loading controls by using ImageJ densitometry.

3.2.6 Current Clamp

Mice were sacrificed between 9 and 11 am, their uteri were removed, and embryos were sacrificed. The uterus was dissected to obtain 1 cm long by 0.5 cm wide strips of longitudinal muscle from all uterine regions, excluding the mesometrial border, in cold Kreb's buffer (133 mM NaCl, 4.7 mM KCl, 11.1 mM glucose, 1.2 mM $MgSO_4$, 1.2 mM KH_2PO_4, 1.2 mM $CaCl_2$, 10 mM TES free acid, pH to 7.4 with NaOH). Muscle strips were maintained in ice cold Kreb's until experiments began (within six hours). For recordings, strips were pinned into a recording chamber on a Nikon Eclipse FN1, and superfused with warm (32 °C) Kreb's solution containing 5 μM wortmannin, to mechanically inhibit contractions while maintaining spontaneous electrical activity. Sharp glass electrodes with tip resistances between 40 mΩ and 110 mΩ were filled with 2 M KCl and used to impale the tissue once contractions had arrested (usually within 15 minutes). Membrane potential was recorded at a 1 kHz sampling rate using an Axon Multiclamp 700B amplifier and Axon Digidata 1550. Data was recorded through the pCLAMP 10.4 software. Burst duration (time between first and last peak (spike)), burst interval (time between last peak of the previous burst and first peak of the next burst), peaks per burst, and peak width were analyzed using a customized Matlab program on Matlab R2015b. In this program, we modified the 'find peaks' function to identify voltage peaks without the need to adjust for changes in baseline, or reduce noise. Peaks were defined by having a minimum prominence of 7 mV, and a minimum width of 20 ms. Clusters of peaks, or bursts, were defined by a minimum duration of 2000 ms, and a minimum interval of 4000 ms. For the across pregnancy data, representative ranges of four bursts and four intervals were selected from a representative

recording for each mouse, chosen by a technician blinded to the pregnancy stage. For the transgenic mouse experiments, all available burst data was analyzed and included in the summative data.

3.2.7 Parturition Phenotyping

Cre control, flox control, smNALCN$^{+/-}$, and smNALCN$^{-/-}$ female mice between the ages of seven weeks and six months were mated with WT C57BL/6J males ages eight weeks to eleven months, for two hours between 2:30 pm and 5:30 pm. At the end of the two-hour period, females were checked for the presence of a copulation plug. On days 17 or 18 of pregnancy, females were placed in individual cages in front of D-Link DCS-932L surveillance cameras (Taipei, Taiwan). Cameras capturing one frame/second began recording at 7pm on day 18 of pregnancy (P18) and were stopped after delivery was completed, or when the female was sacrificed. Dams were sacrificed due to painful delivery if they had not finished delivering by P22. Videos were watched to determine the timing of delivery of each pup. Gestation length was defined as the length of time between when the copulation plug was detected on day zero (about 5:30 pm) and when the first pup was delivered. If a female did not deliver, then the gestational length was taken as the time when she was sacrificed (no later than P22). Duration of labor was defined as the length of time between the delivery of the first and last pups, and adjusted labor duration was calculated by dividing the total labor duration by one less than the total number of pups delivered. Prolonged labor was defined as the adjusted labor taking longer than two standard deviations from the Cre control and flox control mice (>27.5 min). Labor was considered dysfunctional when a dam was unable to deliver her entire litter by P22. Litter size included all fully grown pups or embryos, alive or dead at term or at pregnancy day 19 (P19), i.e.

early pregnancy fetal demises (*in utero* clots) were not counted. Pup weights were taken within 26 hours of birth.

3.2.8 Staging Diestrus

Mice in the diestrus stage of the estrus cycle were identified using previously described methods (25). Briefly, between 2:00 pm and 4:00 pm daily, DPBS vaginal lavages were performed and streaked out on glass slides. Slides were stained with Crystal Violet (Sigma-Aldrich, St. Louis, MO) and visualized on a Leica ICC50 upright microscope. Lavages consisting primarily of leukocytes were considered to be from females in diestrus. Females in diestrus were sacrificed between 3:30 and 5:00 pm and their uteri removed and flash frozen.

3.2.9 MSMC Isolation

Uterine longitudinal muscle was dissected from the same P19 flox control and smNALCN$^{-/-}$ mice used in the sharp electrode experiments. The muscle was dissected in cold DPBS (Gibco, Grand Island, NY), and cut into ~3 mm x 8 mm strips. About 10 – 15 strips were used per experiment. MSMCs were isolated according to previously described methods (26). Tissue was incubated at room temperature in two ml of 0.1% BSA (Research Products International, Mt Prospect, IL) containing dissociation solution (145 mM NaCl, 4 mM KCl, 10 mM HEPES, 10 mM glucose, 0.05 mM $CaCl_2$, 1 mM $MgCl_2$, pH to 7.4 with NaOH) for 10 min. It was then transferred to dissociation solution containing 0.1% BSA, 1.5 mg/ml papain (Worthington, Lakewood, NJ), and 1 mg/ml dithioerythritol (Sigma-Aldrich, St. Louis, MO) at 37 °C for 15 min with occasional mixing. It was then transferred to dissociation solution containing 1.5 mg/ml collagenase blend type H (Sigma, St. Louis, MO), 1 mg/ml soybean trypsin inhibitor (Worthington), and 0.5 mg/ml elastase (Worthington) for 5 min at 37 °C and 2

min on ice. Tissue was transferred to cold dissociation solution, dispersed by gentle pipetting, and transferred to 8 mm coverslips. Cells were kept at 4 °C for 90 minutes before recording.

3.2.10 Whole Cell Voltage Clamp

Coverslips were transferred to a recording chamber containing room temperature bath solution designed to isolate the leak current (125.4 mM NaCl or N-methyl-D-glucamine, 20 mM TEA-Cl, 0.1 mM $MgCl_2$, 5 mM HEPES, 11 mM glucose, 1 μM $CaCl_2$, and 5 μM nifedipine, pH 7.4 (12, 27). TEA and nifedipine were included to inhibit the major contributing K^+ and voltage-gated Ca^{2+} currents in MSMCs. Glass electrodes with resistances between 2 mΩ and 6 mΩ were filled with intracellular solution containing 125 mM Cs-Aspartate, 20 mM TEA-Cl, 5 mM Mg-ATP, 5 mM EGTA, 100 nM free $CaCl_2$, and 10 mM HEPES, pH 7.2. Currents were measured in response to a voltage step protocol in which the holding potential of -55 mV was raised to +40 mV for 100 ms (to inactivate voltage-gated Ca^{2+}-channels), followed by 20 mV, 500 ms voltage steps from 100 mV to +40 mV. Currents were normalized to the cell's average capacitance. The current to voltage relationship was plotted, and the slope of the linear regression from -100 mV to -20 mV was calculated. Slopes that did not reduce by >25% by treatment with 10 μM Gd^{3+} were considered Gd^{3+}-insensitive and excluded from final analysis. Normalized conductance was determined by calculating the slope of the linear regression for currents elicited by voltages between -100 mV and -20 mV, as this was the most linear part of the currents. Reversal potentials were similarly determined by calculating the X-intercept of the linear regressions and calculating the mean ± SEM.

3.2.11 Statistical Analysis

Data comparing more than one group with one dependent variable was analyzed using Kruskal-Wallis one-way ANOVA. Individual differences were further assessed by Dunn's

multiple comparisons test. Experiments with only two groups were compared using Mann Whitney student's t-test. Statistics were done with GraphPad Prism 6 (San Diego, CA, USA) software. Those with P values < 0.05 were considered significant.

3.3 Results

3.3.1 NALCN Expression in the Mouse Uterus

Previously, we have shown that NALCN mRNA and protein are expressed in human myometrium, where it conducts a leak current (12) . In order to better understand the function of NALCN in myometrial physiology and pregnancy outcomes, we elected to use a mouse model of pregnancy. First, to determine whether NALCN is expressed in the mouse uterus, we performed non-quantitative, reverse-transcriptase PCR of NALCN and its complex components, UNC79, UNC80, and NLF-1a, from mouse uterine tissue across pregnancy (Fig 3.1.A). All members of the NALCN complex were present in whole mouse uteri from every stage of pregnancy (non-pregnant (NP), day 14 of pregnancy (P14), day 18 of pregnancy (P18), and day 19 of pregnancy (P19)), though the presence of UNC80 was variable in P19 samples. Quantitative real-time PCR showed that NALCN mRNA levels were attenuated mid-pregnancy, however this did not reach significance (Fig 3.1.B). However, western blot analysis of membrane preparations of mouse uteri taken from mice at different stages of pregnancy showed high levels of NALCN in NP and early pregnant mice (P7 and P10), and showed a decrease in late pregnancy (P14 and P18) (Fig 3.1.C and D). At term (P19) NALCN levels begin to increase again, and they increase further post-partum day 0.5 (PP0.5). Western blot analysis of uterine tissue from a separate pool of P19 mice that were either not in labor or in labor, or within one day post-partum (PP0.5), showed that NALCN levels increased during labor and were significantly different between non-labor and PP0.5. This indicates that NALCN levels increase for labor, and remain high during the highly

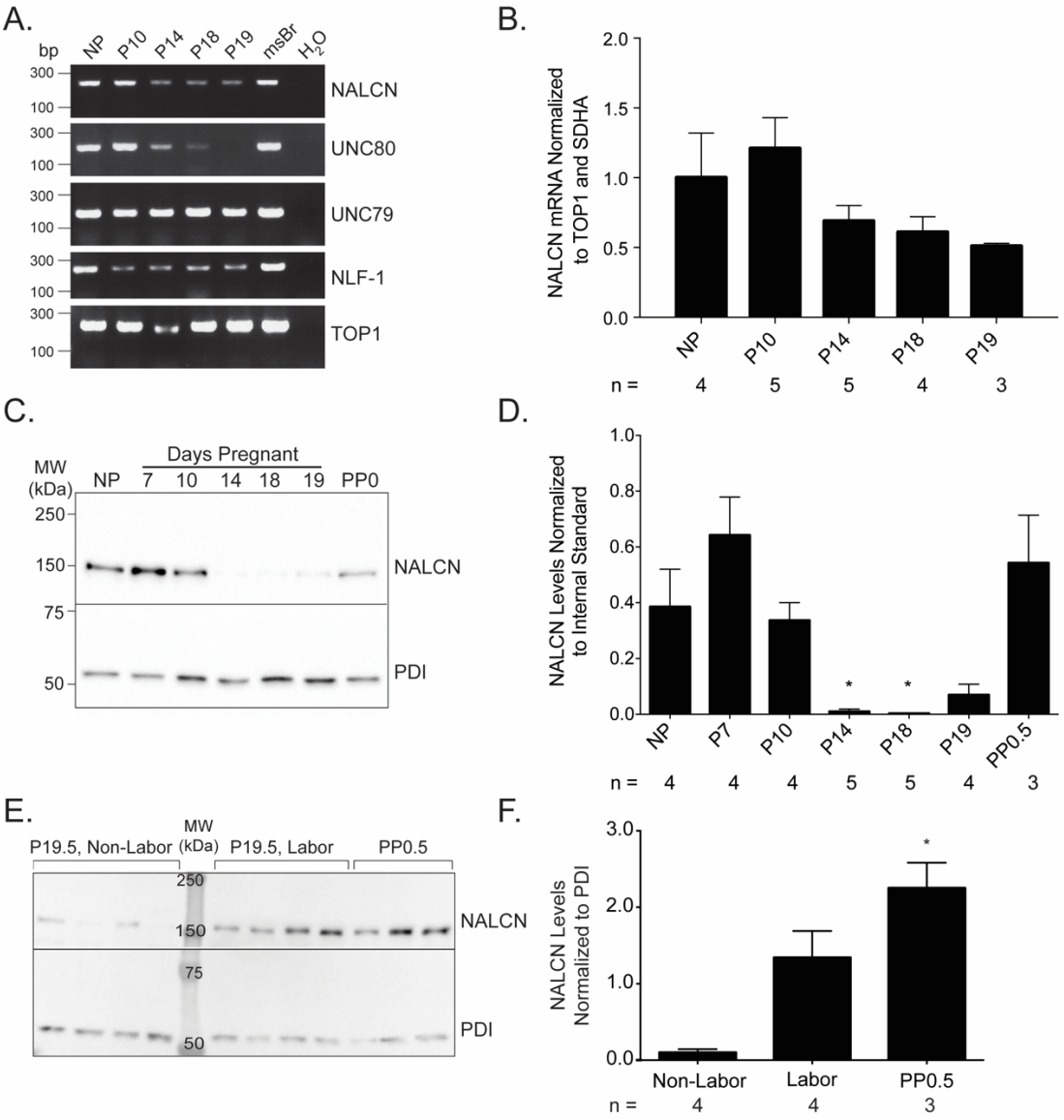

Figure 3.1 NALCN levels throughout pregnancy and post-partum.
A) Reverse transcriptase PCR of NALCN and members of its complex (UNC80, UNC79, and NLF-1a) in the non-pregnant (NP), and pregnant day 10, 14, 18, and 19 mouse uterus. Mouse brain cDNA and water are included as positive and negative controls, respectively. B) Average of qRT-PCR analyses of NALCN mRNA in the mouse uterus across pregnancy. TOP1 and SDHA were included as reference genes. C) Representative western blot of NALCN protein levels across pregnancy in the mouse uterus. PDI is the loading control. D) Quantification of NALCN protein levels in mouse uterine membrane preparations from across pregnancy. NALCN levels were normalized to an internal standard. One-way ANOVA $P < 0.01$, multiple comparisons show P14 and P18 are different from P7 (* $P < 0.05$). E) Western blot of NALCN from mouse uterine membrane preparations of mice at term non-labor, term in labor, and post-partum day 0.5 (PP0.5). F) Quantification of NALCN levels from western blot in (D). PP0.5 is significantly different from non-labor. One-way ANOVA $P < 0.01$, multiple comparisons show non-labor significantly less than PP0.5 (* $P < 0.05$). B, D, and F, n values are printed below the bars.

contractile post-partum estrogen surge.

3.3.2 Myometrial Excitability Throughout Pregnancy

We next sought to investigate whether the changes in NALCN expression that were observed across pregnancy correspond with changes in uterine excitability. To address this question, we performed sharp electrode current clamp experiments on mouse uterine longitudinal muscle to assess electrical activity across pregnancy. These recordings demonstrate the pattern of spontaneous bursts over time (Fig 3.2.A). From these recordings we analyzed the burst duration (time between first spike and last spike of a burst), burst interval (time between last spike of one burst and first spike of the next burst), the number of spikes per burst, and the spike density within each burst. We hypothesized that during stages of pregnancy with higher NALCN expression we would see shorter inter-burst intervals (i.e. higher frequency bursting), and a greater spike density, which would enable more frequent and forceful contractions. P18 myometrium showed a significantly prolonged average burst interval compared to P7 myometrium (Table 3.3, Fig 3.2.B). Interestingly, the burst interval shortened again at term (P19), and was not significantly different from P7. This correlates with high NALCN in the P7 uterus, low levels at P18, and intermediate levels at P19. Unlike burst interval, burst duration increased steadily throughout pregnancy (Table 3.3, Fig 3.2.C). Bursts were significantly longer in duration in P14, P18, and P19 myometrium compared to P7. Interestingly, this does not follow the same pattern as NALCN expression, however, there are many other ion channels important for burst duration which also change expression throughout pregnancy (28-33). Finally, we assessed the number of spikes per burst and normalized these to the burst duration to determine the spike density (spikes/s) (Table 3.3, Fig 3.2.D and E). We saw a high spike

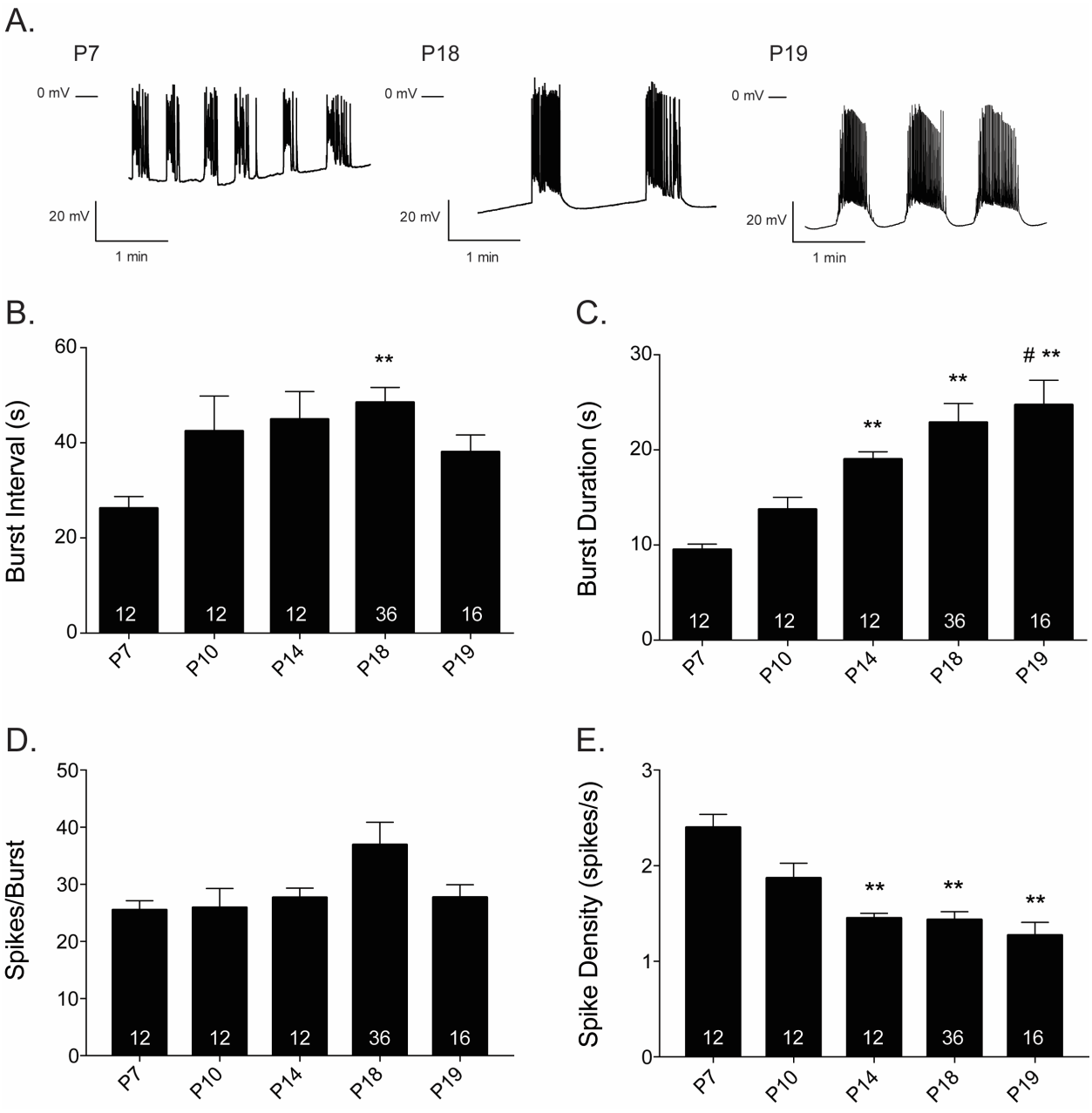

Figure 3.2 Myometrial excitability from across mouse pregnancy.
A) Representative membrane potential traces from P7, P18, and P19. B) Average burst interval from across pregnancy. One-way ANOVA $P < 0.01$, multiple comparisons analysis shows P18 is significantly longer than P7, (** $P < 0.01$. C) Average burst duration from across pregnancy. One-way ANOVA $P < 0.01$, and multiple comparisons analysis shows P14, P18, and P19 are significantly longer than P7 (** $P < 0.01$), and P19 is also significantly longer than P10 (# $P < 0.05$). D) Average spikes per burst from throughout pregnancy. E) Average spike density from throughout pregnancy. One-way ANOVA $P < 0.001$, and multiple comparisons analysis shows P14, P18, and P19 are significantly shorter than P7 (** $P < 0.01$). B – D, n values are printed on the bars.

density at P7 and lower densities at P14, P18, and P19. Although we expected that if NALCN increases the frequency of spikes, then spike density would be highest in P7 and reduced in P14 and P18 when NALCN levels are low, we also expected spike density to increase from P18 to P19. These data suggest that changing NALCN levels may be important for uterine excitability. However, the concurrent regulation of other ion channels across pregnancy, and the lack of an NALCN specific blocker made it difficult to assess the role of NALCN in wild type uteri, and led us to pursue a uterine specific NALCN knockout mouse.

3.3.3 NALCN Smooth Muscle Knockout Mouse (smNALCN$^{-/-}$)

To examine the role of NALCN in modulating myometrial burst activity and the effect that this may have on pregnancy outcomes, we created a smooth muscle specific, NALCN knockout mouse. We crossed the myosin heavy chain-11 promoter driven Cre-IRES-eGFP mouse (smMHC$^{eGFP/Cre}$) (upon recommendation by Francisco DeMayo) with an NALCN$^{fx/fx}$ mouse to create smNALCN$^{-/-}$ mice (Fig 2.3.A) (15, 22). NALCN has not been reported in association with any vascular or severe gastrointestinal phenotypes, and we did not observe any significant non-reproductive phenotypes. Through western blot analysis and fluorescent microscopy, we observed that the myometrial smooth muscle of smNALCN$^{-/-}$ mice expressed GFP, and therefore were also expressing Cre recombinase (Fig 3.3.B and D). Western blot analysis of uterine membrane preparations from non-pregnant mice in the diestrus stage showed a reduction of NALCN expression in smNALCN$^{-/-}$ mice compared to flox controls, although it was incomplete and variable (Fig 3.3.D). Incomplete knockout due to variable Cre expression across smooth muscle cells has been demonstrated before with this Cre line (34). Another likely cause for the incomplete knockout of NALCN in the uterus is because there is remaining NALCN expression in the endometrium. Some ion channels, particularly those involved in

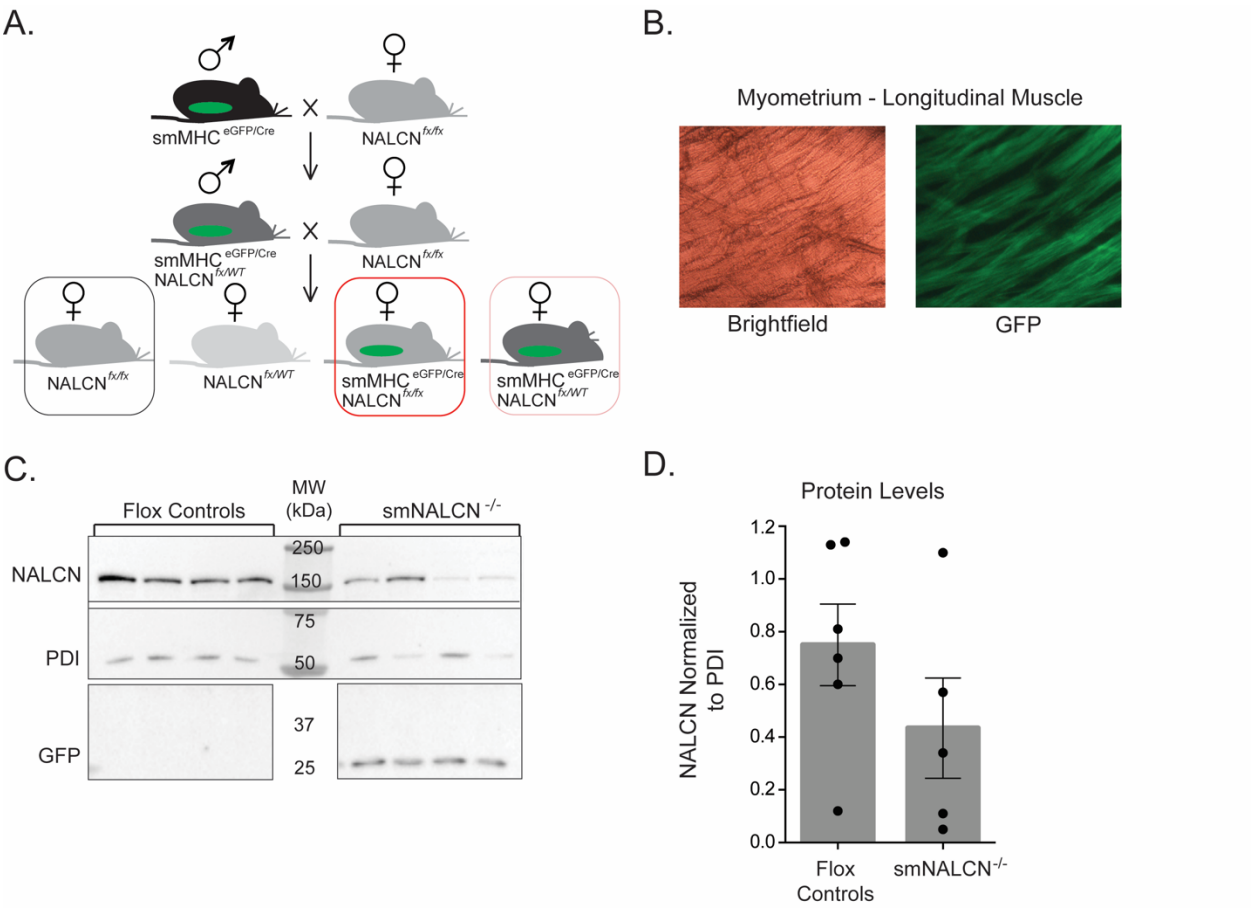

Figure 3.3 Development of the smNALCN$^{-/-}$ mouse.
A) SmMHC$^{eGFP/Cre}$ males were crossed with NALCN$^{fx/fx}$ to produce smNALCN$^{+/-}$ offspring. These males were crossed with NALCN$^{fx/fx}$ females to create the F2 females examined in this study, including flox controls (black box), smNALCN$^{-/-}$ (red box), and smNALCN$^{+/-}$ (pink box). B) Confirmation of GFP expression in the uterine longitudinal muscle of smNALCN$^{-/-}$ uterus. C) Representative western blot of NALCN levels in flox control and smNALCN$^{-/-}$ diestrus uterus. D) Quantification of NALCN levels normalized to PDI.

osmoregulation as NALCN has been reported to be have been identified in the endometrium (35). Additionally, the smNALCN$^{-/-}$ mice used in these experiments were sacrificed after their first or second parity, and had less severe parturition outcomes. Thus, a greater reduction may be observed when the total population, including those mice that have more severe phenotypes, is represented. These data demonstrate the knockout of NALCN specifically in the myometrium, but indicate some degree of variability in the level of NALCN knockout from mouse to mouse.

3.3.4 Parturition Phenotype in smNALCN$^{-/-}$ Mouse

We tested the role of myometrial NALCN expression on pregnancy outcomes by comparing the labor parameters of smNALCN$^{-/-}$, smNALCN$^{+/-}$, Cre control, and flox control females. All genotypes were mated with WT males for two hours and then were checked for the presence of a copulation plug. Beginning on P18, females were observed via surveillance camera for their time and length of delivery. The length of time from copulation to the time of delivery of the first pup (gestation length) was not significantly different between the four genotypes, nor was the duration in labor (Table 3.2, Fig 3.4.A). However, smNALCN$^{-/-}$ dams showed a reduced litter size, averaging 4.9 pups/litter compared to 7.1 pups per litter for flox control littermates (Table 3.2, Fig 3.4.B). Although the mean gestation length did not significantly differ between groups, we observed that the number of pups per litter correlated with the gestation length in smNALCN$^{-/-}$ females, in that smaller litters delivered later (Fig 3.5.A). Likely because of the slightly longer gestation length, and greater maternal resource per pup, pups from smNALCN$^{-/-}$ and Cre control pregnancies were also larger (Fig 3.5.B). These data support the notion that there is a fetal component in determining gestation length (36, 37). In examining labor efficiency, we observed that smNALCN$^{-/-}$ dams experienced an increased

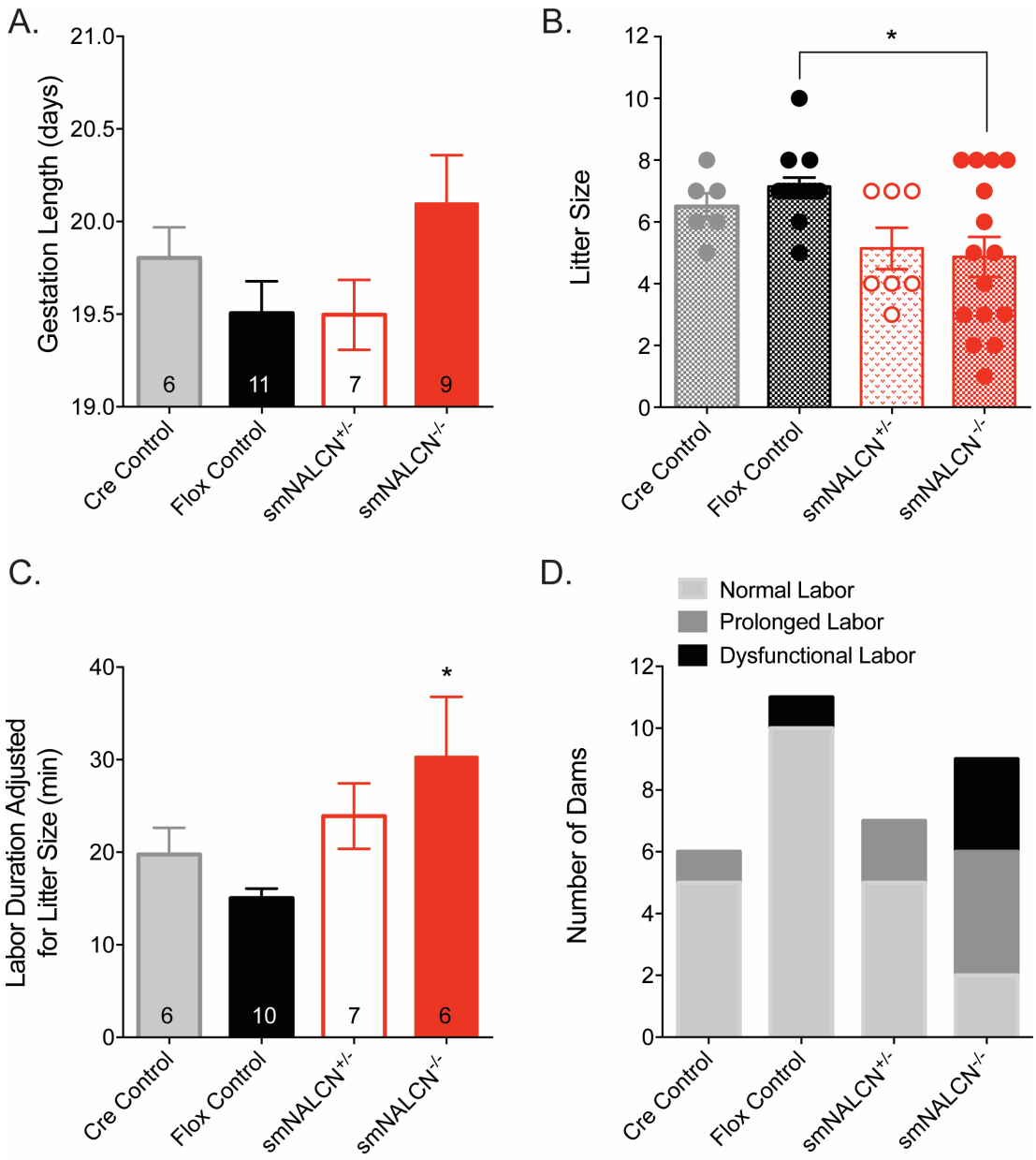

Figure 3.4 Pregnancy parameters in smNALCN$^{-/-}$ mice.
A) Average time to delivery of the first pup. One of the smNALCN$^{-/-}$ females did not deliver; the time that she was sacrificed is included instead. B) Average litter size. These data include mice that were observed via surveillance cameras, as well as the litter sizes of P19 mice sacrificed for electrophysiology experiments. One-way ANOVA $P = 0.05$, multiple comparisons analysis show smNALCN$^{-/-}$ are significanty smaller than flox controls (* $P < 0.05$). C) Labor duration adjusted for litter size. Mice with dysfunctional labor were excluded from this analysis. One-way ANOVA $P = 0.05$, multiple comparisons analysis show smNALCN$^{-/-}$ are significanty longer than flox controls (* $P < 0.05$). D) Rate of prolonged and dysfunctional labor. Chi-square analysis = 0.03. A and B) n values are printed on the bars.

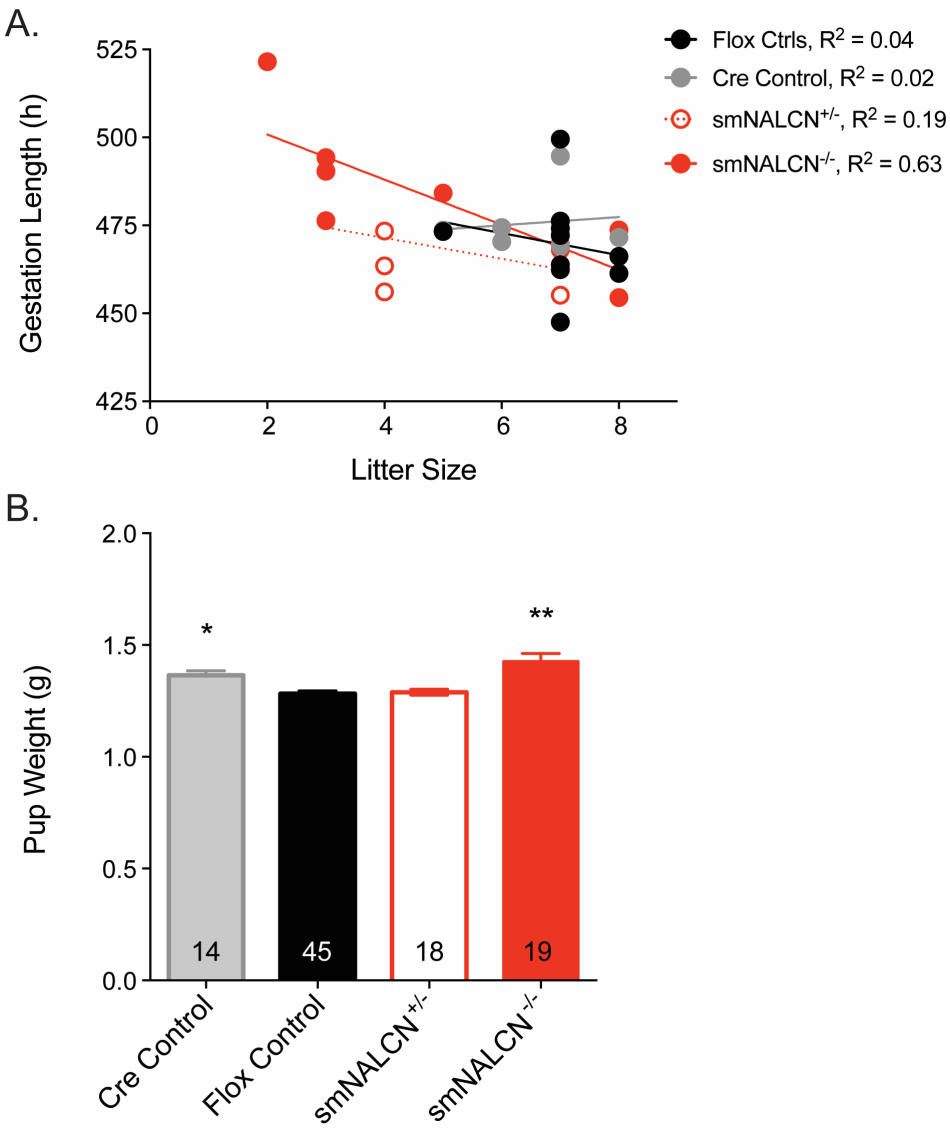

Figure 3.5 (Supplemental) The effect of litter size on gestation length and pup weight.
A) Correlation analysis of litter size and the time to delivery of the first pup, or time of sacrifice (in the case of one smNALCN$^{-/-}$ that was unable to deliver any pups). SmNALCN$^{-/-}$ mice showed a slope that was significantly non-zero, linear regression analysis $P < 0.05$. B) Average pup weights (recorded < 26 hour after birth) by dams of indicated genotypes. Pups weighed are from an 3, 6, 3, and 5 litters, respectively. n value of individual pups is printed on the bars. One-way ANOVA $P < 0.01$, and multiple comparisons anlysis shows that pups of Cre control and smNALCN$^{-/-}$ dams are significantly larger than those from flox controls (* $P < 0.05$, ** $P < 0.01$).

Table 3.2
Pregnancy Parameters

Parameter	Cre Controls (6)	Flox Controls (11)	smNALCN$^{+/-}$ (7)	smNALCN$^{-/-}$ (9)	*P*
Gestation Length (days) ± SEM, (n)	19.80 ± 0.16	19.51 ± 0.17	19.5 ± 0.19	20.10 ± 0.26	0.08
Labor Duration[a] (min) ± SEM, (n)	110.8 ± 20.6, (6)	94.3 ± 10.8, (10)	94.0 ± 17.3, (7)	99.0 ± 67.8, (6)	0.91
Pups/Litter[b]± SD, (n)	6.5 ± 1.0, (6)	7.1 ± 1.1, (14)	5.1 ± 1.8, (7)	**4.9 ± 2.5***, (15)	0.05
Adjusted Labor Duration[c] (min) ± SEM, (n)	19.8 ± 2.9, (6)	15.0 ± 1.0, (10)	23.9 ± 93.5, (7)	**30.3 ± 2.9***, (6)	0.05
Pup Interval[d] (min) ± SEM, (n)	20.4 ± 3.2, (32)	15.0 ± 0.9, (57)	23.0 ± 3.5, (29)	**30.0 ± 6.5***, (21)	0.05
1st to 2nd Pup Interval (min) ± SEM, (n)	18.3 ± 4.4, (6)	18.5 ± 2.1, (11)	43.1 ± 10.7, (7)	385.3 ± 337.5, (7)	0.05
Pup Weight[e] (g) ± SEM, (n)	**1.36 ± 0.02***, (14)	1.28 ± 0.01, (45)	1.29 ± 0.01, (18)	**1.43 ± 0.04****, (19)	**<0.01**
Rate of Prolonged Labor	17% (1/6)	0% (0/11)	29% (2/7)	44% (4/9)	
Rate Dysfunctional Labor	0% (0/6)	9% (1/11)	0% (0/7)	33% (3/9)	**0.032**[f]

[a] Time between delivery of first and last pup. Mice with dysfunctional labor were excluded from this value.
[b] Including all pups born, and in utero from dams studied for pregnancy phenotyping, and P19 dams sacrificed for sharp electrode experiments. Labor duration divided by one less than the total number of pups delivered. Mice with dystocia were excluded from this value.
[c] Labor duration divided by one less than the total number of pups delivered. Mice with dystocia were excluded from this value.
[d] Individual pup delivery time for all pups, excluding those born to mothers with dysfunctional labor.
[e] Pup weight taken within 26 hours of birth. From Cre control (3 litters), flox control (6 litters), smNALCN$^{+/-}$ (3 litters), and smNALCN$^{-/-}$ (5 litters).
[f] Chi-square analysis of the proportion of normal labor for each genotype.
*Adjustment for multiple comparisons finds that these values are are significantly different from flox control values, alpha = 0.05.
**Adjustment for multiple comparisons finds that these values are significantly different from flox control values, alpha = 0.01.

rate of dysfunctional labor (those that were unable to deliver their full litter by P22). 33% of smNALCN$^{-/-}$ dams had dysfunctional labor compared to 9% of flox controls, and 0% of Cre controls and smNALCN$^{+/-}$ dams (Fig 3.4.D). When accounting for the reduced litter size of smNALCN$^{-/-}$ females, we also found that they had an extended time in labor compared to flox controls, taking about 30 min to deliver each pup, compared to the 15 min of flox controls (Table 3.2, Fig 3.4.C). Considering prolonged labor as an adjusted labor duration more than two standard deviations outside of Cre and flox controls (>28 min), we found that smNALCN$^{-/-}$ dams experienced an increased rate of prolonged labor (44% compared to 0% flox controls, 17 % Cre controls, and 29% smNALCN$^{+/-}$ dams) (Table 3.2, Fig 3.4.D). On the whole, smNALCN$^{-/-}$ showed a significant reduction in the rate of normal labor (Table 3.2, Fig 3.4.D). The variability of the smNALCN$^{-/-}$ phenotype is likely associated with the observed variability in NALCN knockdown (Fig 3.3.D). In summary, these data demonstrate the necessity of myometrial NALCN expression in efficient and successful labor outcomes.

3.3.5 Uterine Excitability in smNALCN$^{-/-}$ Mouse

To determine whether the increase in dysfunctional labor in smNALCN$^{-/-}$ mice is related to uterine excitability we again used sharp electrode current clamp to compare P19 smNALCN$^{-/-}$ dams and P19 flox control dams (Fig 3.6.A). We found that myometrium from smNALCN$^{-/-}$ dams showed no significant change in burst interval or spike density (Table 3.3, Fig 3.6.B and E). However, average burst duration and the number of spikes per burst were significantly reduced in smNALCN$^{-/-}$ dams (Table 3.3, Fig 3.6.C and D). This indicates that NALCN is important in sustaining burst duration at P19. Unexpectedly, whole cell patch clamp showed no difference between the Gd^{3+}- sensitive leak current in MSMCs from flox control and

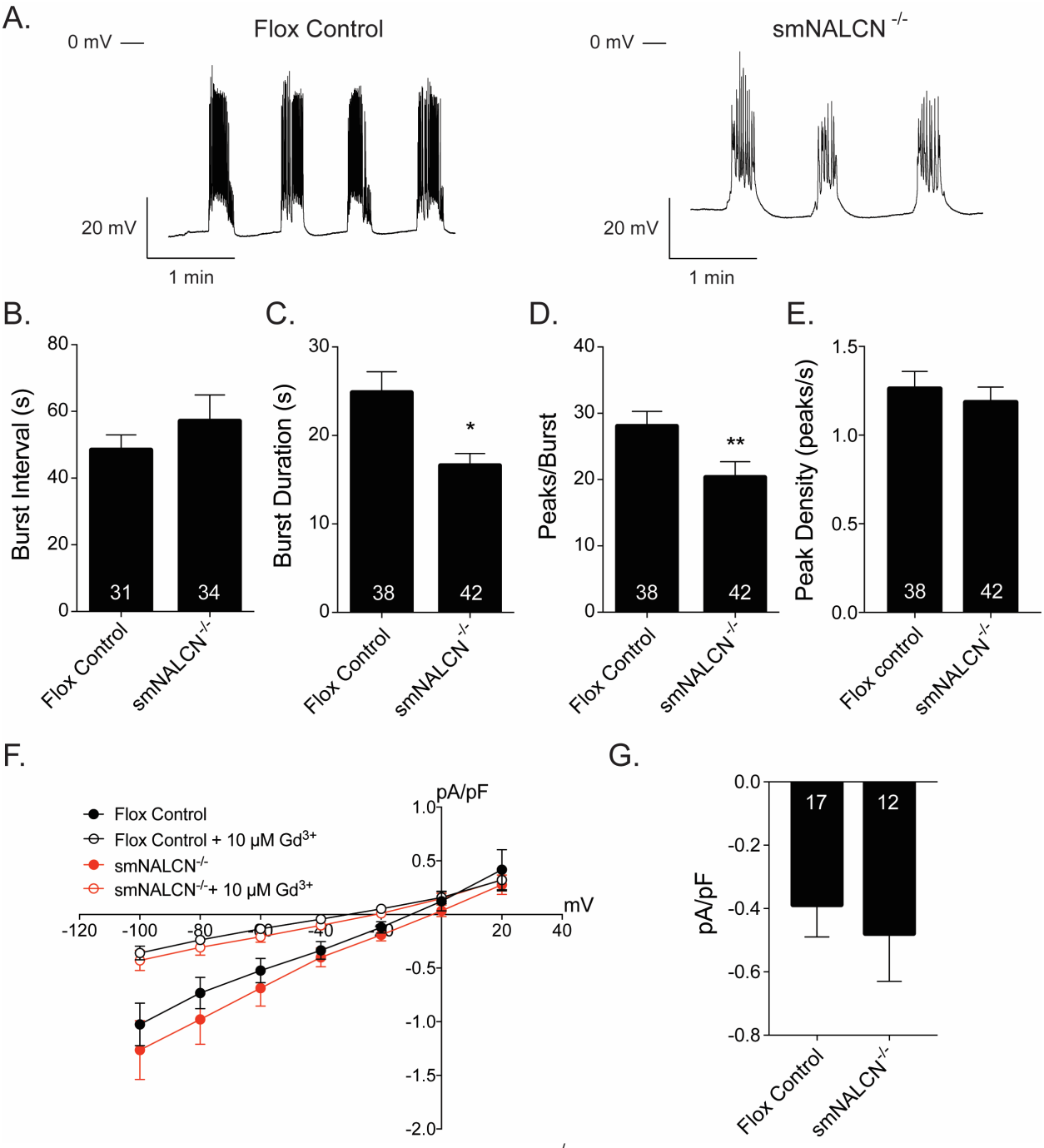

Figure 3.6 Myometrial excitability in smNALCN$^{-/-}$ uterus.
A) Representative membrane potential traces from P19 flox control and smNALCN$^{-/-}$ longitudinal muscle. B – E) Average burst interval, burst duration, number of spikes per burst, and spike density in flox control and smNALCN$^{-/-}$ longitudinal myometrium. Burst duration is decreased in smNALCN$^{-/-}$ (t-test, * $P < 0.05$), and the number of spikes per burst is significantly reduced in smNALCN$^{-/-}$ compared to flox control (t-test, ** $P < 0.01$). F) Average leak current density vs. voltage in smNALCN$^{-/-}$ and flox control mMSMCs. G) Gd^{3+}-sensitive current density evoked at -60 mV in flox control and smNALCN$^{-/-}$ mMSMCs. B – E, and G, n values are printed on the bars.

Table 3.3
Electrophysiology Parameters in Mouse Longitudinal Smooth Muscle.

Genotype	Stage in Pregnancy (n)	Average Burst Interval (s) ± SEM, (N)	Average Burst Duration (s) ± SEM, (N)	Average Spikes/Burst ± SEM	Average Spike Density (spikes/s ± SEM
Wild type	P7 (3)	26.2 ± 2.5, (12)	9.5 ± 0.6, (12)	25.5 ± 1.6	2.40 ± 0.14
	P10 (3)	42.5 ± 7.4, (12)	13.7 ± 1.3, (12)	25.9 ± 3.4	1.87 ± 0.16
	P14 (3)	45.0 ± 5.8, (12)	19.0 ± 0.8**, (12)	27.7 ± 1.7	1.45 ± 0.05**
	P18 (8)	48.5 ± 3.2**, (32)	22.9 ± 2.0**, (32)	36.9 ± 3.9	1.43 ± 0.09**
	P19 (4)	38.1 ± 3.6, (16)	24.7 ± 2.6**,#, (16)	27.7 ± 2.3	1.27 ± 0.14**
Flox Control	P19 (5)	48.4 ± 4.6, (31)	24.9 ± 2.4, (38)	28.0 ± 2.3	1.26 ± 0.10
smNALCN$^{-/-}$	P19 (5)	57.1 ± 7.9, (34)	16.7 ± 1.4[a], (42)	20.3 ± 2.4[a]	1.19 ± 0.09

Genotype	Stage in Pregnancy (n, N)	Calculated Reversal Potential (mV) ± SEM	Normalized Conductance (pS/pF) ± SEM	Current Density[b] (pA/pF) ± SEM
Flox Control	P19 (5, 17)	-12.7 ± 3.0	11.0 ± 2.0	-0.39 ± 0.10
smNALCN$^{-/-}$	P19 (5, 12)	-10.1 ± 5.4	13.6 ± 3.2	-0.49 ± 0.15

* P <0.05 and ** P < 0.01 for Dunn's Multiple Comparisons compared to P7
# P <0.05 for Dunn's Multiple Comparisons compared to P10
[a] P < 0.05 for Mann Whitney t-test comparing flox control and smNALCN$^{-/-}$.
[b]Calculated at -60 mV.
n refers to the number of mice and N refers to the number of bursts, intervals, or cells analyzed.

smNALCN$^{-/-}$ mice (Fig 3.6.F and G). In summary, at P19 NALCN regulates myometrial excitability and does so by sustaining the burst duration.

3.4 Discussion

We previously identified the expression and activity of the Na^+-leak channel, NALCN, in human MSMCs (12). Here, we have gone on to show that NALCN is important in uterine physiology. We found that NALCN is expressed and regulated across pregnancy in the mouse uterus, and its expression is critical for facilitating labor. Specifically, smNALCN$^{-/-}$ females showed an increased incidence of prolonged or dysfunctional labor, and reduced uterine excitability compared to flox control mice. Our study is novel in that it establishes the role of a Na^+ channel in regulating labor efficacy, and expands our understanding of the electrical mechanisms involved in parturition.

Our study supports the findings of others that Na^+ does in fact play an important role in uterine excitability (19-21). Researchers have reported that the regenerative bursting properties of estrogen-treated, non-pregnant rat, and the pregnant rabbit myometrium relied on the presence of Na^+ (19, 20, 21,38). And others have reported the presence of a Na^+-dependent leak current in rat MSMCs (27). Our study identified a specific Na^+ channel in the mouse myometrium, and its necessity in uterine excitability and parturition outcomes. In addition to finding a novel mediator of uterine excitability, this study emphasizes that even subtle changes in ion currents in the myometrium can have a large impact on reproductive success.

Our studies indicate that burst interval correlates with NALCN expression, which was expected based on the established ability of NALCN to increase spontaneous firing (13-15). However, our recordings in smNALCN$^{-/-}$ P19 myometrium did not show a prolonged burst interval, but rather showed a burst duration and number of spikes per burst compared to flox

controls, with no change in spike density. Despite our initial hypothesis that NALCN would contribute mainly to burst interval, our finding that it contributes to burst duration is also unsurprising as NALCN has now been shown to contribute to sustaining depolarization and spike trains in murine interstitial cells of Cajal and hermaphrodite specific neurons in *C. elegans* (16, 39). Even so, NALCN levels are still rather low at P19, and thus a greater role for NALCN in regulating burst interval may be observed in stages with increased NALCN expression, i.e. in labor, or at P7 and P10. Also, because many ion channels are differentially regulated throughout pregnancy, the activity of NALCN, even if constant, may have a different effect on myometrial excitability because of its interaction with other channels. This is likely why we observed a pattern of burst duration that differed from NALCN levels in our wild type burst analysis.

The reduced rate of normal labor, and a decrease in the number of spikes per burst in in the myometrium of smNALCN$^{-/-}$ females suggests that they have insufficient uterine activity to efficiently deliver their pups. Four mice (three smNALCN$^{-/-}$ and one flox control) in our study experienced dysfunctional labor, and were typically able to deliver at least one pup around the normal time, and then were unable to deliver the remaining pups. This suggests that other processes needed for labor to occur, including cervical ripening were proceeding, however the mice lacked the uterine activity to have a normal delivery. SmNALCN$^{-/-}$ mice also showed a reduced litter size, which resulted in a slightly delayed onset to delivery, and larger pup sizes. The reason for the reduced litter size is unknown, but we expect that fetal loss occurs later in pregnancy, as we observed in a small subset of P10 mice (3 of each genotype), that smNALCN$^{-/-}$ had similar litter sizes as flox controls (data not shown). We also noted a larger average pup weight in the smNALCN$^{-/-}$. The slightly longer time in utero, and reduced litter size likely

contributes the increase in pup size, and may contribute to the difficulty the smNALCN$^{-/-}$ dams experienced in labor.

In our study, we focused on the expression and role of only one member of the NALCN complex. We found that NALCN is not only expressed in the mouse myometrium, but that its protein levels are regulated throughout pregnancy. The pattern of NALCN expression suggests that NALCN may be negatively regulated by progesterone. Progesterone levels peak in mid to late gestation (40) when NALCN levels are low, and then decrease for labor, when NALCN levels begin to increase. Beyond reproductive tissues, this may have broad implications in the regulation of NALCN levels in the other tissues in which its expressed, particularly the pancreas and nervous system. Interestingly, we observed that unlike the human, UNC80, an important scaffolding protein for NALCN, was expressed in the non-laboring uterus. It will be important to parse out the regulation of NALCN complex proteins, including UNC80, UNC79, and NLF-1 in the myometrium as these play an fundamental role in regulating NALCN levels and activity (41-44).

It was also surprising to see high levels of NALCN in early pregnancy. Although we do not currently understand the purpose for this, there are a few interesting possibilities. In early pregnancy, when MSMCs are electrically uncoupled and the uterus is less contractile, MSMCs concurrently undergo rapid hyperplasia (45). Depolarizing currents have been shown to contribute to cell proliferation, and therefore it is possible that NALCN may be important in early cell proliferation (46). We did not observe an obvious defect in uterine hyperplasia in smNALCN$^{-/-}$ mice, however there may have been compensatory mechanisms to sustain proliferation, and we did not do intensive histology to determine whether there were architectural differences. Another interesting role for NALCN would be in the endometrium. Regulation of

uterine luminal fluid levels by ion channels ENaC and CFTR, have been suggested to play a role in embryo implantation (35). NALCN has also been linked to osmoregulation (47), and therefore could contribute to this or other unknown processes in the endometrium.

In summary, our study established a novel role for NALCN in regulating myometrial excitability and labor efficiency. Future work should confirm the functional role of NALCN in the human myometrium, in order to validate NALCN as a potential target in the treatment of dysfunctional labor.

3.5 Acknowledgements

We would like to thank Dr. Andrew Blanks and Dr. Conor McCloskey for training us in the technique of sharp electrode current clamp. We would also like to thank Dr. Dejian Ren for his gift of the NALCN$^{fx/fx}$ mouse.

3.6 References

1. Gifford DS, Morton SC, Fiske M, Keesey J, Keeler E, and Kahn KL. Lack of progress in labor as a reason for cesarean. *Obstet Gynecol.* 2000;95(4):589-95.

2. Barber EL, Lundsberg LS, Belanger K, Pettker CM, Funai EF, and Illuzzi JL. Indications contributing to the increasing cesarean delivery rate. *Obstet Gynecol.* 2011;118(1):29-38.

3. Liu S, Liston RM, Joseph KS, Heaman M, Sauve R, Kramer MS, and Maternal Health Study Group of the Canadian Perinatal Surveillance S. Maternal mortality and severe morbidity associated with low-risk planned cesarean delivery versus planned vaginal delivery at term. *CMAJ.* 2007;176(4):455-60.

4. Silver RM, Landon MB, Rouse DJ, Leveno KJ, Spong CY, Thom EA, Moawad AH, Caritis SN, Harper M, Wapner RJ, et al. Maternal morbidity associated with multiple repeat cesarean deliveries. *Obstet Gynecol.* 2006;107(6):1226-32.

5. Clark SL, Belfort MA, Dildy GA, Herbst MA, Meyers JA, and Hankins GD. Maternal death in the 21st century: causes, prevention, and relationship to cesarean delivery. *Am J Obstet Gynecol.* 2008;199(1):36 e1-5; discussion 91-2 e7-11.

6. Hamilton BE, Martin JA, Osterman MJ, Curtin SC, and Matthews TJ. Births: Final Data for 2014. *Natl Vital Stat Rep.* 2015;64(12):1-64.

7. Garfield RE, Maner WL, Maul H, and Saade GR. Use of uterine EMG and cervical LIF in monitoring pregnant patients. *BJOG : an international journal of obstetrics and gynaecology.* 2005;112 Suppl 1(103-8).

8. Garfield RE, Sims S, and Daniel EE. Gap junctions: their presence and necessity in myometrium during parturition. *Science.* 1977;198(4320):958-60.

9. Govindan RB, Siegel E, McKelvey S, Murphy P, Lowery CL, and Eswaran H. Tracking the changes in synchrony of the electrophysiological activity as the uterus approaches labor using magnetomyographic technique. *Reprod Sci.* 2015;22(5):595-601.

10. Marshall JM. Regulation of activity in uterine smooth muscle. *Physiol Rev Suppl.* 1962;5(213-27).

11. Aguilar HN, and Mitchell BF. Physiological pathways and molecular mechanisms regulating uterine contractility. *Hum Reprod Update.* 2010;16(6):725-44.

12. Reinl EL, Cabeza R, Gregory IA, Cahill AG, and England SK. Sodium leak channel, non-selective contributes to the leak current in human myometrial smooth muscle cells from pregnant women. *Mol Hum Reprod.* 2015;21(10):816-24.

13. Lu B, Su Y, Das S, Liu J, Xia J, and Ren D. The Neuronal Channel NALCN Contributes Resting Sodium Permeability and Is Required for Normal Respiratory Rhythm. *Cell.* 2007;129(2):371-83.

14. Lutas A, Lahmann C, Soumillon M, and Yellen G. The leak channel NALCN controls tonic firing and glycolytic sensitivity of substantia nigra pars reticulata neurons. *Elife.* 2016;5(13):e15271.

15. Flourakis M, Kula-Eversole E, Hutchison AL, Han TH, Aranda K, Moose DL, White KP, Dinner AR, Lear BC, Ren D, et al. A Conserved Bicycle Model for Circadian Clock Control of Membrane Excitability. *Cell.* 2015;162(4):836-48.

16. Gao S, Xie L, Kawano T, Po MD, Guan S, Zhen M, Pirri JK, and Alkema MJ. The NCA sodium leak channel is required for persistent motor circuit activity that sustains locomotion. *Nat Commun.* 2015;6(6323).

17. Phillippe M, and Basa A. Effects of sodium and calcium channel blockade on cytosolic calcium oscillations and phasic contractions of myometrial tissue. *J Soc Gynecol Investig.* 1997;4(2):72-7.

18. Miller SM, Garfield RE, and Daniel EE. Improved propagation in myometrium associated with gap junctions during parturition. *Am J Physiol.* 1989;256(1 Pt 1):C130-41.

19. Anderson NC, Ramon F, and Snyder A. Studies on Calcium and Sodium in Uterine Smooth Muscle Excitation under Current-Clamp and Voltage-Clamp Conditions. *J Gen Physiol.* 1971;58(3):322-39.

20. Anderson NC, Jr. Voltage-clamp studies on uterine smooth muscle. *J Gen Physiol.* 1969;54(2):145-65.

21. Kao CY, Zakim D, and Bronner F. Sodium influx and excitation in uterine smooth muscle. *Nature.* 1961;192(1189-90).

22. Xin HB, Deng KY, Rishniw M, Ji G, and Kotlikoff MI. Smooth muscle expression of Cre recombinase and eGFP in transgenic mice. *Physiol Genomics.* 2002;10(3):211-5.

23. Pfaffl MW. A new mathematical model for relative quantification in real-time RT-PCR. *Nucleic acids research.* 2001;29(9):e45.

24. Rosenbaum ST, Svalo J, Nielsen K, Larsen T, Jorgensen JC, and Bouchelouche P. Immunolocalization and expression of small-conductance calcium-activated potassium channels in human myometrium. *J Cell Mol Med.* 2012.

25. McLean AC, Valenzuela N, Fai S, and Bennett SA. Performing vaginal lavage, crystal violet staining, and vaginal cytological evaluation for mouse estrous cycle staging identification. *J Vis Exp.* 201267):e4389.

26. Jackson WF, Huebner JM, and Rusch NJ. Enzymatic isolation and characterization of single vascular smooth muscle cells from cremasteric arterioles. *Microcirculation.* 1997;4(1):35-50.

27. Miyoshi H, Yamaoka K, Garfield RE, and Ohama K. Identification of a non-selective cation channel current in myometrial cells isolated from pregnant rats. *Pflugers Arch.* 2004;447(4):457-64.

28. Lundgren DW, Moore JJ, Chang SM, Collins PL, and Chang AS. Gestational changes in the uterine expression of an inwardly rectifying K^+ channel, ROMK. *Proc Soc Exp Biol Med.* 1997;216(1):57-64.

29. Mershon JL, Mikala G, and Schwartz A. Changes in the expression of the L-type voltage-dependent calcium channel during pregnancy and parturition in the rat. *Biol Reprod.* 1994;51(5):993-9.

30. Collins PL, Moore JJ, Lundgren DW, Choobineh E, Chang SM, and Chang AS. Gestational changes in uterine L-type calcium channel function and expression in guinea pig. *Biol Reprod.* 2000;63(5):1262-70.

31. Curley M, Cairns MT, Friel AM, McMeel OM, Morrison JJ, and Smith TJ. Expression of mRNA transcripts for ATP-sensitive potassium channels in human myometrium. *Mol Hum Reprod.* 2002;8(10):941-5.

32. Pierce SL, Kresowik JD, Lamping KG, and England SK. Overexpression of SK3 channels dampens uterine contractility to prevent preterm labor in mice. *Biol Reprod.* 2008;78(6):1058-63.

33. Matharoo-Ball B, Ashford ML, Arulkumaran S, and Khan RN. Down-regulation of the alpha- and beta-subunits of the calcium-activated potassium channel in human myometrium with parturition. *Biol Reprod.* 2003;68(6):2135-41.

34. Zhang J, Ren C, Chen L, Navedo MF, Antos LK, Kinsey SP, Iwamoto T, Philipson KD, Kotlikoff MI, Santana LF, et al. Knockout of $Na^{+}/Ca2^{+}$ exchanger in smooth muscle attenuates vasoconstriction and L-type Ca^{2+} channel current and lowers blood pressure. *Am J Physiol Heart Circ Physiol.* 2010;298(5):H1472-83.

35. Ruan YC, Chen H, and Chan HC. Ion channels in the endometrium: regulation of endometrial receptivity and embryo implantation. *Hum Reprod Update.* 2014;20(4):517-29.

36. Montalbano AP, Hawgood S, and Mendelson CR. Mice deficient in surfactant protein A (SP-A) and SP-D or in TLR2 manifest delayed parturition and decreased expression of inflammatory and contractile genes. *Endocrinology.* 2013;154(1):483-98.

37. Gao L, Rabbitt EH, Condon JC, Renthal NE, Johnston JM, Mitsche MA, Chambon P, Xu J, O'Malley BW, and Mendelson CR. Steroid receptor coactivators 1 and 2 mediate fetal-to-maternal signaling that initiates parturition. *J Clin Invest.* 2015;125(7):2808-24.

38. Kleinhaus AL, and Kao CY. Electrophysiological actions of oxytocin on the rabbit myometrium. *J Gen Physiol.* 1969;53(6):758-80.

39. Kim BJ, Chang IY, Choi S, Jun JY, Jeon JH, Xu WX, Kwon YK, Ren D, and So I. Involvement of Na(+)-leak channel in substance P-induced depolarization of pacemaking activity in interstitial cells of Cajal. *Cell Physiol Biochem.* 2012;29(3-4):501-10.

40. Virgo BB, and Bellward GD. Serum progesterone levels in the pregnant and postpartum laboratory mouse. *Endocrinology.* 1974;95(5):1486-90.

41. Lu B, Su Y, Das S, Wang H, Wang Y, Liu J, and Ren D. Peptide neurotransmitters activate a cation channel complex of NALCN and UNC-80. *Nature.* 2009;457(7230):741-4.

42. Lu B, Zhang Q, Wang H, Wang Y, Nakayama M, and Ren D. Extracellular calcium controls background current and neuronal excitability via an UNC79-UNC80-NALCN cation channel complex. *Neuron.* 2010;68(3):488-99.

43. Yeh E, Ng S, Zhang M, Bouhours M, Wang Y, Wang M, Hung W, Aoyagi K, Melnik-Martinez K, Li M, et al. A putative cation channel, NCA-1, and a novel protein, UNC-80, transmit neuronal activity in C. elegans. *PLoS Biol.* 2008;6(3):e55.

44. Xie L, Gao S, Alcaire Salvador M, Aoyagi K, Wang Y, Griffin Jennifer K, Stagljar I, Nagamatsu S, and Zhen M. NLF-1 Delivers a Sodium Leak Channel to Regulate Neuronal Excitability and Modulate Rhythmic Locomotion. *Neuron.* 2013;77(6):1069-82.

45. Shynlova O, Lee YH, Srikhajon K, and Lye SJ. Physiologic uterine inflammation and labor onset: integration of endocrine and mechanical signals. *Reprod Sci.* 2013;20(2):154-67.

46. Sundelacruz S, Levin M, and Kaplan DL. Role of membrane potential in the regulation of cell proliferation and differentiation. *Stem Cell Rev.* 2009;5(3):231-46.

47. Sinke AP, Caputo C, Tsaih SW, Yuan R, Ren D, Deen PM, and Korstanje R. Genetic analysis of mouse strains with variable serum sodium concentrations identifies the Nalcn sodium channel as a novel player in osmoregulation. *Physiol Genomics.* 2011;43(5):265-70.

Chapter 4: Hormonal and Post-Translational Regulation of NALCN in the Uterus

Erin L. Reinl[1], Rachael C. Bok[2], K. Joseph Hurt[2], and Sarah K. England[1]

[1] Department of Obstetrics and Gynecology, Center for Reproductive Health Sciences, Washington University in St. Louis School of Medicine, St. Louis, MO 63110

[2] Department of Obstetrics and Gynecology, Basic Reproductive Sciences and Maternal Fetal Medicine, University of Colorado School of Medicine, Aurora, CO 80045

4.1 Introduction

The unique structure and function of specific tissues is established by the distinct regulation of their individual cells. Cells modulate the transcription, translation, post-translational modification, trafficking, and stability of specific gene products in a tissue-specific way. Beyond the establishment of a tissue's structure and function in early development, many tissues alter their functions to adapt to unique physiological or environmental challenges. The myometrium is a striking example of a tissue that changes dramatically over a relatively short period of time in order to accommodate pregnancy. These changes include: hypertrophy and hyperplasia (1), decreasing innervation (2-5), enhanced electrical excitability and connectivity (6-8), and increased mechanical stretch (9, 10). The uterus also undergoes greater regional differentiation including the development of the embryo implantation site, as well as increased contractility at term in the upper segment compared to the lower segment. Focusing our work on one gene in the mouse uterus, *NALCN*, we have demonstrated that it too shows dynamic regulation of its protein levels throughout pregnancy (Fig 3.1.C and D), and that this regulation is

likely important in the modulation of uterine excitability necessary for successful parturition. However, mechanisms by which NALCN protein levels are modulated in the myometrium are unknown.

Proper uterine function during pregnancy relies on differential gene expression across different regions of the uterus (11). Beyond the endometrial and muscular layers, the mouse uterus can be superficially subdivided into broad regions 1) longitudinally into the cervical, mid, and ovarian sections, and 2) transversely into the mesometrial border (placental side) and anti-mesometrial section (Fig 4.1). It has been suggested that the ovarian end, much like the upper segment (fundus) of the human uterus, is the site of contraction initiation while the cervical end and lower segment are the sites with greater relaxation to allow expulsion of the fetus (12). Differences in gene expression have been observed across these regions (11, 13, 14). Agonist sensitivity, especially carbachol-responsiveness was also demonstrated to be more dominant in the ovarian end than in the cervical end, likely due to differing levels of muscarinic receptor 3 (15). However, observations of electrical activity in the guinea pig uterus have shown that neither the ovarian nor cervical end are dominant in burst initiation (16). Additionally, reports differ in their findings of the levels of excitability in the mesometrial border, the site of placentation in the mouse uterus, and the anti-mesometrial border. Several reports have shown less electrical activity in the mesometrial border (17, 18) compared to the anti-mesometrial side. However, recently, Lammers et al. demonstrated a greater prevalence of bursting initiation and contraction origination at the mesometrial border in the rat and guinea pig uteri (19). Based on these observations of regional differences in electrical activity, we hypothesized that NALCN may be differentially expressed across specific regions of the uterus.

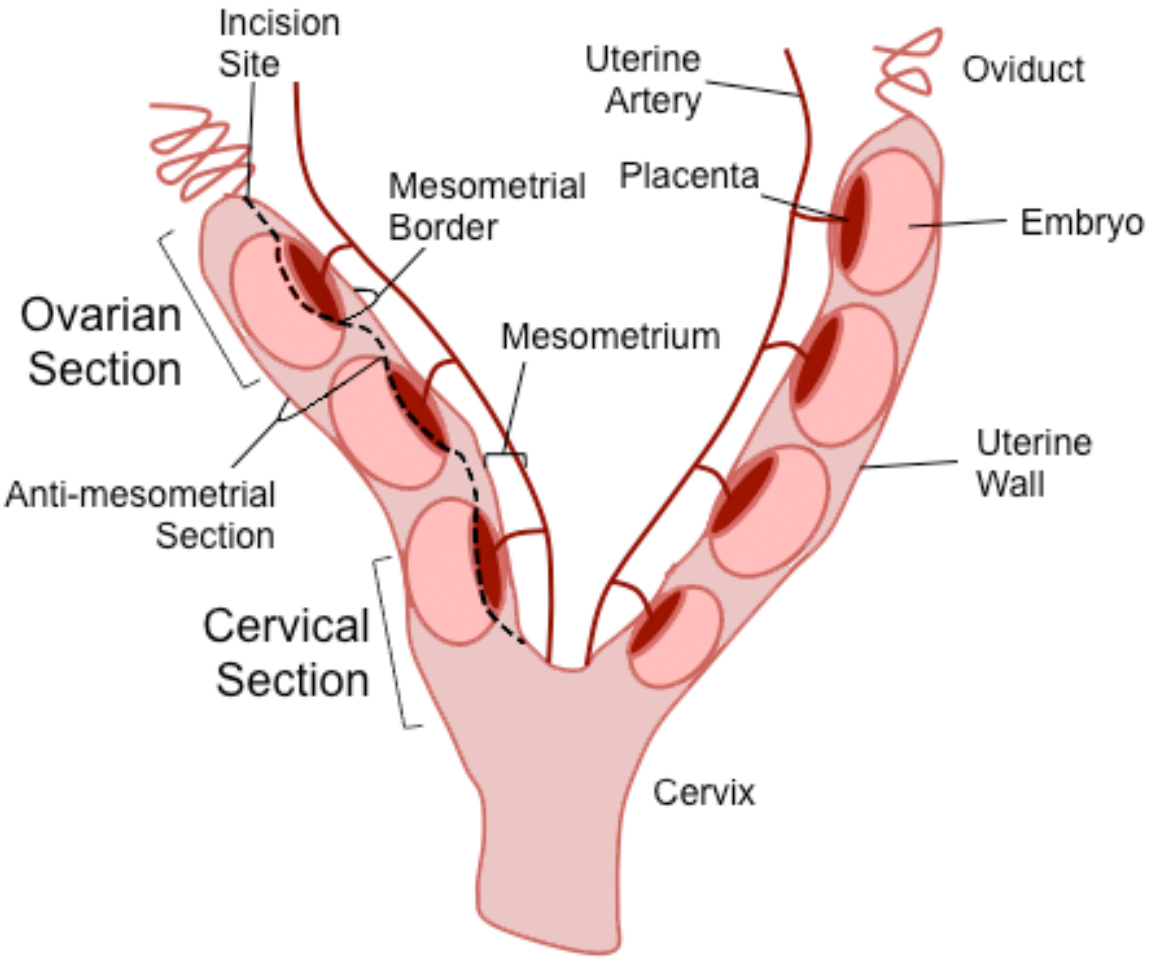

Figure 4.1 Schematic of the gravid mouse uterus.
The uterus can be subdivided longitudinally into ovarian and cervical sections, and transversely into the mesometrial border and anti-mesometrial section. The mesometrial border includes the implantation sites where the placenta and maternal vasculature interact.

Beyond regional localization differences, proteins may also be individually modified to contribute to functional differences in the tissue. We observed that NALCN mRNA and protein levels changed across pregnancy in the mouse uterus (chapter 3), but the assessment of mRNA levels and even total protein levels often fail to capture differences in intracellular localization, and post-translational modifications that can affect protein function. One example in the case of NALCN, is its dependence on the accessory protein, NLF-1, for its localization to the cell membrane. Alterations in NLF-1 expression can directly affect NALCN protein levels at the plasma membrane (20, 21). Alternatively, ion channel function may also be regulated by post-translational modifications, such as glycosylation. Glycosylation, which occurs in the ER and Golgi apparatus, is an important post-translational modification that mediates proper protein folding, and trafficking to the cell membrane. The specific sequence of carbohydrate chains adjoined to glycosylated ion channels can have a direct effect on channel function (22). For example, preventing the glycosylation of the voltage-gated K^+ channel, Kv1.1, results in slower activation kinetics (23). Interestingly, the pregnancy hormone progesterone has been associated with increased glycosylation of IgG1 antibodies (24), and therefore may have an unexplored function in regulating protein glycosylation in MSMCs. We have not observed dramatic changes in *NALCN* mRNA across pregnancy in the mouse (Figure 3.1.B) or human (Figure 2.4) uterus, therefore we hypothesized that changes in NALCN protein levels may be mediated through post-translational mechanisms, which regulate protein stability.

Hormones, particularly progesterone and estrogen, are the major orchestrators of change in reproductive tissues like the uterus, and therefore are often the first candidates associated with pregnancy-mediated expression changes. As previously mentioned, these hormones bind to their intracellular receptors (PR and ER) and enact changes in gene transcription by translocating to

the nucleus and binding to response elements in the promoter regions of an array of target genes to drive transcriptional activity (25). They can also modulate the expression of genes lacking response elements by interacting with other transcription factors such as Sp1 and members of the AP-1 family (26, 27). Progesterone and estrogen are thought to work in opposition, promoting the expression of target genes with opposing functions, or inhibiting expression of the other's target genes (28). Progesterone levels increase during pregnancy and are essential for maintaining pregnancy (29). In the mouse, progesterone levels drop at term as a result of luteolysis, and this decrease precipitates labor. Interestingly, uterine NALCN levels inversely correlate with serum progesterone levels. We showed that uterine NALCN protein levels were high in early pregnancy, reduced in mid to late pregnancy, and then increased during labor and into the post-partum period (Figure 3.1.D and F). In the mouse, the serum progesterone concentration reaches its peak during mid to late gestation, when NALCN protein levels are at their lowest (30). Based on these data, we hypothesized that NALCN protein levels may be negatively regulated by progesterone.

4.2 Materials and Methods

4.2.1 Animal Studies

All animal procedures complied with guidelines for the care and use of animals set forth by the National Institutes of Health. All protocols were approved by the Animal Studies Committee at Washington University in St. Louis and the University of Colorado Institutional Animal Care and Use Committee. C57BL/6 mice were obtained from Jackson Laboratories (those used in estrus cycle experiments) or from Charles River Laboratories (those used in progesterone and RU486 experiments).

4.2.2 Staging the Estrus Cycle

The estrus cycle of non-pregnant mice was tracked by using previously described methods (31) summarized in chapter 3. Mice were tracked for a minimum of one complete estrus cycle before they were sacrificed. Four were sacrificed at each stage of the estrus cycle (proestrus, estrus, metestrus, and diestrus) between 2:00 and 5:00 pm. Their uteri were removed and flash frozen, and eventually their plasma membranes were isolated.

4.2.3 Progesterone and RU486 Treatment

Samples were a kind gift from K. Joseph Hurt, MD, PhD. Briefly, one group of mice was treated in the evening with the progesterone receptor antagonist, RU486 (0.5 mg diluted in 150 μL EtOH), or vehicle (150 μL EtOH) at P14.5 via subcutaneous injection. Mice (controls and RU486 treated) were sacrificed at the time of delivery of the first pup in the RU486 group (< 24 hours after treatment), their uterus was removed, cleared of its contents, and flash frozen in liquid nitrogen. Females that did not go into preterm labor (~20%) were excluded. A second group of mice was treated with progesterone (1 mg in 150 μL sesame oil) or vehicle (150 μL sesame oil) at P17.5 and a second dose was administered at P18.5. Vehicle and progesterone treated mice were sacrificed after the delivery of the first pups of the vehicle treated mice (progesterone treated mice do not deliver). The uteri from these mice were removed, the embryonic contents were cleared, and the uterus was flash frozen.

4.2.4 Membrane Preparations

Uterine tissue was minced and homogenized for isolation of their cell membranes. The same membrane preparation protocol described in the methods section of chapter 3 was employed here.

4.2.5 Immunoblot

Immunoblots were run in the same way as described in the methods section of chapter 3. Pretreatment with the antigenic peptide is described in chapter 2.

4.2.6 Glycosidase Treatment

Endoglycosidase H (endo H) and Peptide-*N*-glycosidase F (PNGase F) deglycosylation of mouse uterine membrane preps were performed using the associated kits from New England BioLabs. Mouse uterine membrane preparations (30 µg in 15 µl) were denatured using the 10X Denaturing Buffer for 10 min at 100 °C. For endo H reactions, 3 µl of 10X GlycoBuffer #3, 4.5 µl water, and 7.5 µl (~3750 units) of endo H were added (30 µl total volume). For PNGase F reactions, 3 µl of 10X GlycoBuffer #2, 3 ul 10% NP40, 6 µl water, and 3 µl PNGase F (~1500 units) were added (30 µl total volume). Reactions were incubated for one hour at 37 °C, then stopped with 10 µl of 4X Laemmli loading buffer and stored at -20 °C until SDS-PAGE.

4.2.7 HEK293 Transduction with NALCN

Lentiviral vectors were produced by the Washington University in St. Louis Hope Center Viral Vectors core using a pWPXL plasmid containing an HA tag-NALCN-IRES-NeoR cassette (a generous gift from Arnaud Monteil at the Institut de Génomique Fonctionnelle, Universités Montpellier). HEK293 cells were suspended via 0.25% Trypsin-EDTA (Gibco), and washed twice with DMEM-Ham's F-12 with 10% FBS and 25 µg/ml gentamicin (standard media). HEK293 cells were transferred to a conical tube containing 2 ml of standard media supplemented with 16 µg/ml polybrene and viral vectors, consisting of a multiplicity of infection of two. The suspension was mixed briefly and then transferred to a cell culture-treated flask containing 2 ml of standard media. Media was changed 16 hours later, and transduced cells were selected for with G418 treatment (200 µg/ml) beginning 70 hours post-transduction.

4.3 Results

4.3.1 Regional Localization of NALCN Isoforms

In contemplating NALCN regulation, we first asked whether NALCN levels may differ according to the specific region within the uterus thus contributing to reported regional differences of excitability in the uterus. NALCN levels in the ovarian end of the uterus were compared to the cervical end, as well as from the mesometrial border compared to the anti-mesometrial border. Western blot analysis on membrane preparations from these regions at NP and P18 showed no evidence for a difference in NALCN levels between the cervical and ovarian regions (Fig 4.1.A). However, in comparing the mesometrial border and anti-mesometrial section, we observed an increased prevalence of a novel ~180 kDa band in P14 and P18. In the P19 uteri we detected a combination of the standard ~160 kDa band and the ~180 kDa band in the mesometrial border and anti-mesometrial sections (Fig 4.2.B). To confirm the specificity of the NALCN antibody, I performed a western blot on lysates of HEK293 cells that had been transduced with a lentiviral vector to overexpress NALCN. Figure 4.2.C shows increased intensity of the ~160 kDa band in the NALCN overexpressing cells compared to the vehicle treated cells, with no change in the loading control (GAPDH). As an additional control, I performed a western blot on the P18 and P19 mesometrial border samples in which I pre-incubated the primary antibody with the antigenic peptide, or used the secondary antibody alone. I did not observe any non-specific bands that remained in either of these control conditions (Fig 4.2.D), indicating NALCN-specificity of the antibody. The induction of a putative higher molecular weight isoform of NALCN in the mesometrial border lead us to hypothesize that NALCN may be differentially post-translationally modified in this region.

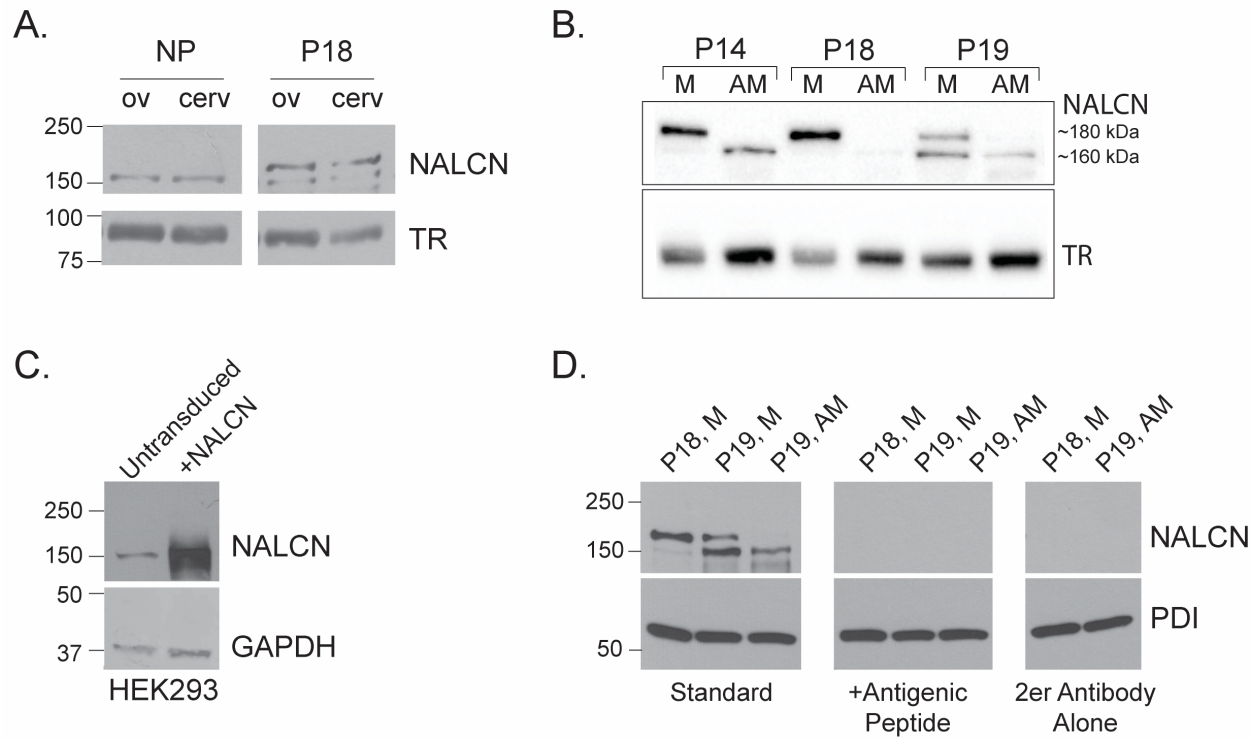

Figure 4.2 Regional localization of NALCN.
A) Western blot of mouse uterine membrane preparations from the ovarian (ov) and cervical (cerv) sections of the non-pregnant (NP) and pregnancy day 18 (P18) uteri. TR is the loading control. B) Western blot of mouse uterine membrane preparations from the mesometrial border (M) and anti-mesometrial section (AM) of the P14, P18, and P19 uterus. TR is the loading control. C) Western blot of HEK293 cells transduced with a lentivirus overexpressing NALCN. GAPDH is the loading control. D) Western blots of the P18 mesometrial border (P18, M), P19 mesometrial border (P19, M), and P19 anti-mesometrial border (P19, AM). The first blot is under standard conditions. In the second blot, the primary antibody was pre-incubated with the antigenic peptide. In the third blot, the primary antibody was excluded.

4.3.2 *N*-Linked Glycosylation of NALCN

As mentioned, the mesometrial border has been found to be a less excitable region of the uterus (17, 18). Therefore, we hypothesized that there may be a mechanism to sequester an excitatory ion channel like NALCN to the endoplasmic reticulum in this region. Many transmembrane proteins that are trafficked to the plasma membrane are glycosylated within the ER and Golgi apparatus, and the type of glycosylation can denote a protein's intracellular location. We hypothesized that the higher molecular weight band observed in NALCN western blots of the mesometrial border is a glycosylated form of the channel that may be sequestered to the endoplasmic reticulum. First we asked whether NALCN contained putative asparagine (*N*)-linked glycosylation sites. These consist of an asparagine followed by any amino acid (except proline), and a serine or threonine (N-X-S/T). We found six putative glycosylation sites. Two of the sites are located on the cytoplasmic face of the protein, and although cytoplasmic proteins can be glycosylated, this form of glycosylation is less common (32). The other four sites are located in the extracellular portion of the S5-S6 linkers in repeats I, III, and IV, outside of the pore regions, and are more likely candidates (Fig 4.3.A).

To determine the glycosylation status of NALCN, we employed the glycosidases, PNGase F and endo H. These enzymes are commonly used to determine whether a protein has undergone *N*-linked glycosylation and whether it localizes to the ER, respectively (33). We incubated mesometrial border membrane preparations from P18 and P19 mice with both PNGase F and endo H. Neither PNGase F nor endo H caused any shift of the ~160 kDa band, indicating that this band is not *N*-glycosylated or sequestered to the ER (Fig 4.3.B and C). However, the ~180 kDa band was reduced to nearly 140 kDa by PNGase F treatment (Fig 4.3.B). This indicates that the ~180 kDa band is a glycosylated protein. However, endo H treatment did not

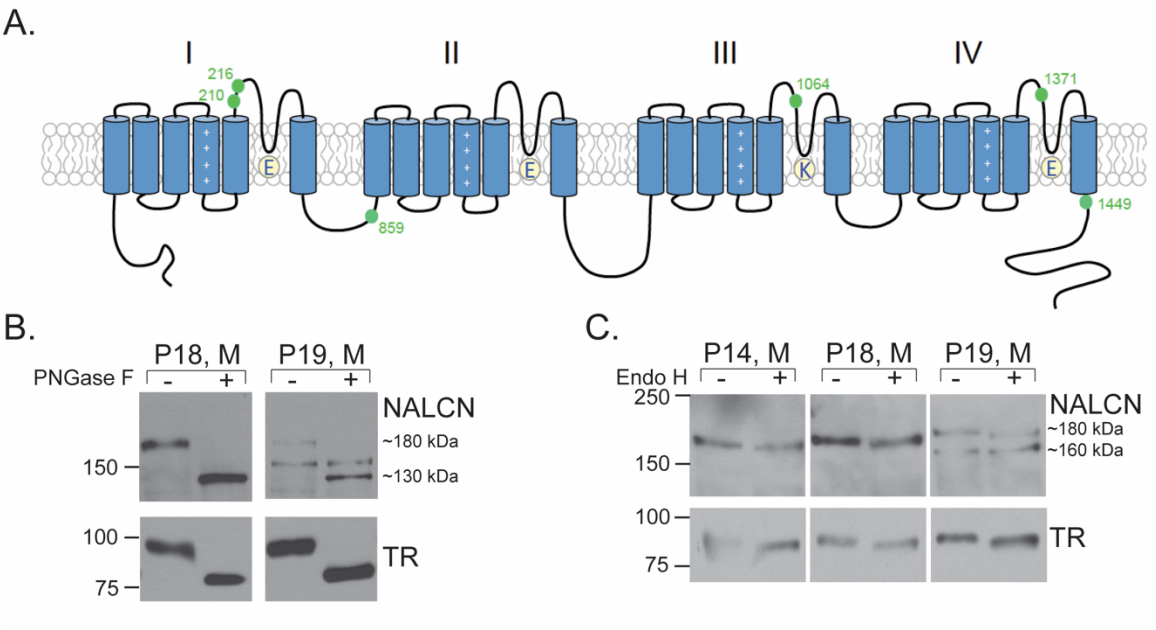

Figure 4.3 NALCN *N*-linked Glycosylation.
A) Schematic of NALCN with putative glycosylation sites denoted with green circles. B) Pregnancy day 18 (P18) and P19 mesometrial border (M) treated with and without PNGase F. TR is a positive control. C) P14, P18, and P19 mesometrial borders treated with endo H. TR is a positive control.

cause a significant shift in the molecular weight of the ~180 kDa band, indicating that NALCN is not sequestered to the ER (Fig 4.3.C). Interestingly, the PNGase F-induced shift reduced the protein to a size that is even smaller than the non-glycosylated ~160 kDa form. This indicates that two core forms of NALCN may exist, one that is ~160 kDa, and one that is ~140 kDa, with only the ~140 kDa protein showing end stage glycosylation. These experiments indicate that at the mesometrial border, there is a greater prevalence of a glycosylated, smaller core NALCN protein. Further work needs to be done to determine the identity of the 140 kDa protein.

4.3.3 NALCN Levels During the Estrus Cycle

Based on our findings that NALCN levels are regulated throughout pregnancy, we hypothesized that NALCN may be negatively regulated by progesterone, and that progesterone may play a role in the regional differences observed in NALCN glycosylation. First, to test the hypothesis that NALCN is regulated by progesterone, NALCN protein levels in the mouse uterus were assayed from tissue collected throughout the hormonally driven estrus cycle (Fig 4.4.A). The estrus cycle is broken down into four stages, diestrus, proestrus, estrus, and metestrus. During late diestrus and proestrus ovarian follicles are formed, and circulating estrogen levels increase to signal the release of follicle stimulating hormone and luteinizing hormone from the pituitary gland. These hormones stimulate ovulation and the transition to the estrus stage, when the female becomes sexually receptive. Following estrus is metestrus, in which the corpus luteum is formed in preparation for pregnancy, and progesterone levels increase. In the absence of pregnancy, the mouse reenters the diestrus phase (34). We hypothesized that NALCN levels would peak during proestrus, when progesterone levels are at their lowest, and the estrogen to progesterone ratio is at its highest. Estrus stages of mice were assessed via vaginal cytological evaluation, and whole uteri were collected from four mice at each stage and flash frozen for later

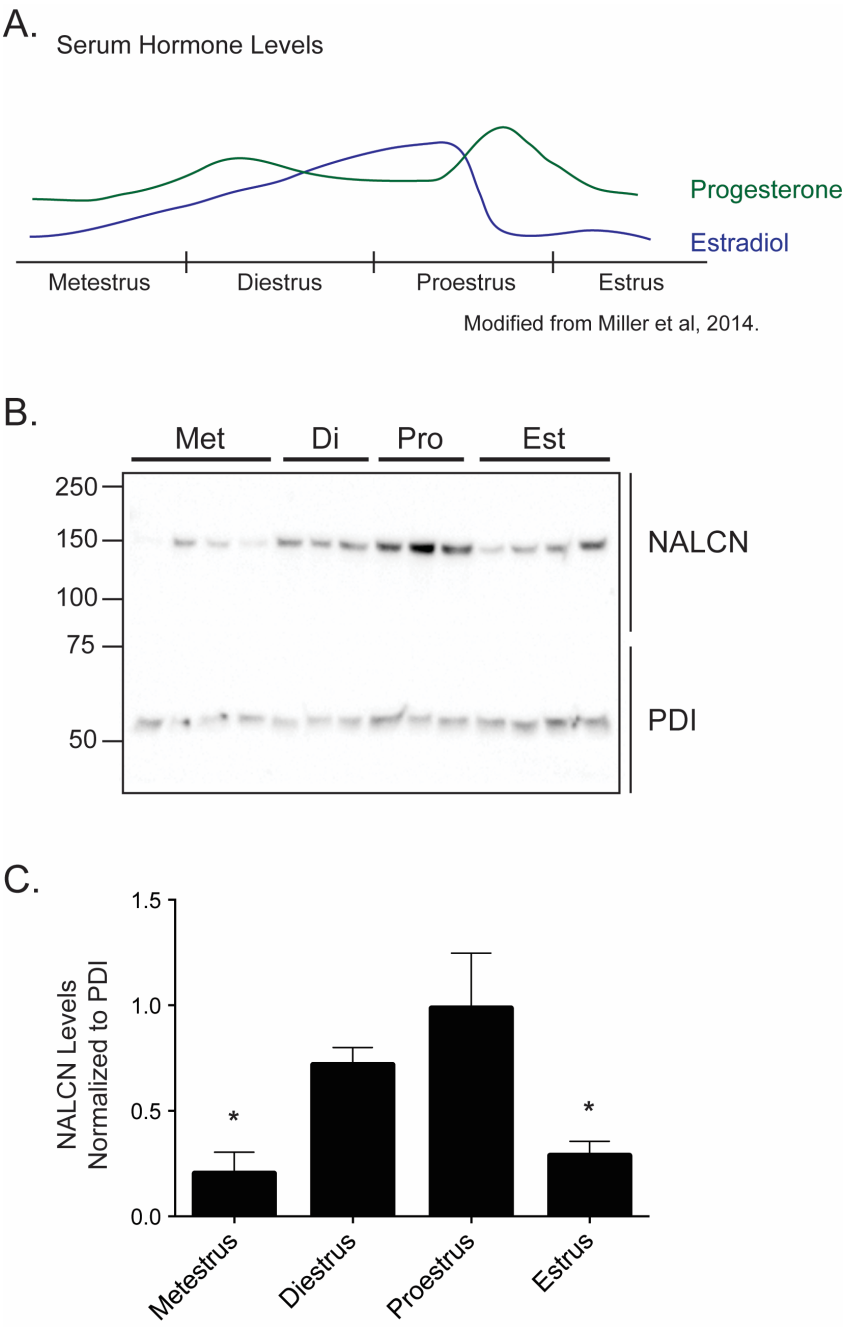

Figure 4.4 NALCN levels in the mouse uterus across the estrus cycle.
A) Schematic of the relative circulating progesterone and estradiol levels throughout the mouse estrus cycle. B) Representative western blot of NALCN from membrane preparations of mouse uterus collected from different stages of the estrus cycle. PDI is the loading control. C) Quantification of NALCN levels from across the estrus cycle. n is four for all stages. One-way ANOVA $P < 0.01$, and multiple comparisons show that metestrus and estrus are significantly less than proestrus (* $P < 0.05$).

processing. Importantly, uteri were collected at a similar time each day, as the estrus cycle is also affected by circadian rhythms (35, 36). Western blot analysis was performed on membrane preparations, tagging for NALCN and protein disulfide isomerase (PDI) as the loading control (37). As predicted, NALCN levels peaked in proestrus and were at their lowest in metestrus (Figure 4.4.B and C). Interestingly, NALCN levels were also elevated during diestrus, when progesterone remains high. However, despite high progesterone levels, during diestrus the estrogen to progesterone ratio begins to increase (Figure 4.4.A). This suggests that beyond the serum progesterone levels, the overall estrogen to progesterone ratio may play an important role in regulating NALCN levels. Taken together, the assessment of NALCN protein levels in the uterus across pregnancy and the estrus cycle demonstrate that NALCN levels are dynamically regulated in the uterus to accommodate the unique stages of the reproductive cycle, and that NALCN levels are dependent on circulating estrogen and progesterone levels.

4.3.4 NALCN Levels in Response to Progesterone and RU486 Treatments

To more directly ascertain whether NALCN is downregulated by progesterone, we assayed NALCN levels in the uteri of mice that had been injected with exogenous progesterone at term. We obtained uterine tissue from our collaborator Dr. K. Joseph Hurt at the University of Colorado. Mice were subcutaneously injected with 1 mg of progesterone or vehicle on days 17.5 and 18.5 of pregnancy. Vehicle and progesterone treated mice were sacrificed at the time of delivery of the first pups in the vehicle treated group, and uteri were collected. The progesterone treated mice, because they do not experience progesterone withdrawal, do not go into labor. Western blot analysis of uterine membrane preparations revealed that delaying the progesterone withdrawal in mice, prevented the term increase in NALCN levels. Uterine tissue from progesterone-injected mice had an 86% reduction in NALCN (~160 kDa band) compared to

vehicle-injected mice (Fig. 4.4.A and B). Surprisingly, we again saw the appearance of the higher molecular weight (~180 kDa) band in some of the progesterone treated tissues (6 of 10 progesterone treated samples compared to 1 of 8 control samples).

To further examine NALCN regulation by progesterone, we also performed the reverse experiment by blocking progesterone receptors with the antagonist, RU486, at P14.5 when progesterone levels are naturally high. Mice were subcutaneously injected with 0.5 mg of RU486 or vehicle in the evening of P14.5. They were sacrificed at the time of delivery of the first pup of the RU486 treated mice, < 24 hours later (vehicle mice do not deliver during this time). We hypothesized that blocking progesterone signaling during mid-gestation would relieve the inhibition on NALCN expression and uterine NALCN levels would rise. We saw a subtle increase in NALCN levels, but this increase was not significant (Fig. 4.5.C and D). Interestingly, while overall NALCN levels were still lower in the control P15.5 samples compared to the P19.5 samples (Fig 4.5.E), when films were exposed longer to better visualize the NALCN bands at P15.5, we again saw an increased prevalence of the higher molecular weight band in the vehicle treated P15.5 (high progesterone) uterine tissue compared to the tissue from RU486 treated mice. These data reiterate the upregulation of the ~180 kDa band in the presence of both exogenous and endogenous progesterone. The induction of the ~180 kDa band during periods of higher progesterone levels suggests that progesterone may also be behind the *N*-linked glycosylation observed in the mesometrial border of P14, P18, and P19 mice. To confirm, we also analyzed the effects of PNGase F and endo H on the progesterone treated tissue. Again, we observed that the ~160 kDa band was insensitive to treatment by PNGase F and endo H, but that the ~180 kDa band was dramatically shifted by PNGase F to a core structure of ~140 kDa. Thus, we concluded that there is a common mechanism in high

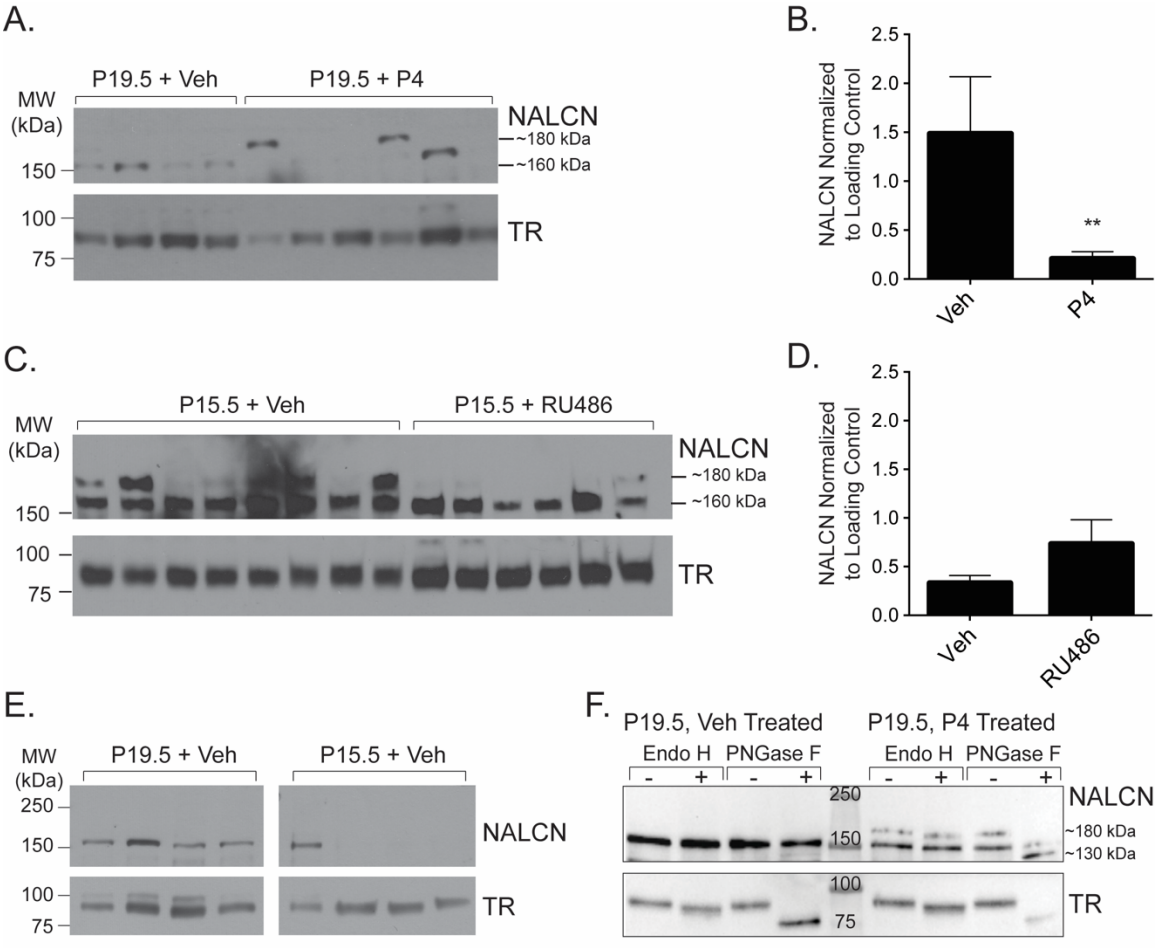

Figure 4.5 Progesterone-mediated regulation of NALCN.
A) Representative western blot of uterine membrane preparations from mice at pregnancy day 19.5 (P19.5) after treatment with vehicle or progesterone (P4) on P17.5 and P18.5. TR is the loading control. B) Quantification of NALCN levels from vehicle and progesterone treated mice. n's are 8 and 10, respectively. Mann-Whitney t-test, ** $P < 0.01$. C) Representative western blot of uterine membrane preparations from mice at P15.5 after treatment with RU486 or vehicle on P14.5. TR is the loading control. D) Quantification of NALCN levels from vehicle and RU486 treated mice. n's are 12 and 10, respectively. E) Western blot of NALCN levels in mouse uterine membrane preparations from the P19.5 and P15.5 vehicle treated mice at the same exposure. F) Western blot of endo H and PNGase F treated uterine membrane preps from a P19.5 vehicle treated mouse and a P19.5 progesterone treated mouse. TR is the positive control.

progesterone states and the mesometrial border that induces the expression of a glycosylated form of NALCN.

4.4 Discussion

In an organ that undergoes extreme change, like the uterus, the specific genes that are important for its function undergo dynamic regulation to facilitate these changes. We found that NALCN is dynamically regulated in the uterus on multiple levels. First, we demonstrated by western blot the differential expression of two NALCN isoforms (~160 kDa and ~180 kDa) in the mesometrial border and anti-mesometrial section, and that the larger isoform undergoes *N*-linked glycosylation. We also showed that NALCN levels change over the estrus cycle, and in response to progesterone and RU486 treatment. Increases in progesterone, and stages of the estrus cycle when the estrogen to progesterone ratio is decreased, downregulates NALCN protein levels. During periods with higher levels of progesterone, we also saw an increased incidence of the ~180 kDa, PNGase F-sensitive protein. Our discovery that NALCN undergoes dynamic regulation in the uterus, takes our findings beyond the modest concept that NALCN is expressed and active in the uterus, to supporting the notion that NALCN is an important contributor to uterine function and therefore needs to be modulated in order to drive changes in uterine activity.

Our results reinforce the findings of others who have shown the regulation of a number of ion channels in the uterus throughout pregnancy. L-type calcium channels are the main ion channel responsible for the influx of calcium that initiate signaling processes and induce contraction. These channels have been shown to gradually increase throughout pregnancy (38, 39). Potassium channels are also regulated throughout pregnancy. Many potassium channels, including SK3, BK_{Ca}, ROMK, and K_{ATP}, are down regulated in the uterus near term to facilitate membrane depolarization for the contractions of parturition (40-44). However, some potassium

channels, primarily KCNQ, have been shown to be upregulated towards term as potassium currents are still essential in the contracting uterus to repolarize the membrane potential and avoid tonic contractions (45). Additionally, the gap junction protein connexin-43, known for its role in increasing electrical connectivity in the uterus for parturition, is highly upregulated during labor and this process has also been shown to be dependent on the estrogen to progesterone ratio (46, 47). Thus, changes in NALCN expression do not occur in isolation, but rather in coordination with the overall changing electrical dynamics of MSMCs.

Differential expression of NALCN between the mesometrial border and the anti-mesometrial section supports literature demonstrating differing electrical properties between these two sections. Kanda and Kuriyama demonstrated that myometrium from the mesometrial border was more hyperpolarized, showed a slower conduction velocity, and reduced oxytocin-responsiveness (17). Reduced excitability of this region has been corroborated by others (16, 18). Increased expression of the ~180 kDa NALCN band in the mesometrial border, and in progesterone treated uteri, suggests that this form of the channel may be inhibitory. It is possible that this form of the channel is alternatively spliced, as the de-glycosylated core protein is smaller than the ~160 kDa non-glycosylated form. Progesterone and estrogen have been shown to regulate alternative splicing of their target genes (48, 49) including ion channels (50, 51). In the myometrium, estrogen downregulates an alternatively spliced isoform of the BK_{Ca} channel which is uniquely inhibited by protein kinase A (50). Thus, although glycosylation of ion channels has been overwhelmingly associated with increased trafficking and activity of those channels (22), because this form of NALCN also may be alternatively spliced, glycosylation in this case may be stabilizing an inhibitory form of the channel. If this isoform of NALCN is alternatively spliced, it is likely a novel isoform. Alternatively spliced isoforms of NALCN have

been reported (52), but not extensively studied, and none of them closely match the isoform described here. Finally, outside of alternative splicing, in the mesometrial border NALCN may differentially associate with accessory proteins like the calcium sensing receptor (CaSR) which negatively regulates NALCN, or with Na^+-activated potassium channels which in the presence of the Na^+-leak current, would actually cause membrane polarization.

A limitation to these studies was that we did our analyses in whole uterine sections, meaning that our membrane preparations included myometrial and decidual tissue. We expected that NALCN expression would be concentrated in the myometrium as ion channels are thought to play a greater role there, since the endometrium and decidua are thought to be less excitable tissues. Furthermore, knocking out NALCN in the smooth muscle alone of mice resulted in a parturition phenotype indicating its specific importance in the myometrium. However, ion channels including ENaC and CFTR are expressed in the endometrial epithelium and suggested to contribute to embryo implantation by controlling luminal fluid volume (reviewed in (53). It is feasible that NALCN could also play a role in this process, as it has been linked to osmoregulation and hypernatremia (54). Additionally, the progesterone receptor has been shown to be upregulated in the decidua of the mesometrial border compared to the anti-mesometrial section (55). The co-occurrence of the ~180 kDa band in both the mesometrial border samples and the high progesterone samples, suggests that this mode of regulation of NALCN may be mediated by the progesterone receptor localized in the decidua of the mesometrial border. Therefore, future studies will determine whether NALCN levels differ between the endometrium or decidua, and the myometrium, and whether post-translational modifications of NALCN differ in these regions or even in individual cell types.

Our findings have important implications in myometrium research as well as beyond. NALCN is expressed in a variety of tissues, including the pancreas, GI tract, and nervous system. Hormonal control of this channel, if it occurs in these tissues, could have implications in sexually dimorphic diseases related to these systems. Additionally, the discovery of a potentially novel isoform of the channel would have implications in the regulation of NALCN regardless of tissue.

4.5 References

1. Shynlova O, Lee YH, Srikhajon K, and Lye SJ. Physiologic uterine inflammation and labor onset: integration of endocrine and mechanical signals. *Reprod Sci.* 2013;20(2):154-67.

2. Haase EB, Buchman J, Tietz AE, and Schramm LP. Pregnancy-induced uterine neuronal degeneration in the rat. *Cell Tissue Res.* 1997;288(2):293-306.

3. Latini C, Frontini A, Morroni M, Marzioni D, Castellucci M, and Smith PG. Remodeling of uterine innervation. *Cell Tissue Res.* 2008;334(1):1-6.

4. Marshall JM. Effects of ovarian steroids and pregnancy on adrenergic nerves of uterus and oviduct. *Am J Physiol.* 1981;240(5):C165-74.

5. Wikland M, Lindblom B, Dahlstrom A, and Haglid KG. Structural and functional evidence for the denervation of human myometrium during pregnancy. *Obstet Gynecol.* 1984;64(4):503-9.

6. Garfield RE, Sims S, and Daniel EE. Gap junctions: their presence and necessity in myometrium during parturition. *Science.* 1977;198(4320):958-60.

7. Miller SM, Garfield RE, and Daniel EE. Improved propagation in myometrium associated with gap junctions during parturition. *Am J Physiol.* 1989;256(1 Pt 1):C130-41.

8. Govindan RB, Siegel E, McKelvey S, Murphy P, Lowery CL, and Eswaran H. Tracking the changes in synchrony of the electrophysiological activity as the uterus approaches labor using magnetomyographic technique. *Reprod Sci.* 2015;22(5):595-601.

9. Reynolds SRM. In: Reynolds SRM ed. *Physiology of the Uterus*. New York: Paul B. Hoeber. Inc.; 1949:218-34.

10. Csapo A, Erdos T, De Mattos CR, Gramss E, and Moscowitz C. Stretch-induced uterine growth, protein synthesis and function. *Nature.* 1965;207(5004):1378-9.

11. Bukowski R, Hankins GD, Saade GR, Anderson GD, and Thornton S. Labor-associated gene expression in the human uterine fundus, lower segment, and cervix. *PLoS Med.* 2006;3(6):e169.

12. Euliano TY, Marossero D, Nguyen MT, Euliano NR, Principe J, and Edwards RK. Spatiotemporal electrohysterography patterns in normal and arrested labor. *Am J Obstet Gynecol.* 2009;200(1):54 e1-7.

13. Sparey C, Robson SC, Bailey J, Lyall F, and Europe-Finner GN. The differential expression of myometrial connexin-43, cyclooxygenase-1 and -2, and Gs alpha proteins in the upper and lower segments of the human uterus during pregnancy and labor. *J Clin Endocrinol Metab.* 1999;84(5):1705-10.

14. Smith GC, Baguma-Nibasheka M, Wu WX, and Nathanielsz PW. Regional variations in contractile responses to prostaglandins and prostanoid receptor messenger ribonucleic acid in pregnant baboon uterus. *Am J Obstet Gynecol.* 1998;179(6 Pt 1):1545-52.

15. Kitazawa T, Hirama R, Masunaga K, Nakamura T, Asakawa K, Cao J, Teraoka H, Unno T, Komori S, Yamada M, et al. Muscarinic receptor subtypes involved in carbachol-induced contraction of mouse uterine smooth muscle. *Naunyn Schmiedebergs Arch Pharmacol.* 2008;377(4-6):503-13.

16. Lammers WJ, Mirghani H, Stephen B, Dhanasekaran S, Wahab A, Al Sultan MA, and Abazer F. Patterns of electrical propagation in the intact pregnant guinea pig uterus. *Am J Physiol Regul Integr Comp Physiol.* 2008;294(3):R919-28.

17. Kanda S, and Kuriyama H. Specific features of smooth muscle cells recorded from the placental region of the myometrium of pregnant rats. *J Physiol.* 1980;299(127-44).

18. Daniel EE, and Renner SA. Effect of the placenta on the electrical activity of the cat uterus in vivo and in vitro. *Am J Obstet Gynecol.* 1960;80(229-44).

19. Lammers WJ, Stephen B, Al-Sultan MA, Subramanya SB, and Blanks AM. The location of pacemakers in the uteri of pregnant guinea pigs and rats. *Am J Physiol Regul Integr Comp Physiol.* 2015;309(11):R1439-46.

20. Flourakis M, Kula-Eversole E, Hutchison AL, Han TH, Aranda K, Moose DL, White KP, Dinner AR, Lear BC, Ren D, et al. A Conserved Bicycle Model for Circadian Clock Control of Membrane Excitability. *Cell.* 2015;162(4):836-48.

21. Xie L, Gao S, Alcaire Salvador M, Aoyagi K, Wang Y, Griffin Jennifer K, Stagljar I, Nagamatsu S, and Zhen M. NLF-1 Delivers a Sodium Leak Channel to Regulate Neuronal Excitability and Modulate Rhythmic Locomotion. *Neuron.* 2013;77(6):1069-82.

22. Baycin-Hizal D, Gottschalk A, Jacobson E, Mai S, Wolozny D, Zhang H, Krag SS, and Betenbaugh MJ. Physiologic and pathophysiologic consequences of altered sialylation

and glycosylation on ion channel function. *Biochem Biophys Res Commun.* 2014;453(2):243-53.

23. Watanabe I, Wang HG, Sutachan JJ, Zhu J, Recio-Pinto E, and Thornhill WB. Glycosylation affects rat Kv1.1 potassium channel gating by a combined surface potential and cooperative subunit interaction mechanism. *J Physiol.* 2003;550(Pt 1):51-66.

24. Canellada A, Blois S, Gentile T, and Margni Idehu RA. In vitro modulation of protective antibody responses by estrogen, progesterone and interleukin-6. *Am J Reprod Immunol.* 2002;48(5):334-43.

25. Mesiano S, and Welsh TN. Steroid hormone control of myometrial contractility and parturition. *Semin Cell Dev Biol.* 2007;18(3):321-31.

26. Dong X, Yu C, Shynlova O, Challis JR, Rennie PS, and Lye SJ. p54nrb is a transcriptional corepressor of the progesterone receptor that modulates transcription of the labor-associated gene, connexin 43 (Gja1). *Mol Endocrinol.* 2009;23(8):1147-60.

27. Jacobson D, Pribnow D, Herson PS, Maylie J, and Adelman JP. Determinants contributing to estrogen-regulated expression of SK3. *Biochem Biophys Res Commun.* 2003;303(2):660-8.

28. Mesiano S, Chan EC, Fitter JT, Kwek K, Yeo G, and Smith R. Progesterone withdrawal and estrogen activation in human parturition are coordinated by progesterone receptor A expression in the myometrium. *J Clin Endocrinol Metab.* 2002;87(6):2924-30.

29. Csapo A. Progesterone block. *Am J Anat.* 1956;98(2):273-91.

30. Virgo BB, and Bellward GD. Serum progesterone levels in the pregnant and postpartum laboratory mouse. *Endocrinology.* 1974;95(5):1486-90.

31. McLean AC, Valenzuela N, Fai S, and Bennett SA. Performing vaginal lavage, crystal violet staining, and vaginal cytological evaluation for mouse estrous cycle staging identification. *J Vis Exp.* 201267):e4389.

32. Hart GaW, CM. In: Varki A CR, Esko JD, et al. ed. *Essentials of Glycobiology*. Cold Spring Harbor, NY: Cold Spring Harbor Laboratory Press; 2009.

33. Freeze HH, and Kranz C. Endoglycosidase and glycoamidase release of N-linked glycans. *Curr Protoc Mol Biol.* 2010;Chapter 17(Unit 17 3A).

34. *The Guide to Investigation of Mouse Pregnancy.* Academic Press; 2013.

35. Miller BH, and Takahashi JS. Central circadian control of female reproductive function. *Front Endocrinol (Lausanne).* 2013;4(195).

36. Norman RL, Blake CA, and Sawyer CH. Estrogen-dependent 24-hour periodicity in pituitary LH release in the female hamster. *Endocrinology.* 1973;93(4):965-70.

37. Suresh A, Subedi K, Kyathanahalli C, Jeyasuria P, and Condon JC. Uterine endoplasmic reticulum stress and its unfolded protein response may regulate caspase 3 activation in the pregnant mouse uterus. *PLoS One.* 2013;8(9):e75152.

38. Mershon JL, Mikala G, and Schwartz A. Changes in the expression of the L-type voltage-dependent calcium channel during pregnancy and parturition in the rat. *Biol Reprod.* 1994;51(5):993-9.

39. Collins PL, Moore JJ, Lundgren DW, Choobineh E, Chang SM, and Chang AS. Gestational changes in uterine L-type calcium channel function and expression in guinea pig. *Biol Reprod.* 2000;63(5):1262-70.

40. Curley M, Cairns MT, Friel AM, McMeel OM, Morrison JJ, and Smith TJ. Expression of mRNA transcripts for ATP-sensitive potassium channels in human myometrium. *Mol Hum Reprod.* 2002;8(10):941-5.

41. Pierce SL, Kresowik JD, Lamping KG, and England SK. Overexpression of SK3 channels dampens uterine contractility to prevent preterm labor in mice. *Biol Reprod.* 2008;78(6):1058-63.

42. Lundgren DW, Moore JJ, Chang SM, Collins PL, and Chang AS. Gestational changes in the uterine expression of an inwardly rectifying K^+ channel, ROMK. *Proc Soc Exp Biol Med.* 1997;216(1):57-64.

43. Matharoo-Ball B, Ashford ML, Arulkumaran S, and Khan RN. Down-regulation of the alpha- and beta-subunits of the calcium-activated potassium channel in human myometrium with parturition. *Biol Reprod.* 2003;68(6):2135-41.

44. Gao L, Cong B, Zhang L, and Ni X. Expression of the calcium-activated potassium channel in upper and lower segment human myometrium during pregnancy and parturition. *Reprod Biol Endocrinol.* 2009;7(27).

45. McCallum LA, Pierce SL, England SK, Greenwood IA, and Tribe RM. The contribution of Kv7 channels to pregnant mouse and human myometrial contractility. *J Cell Mol Med.* 2011;15(3):577-86.

46. Petrocelli T, and Lye SJ. Regulation of transcripts encoding the myometrial gap junction protein, connexin-43, by estrogen and progesterone. *Endocrinology.* 1993;133(1):284-90.

47. Chow L, and Lye SJ. Expression of the gap junction protein connexin-43 is increased in the human myometrium toward term and with the onset of labor. *Am J Obstet Gynecol.* 1994;170(3):788-95.

48. Auboeuf D, Honig A, Berget SM, and O'Malley BW. Coordinate regulation of transcription and splicing by steroid receptor coregulators. *Science.* 2002;298(5592):416-9.

49. Iannone C, Pohl A, Papasaikas P, Soronellas D, Vicent GP, Beato M, and ValcaRcel J. Relationship between nucleosome positioning and progesterone-induced alternative splicing in breast cancer cells. *RNA.* 2015;21(3):360-74.

50. Zhu N, Eghbali M, Helguera G, Song M, Stefani E, and Toro L. Alternative splicing of Slo channel gene programmed by estrogen, progesterone and pregnancy. *FEBS letters.* 2005;579(21):4856-60.

51. Benkusky NA, Fergus DJ, Zucchero TM, and England SK. Regulation of the Ca2+-sensitive domains of the maxi-K channel in the mouse myometrium during gestation. *J Biol Chem.* 2000;275(36):27712-9.

52. Cochet-Bissuel M, Lory P, and Monteil A. The sodium leak channel, NALCN, in health and disease. *Front Cell Neurosci.* 2014;8(132.

53. Ruan YC, Chen H, and Chan HC. Ion channels in the endometrium: regulation of endometrial receptivity and embryo implantation. *Hum Reprod Update.* 2014;20(4):517-29.

54. Sinke AP, Caputo C, Tsaih SW, Yuan R, Ren D, Deen PM, and Korstanje R. Genetic analysis of mouse strains with variable serum sodium concentrations identifies the Nalcn sodium channel as a novel player in osmoregulation. *Physiol Genomics.* 2011;43(5):265-70.

55. Chien Y, Cheng WC, Wu MR, Jiang ST, Shen CK, and Chung BC. Misregulated progesterone secretion and impaired pregnancy in Cyp11a1 transgenic mice. *Biol Reprod.* 2013;89(4):91.

Chapter 5: Discussion and Proposed Future Directions

5.1 The Field of Myometrial Physiology

Of all the unresolved questions in human and animal physiology, the question of what initiates labor and specifically how the uterus is able to remain quiescent for 40 weeks and then transition to a fully contractile state to deliver a baby, at first seems like a simple one. However, after decades of both descriptive and mechanistic research, we still lack knowledge in some of the key aspects of normal labor physiology that would allow us to fully prevent and treat obstetric pathologies like preterm labor and dysfunctional labor. Attempts to model the uterus after other well-studied contractile organs such as the heart or gastro-intestinal tract have only demonstrated that the uterus is fundamentally different, and therefore presents novel challenges. At present, researchers in the field of myometrial biology focus their efforts into three major areas that when taken as a whole, provide a clear picture of the regulation of uterine contractions across pregnancy and during labor. These areas include 1) understanding the individual building blocks of the myometrium, the MSMCs, 2) understanding the changing local environment and tissue level signaling which alter the activity of MSMCs, and 3) understanding the regulation of uterine contractions at the whole organ level. In my thesis work I attempted to study the role of the Na^+ leak channel, NALCN, at all three levels of myometrial physiology. Like the work of those before me, my research has answered some important questions and has also provided the basis for many new questions for future research.

5.2 NALCN as a Contributor of Na^+ Current in MSMCs

As discussed extensively in the previous chapters, the electrical and contractile coupling of MSMCs is the driving mechanism behind uterine contractions. Thus, the changes in uterine contractility necessary for labor to ensue are mediated by changes in the excitability of individual MSMCs. It has long been understood that the duration, amplitude, and frequency of Ca^{2+} spikes in myometrial tissue are associated with the duration, force, and frequency of contractions (1). It has also been demonstrated that the resting membrane potential in human and rodent myometrium becomes more depolarized over the course of pregnancy and at labor, contributing to increased uterine excitability needed for effective uterine contractions (2, 3). Both RMP and the bursting pattern of the myometrium can be modified by changing the expression of the array of ion channels expressed in the myometrium (4, 5). Most studies have focused solely on the regulation and activity of K^+ and Ca^{2+} channels in the myometrium despite the known, but unclear role for Na^+ currents. In my thesis work, I discovered a novel Na^+ leak current in human MSMCs, and determined that the recently identified Na^+-leak channel, NALCN, contributes to this current (chapter 2). This channel has been shown to increase spontaneous firing and burst activity in the tissues in which it is expressed (6-10). In our genetic mouse model where NALCN is deleted in the myometrium, we determined that at term pregnancy, NALCN is necessary to sustain burst duration and the number of spikes per burst (chapter 3). These data support the hypothesis that NALCN is an important modulator of uterine excitability in MSMCs.

Our finding that NALCN regulates burst duration in P19 myometrium corroborates the findings of others studying NCA (*C. elegans* NALCN equivalent) in *C. elegans* pre-motor interneurons, NALCN in the murine brain stem and pars reticulata neurons of the substantia nigra (8), and NALCN in murine interstitial cells of Cajal (ICCs) (11). In *C. elegans,* a

depolarizing pulse to pre-motor interneurons initiates a train of rhythmic post-synaptic current bursts (rPSCs) that corresponded with bursting action potentials (9). In NCA loss of function mutants, the initial action potential in response to the depolarizing pulse remained, but the rhythmic post-stimulation bursts were lost. In this model, NCA seems to have no role in initiating the primary burst, but plays an integral role in sustaining persistent bursting activity required for sustained locomotion in these worms. In studies examining spontaneous firing in the murine nervous system, NALCN knockouts exhibited hyperpolarized resting membrane potential and a decreased spontaneous firing rate (6, 8). In murine ICCs, substance P (SP) induces temporary prolonged depolarization of the membrane potential through a tachykinin receptor, and SFK dependent mechanism (11). In $NALCN^{-/-}$ ICCs, SP-induced depolarization is significantly reduced. This agrees with our finding that NALCN contributes to mechanisms of sustained depolarization required for rhythmic activity. The study of NALCN in ICCs also demonstrated that NALCN activity can be modulated by agonists including SP and acetylcholine, the mechanism for which requires the interaction of other members of what is now known as the NALCN complex.

Members of the NALCN complex, UNC79 and NLF-1 were expressed at the mRNA level in all human myometrium and mouse uterus samples analyzed (chapters 2 and 3). Another member of the complex, UNC80 was expressed only in some laboring human samples, and some term non-laboring mouse uterus samples. UNC80 has been found to be essential for NALCN activation by SP (TACR1) and low extracellular Ca^{2+} (removal of inhibition by CaSR), and may also be required for activation by acetylcholine (M3R) (12-14). Future experiments parsing out the spatial and temporal regulation of UNC80 in human and mouse uterus will shed light on an important mode of NALCN regulation, and whether this channel may be modulated by agonists

in the myometrium. Furthermore, because NLF-1 has been associated with coordinating the temporal regulation of NALCN in the circadian rhythm neurons of fruit flies, it will be important to assess NLF-1 and the entire NALCN complex levels in the myometrium across a 24-hour period (7). This has additional implications in that spontaneous labor demonstrates a circadian dependence, with more labor initiating at night (15, 16). Related to this, a pilot experiment assessing bursting activity in the mouse uterus during the night just before labor (performing the experiment 12 hours later than normal), showed myometrium had a longer burst duration and shorter burst interval than most P19 samples (Fig 5.1). This agrees with findings of circadian regulation of NALCN, and increased expression of NALCN in the uterus in preparation for the onset of labor. Future experiments may include assessment of myometrial bursting activity in smNALCN$^{-/-}$ during different light cycles to determine whether NALCN facilitates the prolonged bursts seen in the pilot experiment.

5.3 Uterine NALCN in the Context of Pregnancy and Labor

Myometrial excitability changes across pregnancy in response to the changing hormonal milieu. We found that burst duration, interval, and spike density of mouse myometrium changed throughout pregnancy. However, many other ion channels are regulated throughout pregnancy that could be playing a role in these changes. Furthermore, there are no specific blockers of NALCN to test the specific role of NALCN in myometrial excitability. Thus, in order to determine whether NALCN regulates burst activity, we created the smNALCN$^{-/-}$ mouse and performed sharp electrode current clamp from P19 myometrium. To address the role of NALCN in myometrial excitability throughout pregnancy, these experiments will need to be continued in myometrium samples from earlier stages of pregnancy. It would be especially interesting to determine the role of NALCN in the burst parameters in the myometrium from P7 and P18

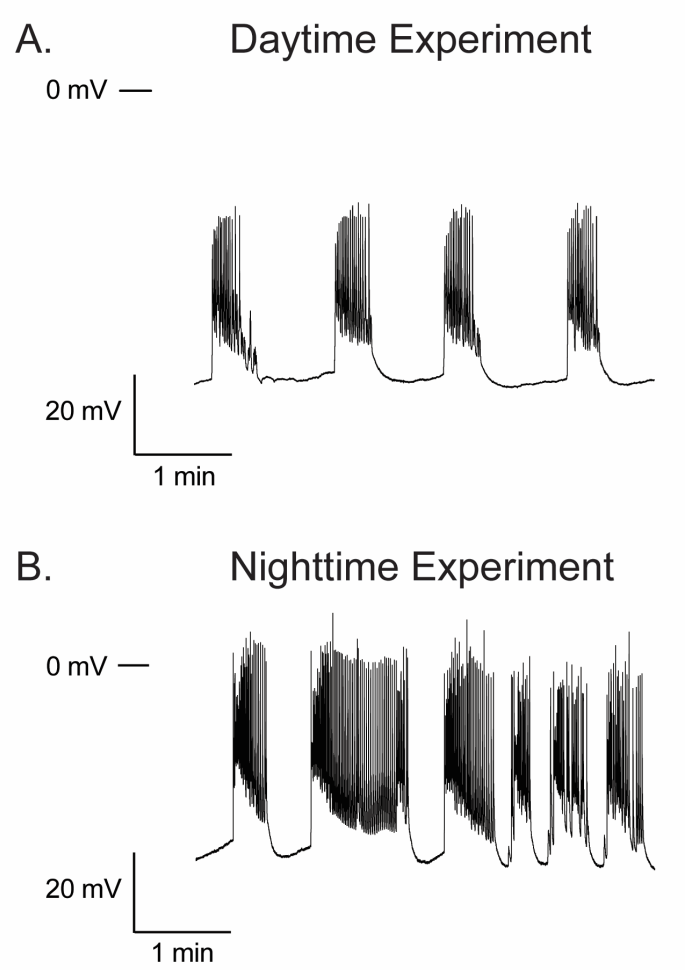

Figure 5.1 Effect of time of day and proximity to labor on uterine excitability.
A) Representative membrane potential trace from a pregnancy day 19 (P19) recorded during the day. This mouse was sacrificed about 18 hours before normal delivery time. B) Membrane potential trace from a P19.5 mouse recorded at night. This mouse was sacrificed about 6 hours before normal delivery time.

myometrium, when NALCN levels are at high and low levels, respectively. We originally hypothesized that NALCN would play a greater role in regulating the burst interval, and not the burst duration. This hypothesis was not correct in P19 myometrium, but it may be true of other stages of pregnancy when the levels of NALCN are higher.

In addition to finding NALCN-dependent regulation of uterine excitability, we found that NALCN levels and putative NALCN isoforms were differentially regulated throughout pregnancy and the estrus cycle (chapter 3 and 4). NALCN expression was inversely correlated with progesterone levels, and in fact, treating mice with progesterone reduced NALCN expression at P19.5. These data suggest that NALCN is downregulated by progesterone in the mouse uterus, though the mechanism behind this downregulation is unknown.

Progesterone signaling is classically thought to alter expression of target genes at the transcriptional level. We saw a subtle reduction in NALCN mRNA later in pregnancy, but this change was not statistically significant. It may be that NALCN transcription is subtly inhibited by progesterone through progesterone receptor-mediated transcriptional repression. The NALCN promoter region contains a number of putative hormone receptor binding sites (Fig 5.2). Regulation of NALCN at the transcriptional level could be determined by further qRT-PCR analysis of NALCN mRNA levels in control P19.5 uterine tissue compared to tissue from a P19.5 mouse treated with progesterone. Alternatively, progesterone may indirectly reduce NALCN stability. It may do so by regulating the expression of NALCN complex proteins, NLF-1, UNC79, or UNC80, which can aid in its localization to the plasma membrane. Additionally, other progesterone targets may contribute to NALCN stability. For example, progesterone was shown to reduce GATA3 stability by increasing phosphorylation-dependent GATA3 degradation

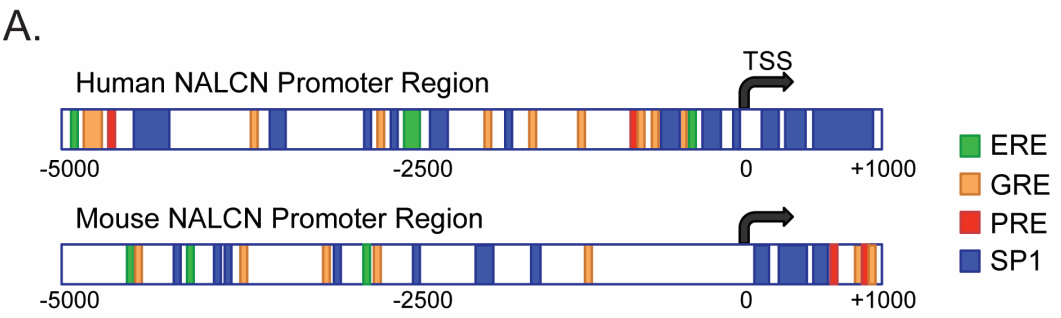

Figure 5.2 Transcription factor consensus sites in the NALCN promoter.
NALCN promoter regions in the human and mouse with highlighted transcription factor consensus sequence sites. Transcription start site (TSS), estrogen response element (ERE), glucocorticoid response element (GRE), progesterone response element (PRE), and specificity protein 1 consensus sequence (SP1).

in the proteasome (17). Future studies could include time course experiments to determine whether progesterone affects the stability of NALCN protein.

Progesterone withdrawal, an initiator of labor, occurs by a different mechanism in human myometrium compared to the rodent. In humans, circulating progesterone levels remain high, and the human myometrium undergoes a functional withdrawal of progesterone (discussed in chapter 1). This functional withdrawal is in part mediated by the differential expression and functionality of progesterone receptors A and B. PR-B is associated with the conventional function of progesterone in maintaining quiescence, whereas PR-A is associated with the term related increase in uterine excitability. Although we did not see a significant change in NALCN mRNA levels from the myometrium of women in PTNL, TNL, PTL, or TL (chapter 2), this is likely due to the variability in the timing (both time of day and gestational length) of sample acquisition, the variability across a human population, and the fact that the samples were taken from the less contractile lower uterine segment. Thus, to determine whether NALCN is regulated by progesterone in human MSMCs, cell lines may present a more consistent model. I performed studies in a human myometrial cell line that had been engineered to express PRA and PRB under the control of the Tet-ON and RheoSwitch promoters (18). In these cells the PRA:PRB ratio can be controlled by the dose of doxycycline or rheostat ligand. I observed no clear pattern of NALCN regulation by progesterone, regardless of the PRA:PRB ratio in these cells. This was possibly due to the fundamental changes that can occur in cell lines when they are immortalized. Additionally, there were many NALCN antibody-reactive bands that made it difficult to parse out true changes in NALCN levels. Preliminary experiments in cultured primary human MSMCs have shown that NALCN is upregulated by progesterone when the PRA:PRB ratio is high, compared to no change when the PRA:PRB level is reduced (Fig 5.3).

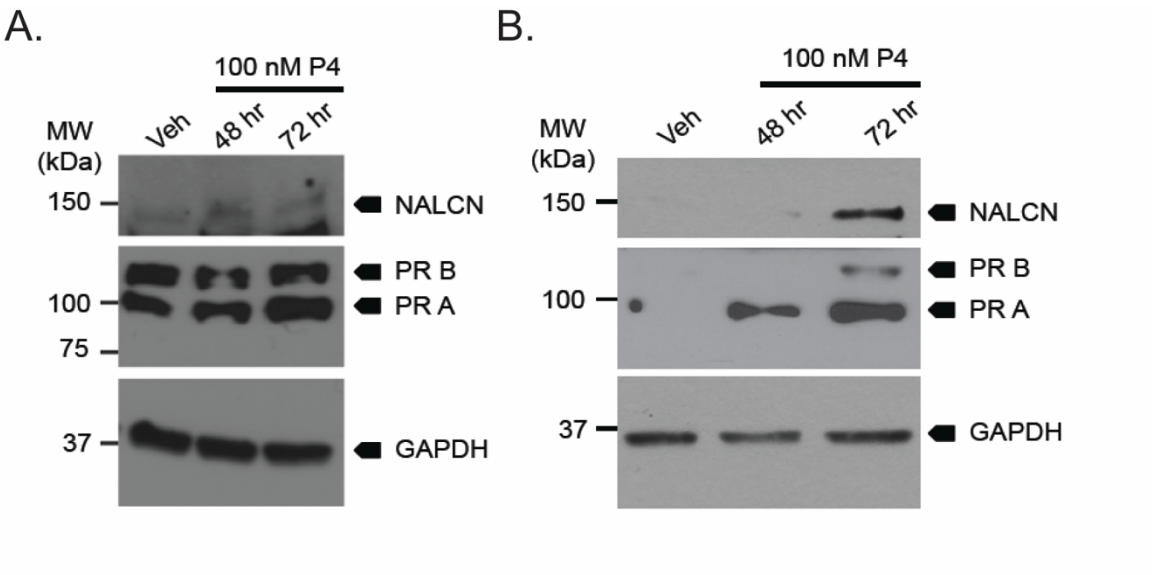

Figure 5.3 Progesterone-mediated regulation of NALCN in primary human MSMCs.
A) MSMCs from a term, non-laboring woman, treated with 100 nM progesterone (P4) for 48 and 72 hours. PR-A and PR-B levels are near equal. B) MSMCs from a term, non-laboring woman, treated with 100 nM P4 for 48 and 72 hours. PR-A is dominant. A and B) GAPDH is used as a loading control.

However, more experiments will need to be performed to determine if this is a mechanism for NALCN regulation, and they may need to be performed in large number to increase the number of samples with a high PRA:PRB ratio.

We also found that progesterone has an effect on NALCN post-transcriptional regulation. In the whole uterus under high progesterone states, and specifically in the mesometrial border, we saw increased expression of a PNGase F-sensitive ~180 kDa isoform of NALCN. Interestingly, when deglycosylated, this isoform ends up being smaller than the original, at only ~140 kDa. This indicates that the ~160 kDa band is either resistant to deglycoslation by PNGase F, perhaps because it is O-glycosylated instead of N-glycosylated, or that the two isoforms have a different core structure. Future studies using immunoblot analysis of the mesometrial border from P14 and P18 smNALCN$^{-/-}$ mice will confirm the identity of the ~180 kDa band as NALCN. Additionally, RT-PCR analysis of NALCN from the mesometrial border would enable identification of alternative splicing isoforms. Currently, there are no reports of glycosylation of NALCN and thus we do not know if this would alter channel function. Further investigation using western blot analysis and patch clamp recordings of NALCN mutants lacking glycosylation sites, would enable us to define the role of glycosylation on NALCN function.

Progesterone is thought to serve its 'anti-labor' function, by downregulating inflammatory genes (18), known risk factors in initiating labor. Intrauterine infection is a leading cause of preterm birth. In mice, intrauterine injection of lipopolysaccharide (LPS) induces preterm labor. Many of the mechanisms associated with infection associated preterm birth are similar to those found in term, spontaneous labor. For example, myometrial samples from term laboring women show a large increase in the presence of leukocytes including macrophages and neutrophils (19, 20), and increased expression of cytokines and chemokines

including IL-6, IL-1β, TNF-α, and IL-8 (20). These induce labor by stimulating the production of the uterotonin, prostaglandin $F_{2\alpha}$. Thus, future experiments should determine if NALCN levels in the myometrium are regulated by pro-inflammatory genes and whether progesterone inhibition of NALCN is actually an indirect effect of progesterone's anti-inflammatory actions. Additionally, future experiments could address whether NALCN is an important mediator of infection-induced preterm birth by performing intrauterine injections of LPS in smNALCN$^{-/-}$ and comparing outcomes to flox control mice.

5.4 NALCN in Achieving Organ-level Uterine Contractions

Beyond understanding the role of a particular target gene in myometrial cell and tissue-level excitability, and knowing its regulation in the context of pregnancy, it is essential to determine whether this function is substantial enough to translate into a change at the whole organ level. For labor to be successful, uterine contractions must not only be forceful and rhythmic, but must also be coordinated throughout the entire uterus. In women, physicians monitor labor progress by measuring cervical dilation, as well as contraction frequency and amplitude via a tocodynamometer (at the abdominal surface), or by an inserted intrauterine pressure catheter. Although these are still the main methods of assessing labor progress, they are imprecise in their measurement. These measurements also cannot address key questions about uterine contractility such as how contractions propagate throughout the organ, where the contractions originate, whether there is a pacemaker region, and whether the contractions will be effective and represent true labor. Whole organ measurements of electrical activity, such as those derived from electromyography or magnetomyography are better suited to answer these questions.

One device that was developed to study organ level electrical activity of the uterus in women is the SQUID array, which is a non-invasive magnetomyography device. It measures electrical activity across the front surface of the human uterus, and it is being used to understand patterns of uterine contractility so that physicians may be able to better predict preterm labor and/or false labor. Data from the SQUID array, as well as some electromyographical studies (21, 22) and an *in vitro* electrode array study of the guinea pig uterus (23), have been unable to identify a specific region of the uterus with pacemaking activity. Although the spontaneous and reliable nature of uterine contractions suggests that uterine activity is driven by a biological pacemaker, studies indicate that electrical activity could initiate anywhere (23). Additionally, the theory that the electrical signal could begin in one part of the uterus and then spread evenly throughout the entire organ has been discounted by many investigators, in which they found propagation distances were shorter than that required to cover the whole organ, and did not follow any distinct path (23-25). This has left many wondering how synchronous contractions could occur at the whole organ level.

With no strong evidence for a distinct pacemaking node or path of propagation, accumulating experimental evidence and mathematical models suggest that the rhythmicity of uterine contractions during labor are driven by the increased connectivity of MSMCs and mechanical stimulation (24, 26). Smith et al. suggest that depolarizations of MSMCs during mid-pregnancy remain locally isolated, while at term because of increased cell-to-cell connectivity driven by the upregulation of gap junctions, local depolarization can spread to surrounding tissue (26). This creates depolarized areas large enough to produce regional contractions, which induce mechanically-stimulated contraction of the neighboring tissue. This drives a chain reaction resulting in organ level contractions. Smith et al. relate this to the activity

of a soccer stadium crowd, wherein spontaneous local activity of individual members (MSMCs), spreads through increased connectivity to form coordinated chants and waves (electrical bursts). This model wonderfully conceptualizes the intricate coordination of MSMC activity that occurs during parturition. Although it mainly focuses on the activity of MSMCs as a group, it also implies that the individual MSMCs must be able to initiate and propagate spontaneous bursting activity. In studying NALCN, we sought to address the physiological mechanisms which make the individual members prone to initiate and sustain excitable activity.

We addressed the role of NALCN in organ level activity by creating a smooth muscle specific NALCN knockout mouse and assessing its labor outcomes. We found that smNALCN$^{-/-}$ mice had a higher rate of either prolonged or dysfunctional labor. Because our data showed reduced burst duration in smNALCN$^{-/-}$ myometrium, and because it is well known that NALCN regulates tissue excitability, we associated the labor problems in the smNALCN$^{-/-}$ mice with inefficient uterine contractility. Although the current evidence supports our assumption, future studies measuring uterine contractions in smNALCN$^{-/-}$ mice need to be performed. Contractions can be studied in an *in vitro* setting by isometric tension recording of myometrial strips and these provide baseline information about the contractility pattern of a piece of uterine tissue. Mouse uterine activity can also be measured *in vivo* with the use of intrauterine pressure catheters, the method for which our lab was first to establish (27, 28). These experiments would provide an important validation of our hypothesized mechanism of smNALCN$^{-/-}$ labor dysfunction.

5.5 Concluding Remarks

Labor contractions are an essential component to the evolutionary success of placental viviparous species, and yet they are often taken for granted. In humans especially, labor contractions must be well-coordinated to deliver a live offspring and maintain maternal health.

Evolutionary selection in humans for both bipedalism and an enlarged brain has made the infant head to maternal pelvis a tighter fit and more tortuous passage, and also unique to humans, it forces the need for assisted birth (29, 30). Although many births carried out in the home or the hospital proceed without complication, still many women will require medical intervention (31). Physicians rely heavily on methods including labor induction and augmentation by oxytocin, or surgical delivery by caesarean section, which still sustain a substantial risk of morbidity and mortality for mother and baby (32-35). Thus, endeavors to increase our understanding of the mechanisms behind uterine contractions are crucial in the efforts to improve medical assistance to women undergoing dysfunctional labor.

In our studies, we identified the novel expression of the Na^+-leak channel in human MSMCs. Through the use of a smooth muscle NALCN knockout mouse model, we established the role for this channel in modulating uterine excitability and in facilitating successful and efficient parturition. In the future, it will be important to establish the role and regulation of this channel in coordinating human uterine contractility. Additionally, high-throughput small molecule screening methods to identify NALCN-specific agonists and antagonists will be essential in the application of this knowledge to the treatment of women, as well as to those suffering from diseases associated with NALCN mutations. As is often the case in medical research, our findings of a novel mediator of uterine contractions creates optimism for the implications of its future applications, but also generates many new questions to be addressed.

5.6 References

1. Marshall JM. Regulation of activity in uterine smooth muscle. *Physiol Rev Suppl.* 1962;5(213-27).

2. Parkington HC, Tonta MA, Brennecke SP, and Coleman HA. Contractile activity, membrane potential, and cytoplasmic calcium in human uterine smooth muscle in the

third trimester of pregnancy and during labor. *Am J Obstet Gynecol.* 1999;181(6):1445-51.

3. Kuriyama H, and Suzuki H. Changes in electrical properties of rat myometrium during gestation and following hormonal treatments. *J Physiol.* 1976;260(2):315-33.

4. Atia J, McCloskey C, Shmygol AS, Rand DA, van den Berg HA, and Blanks AM. Reconstruction of Cell Surface Densities of Ion Pumps, Exchangers, and Channels from mRNA Expression, Conductance Kinetics, Whole-Cell Calcium, and Current-Clamp Voltage Recordings, with an Application to Human Uterine Smooth Muscle Cells. *PLoS Comput Biol.* 2016;12(4):e1004828.

5. Chan YW, van den Berg HA, Moore JD, Quenby S, and Blanks AM. Assessment of myometrial transcriptome changes associated with spontaneous human labour by high-throughput RNA-seq. *Experimental physiology.* 2014;99(3):510-24.

6. Lu B, Su Y, Das S, Liu J, Xia J, and Ren D. The Neuronal Channel NALCN Contributes Resting Sodium Permeability and Is Required for Normal Respiratory Rhythm. *Cell.* 2007;129(2):371-83.

7. Flourakis M, Kula-Eversole E, Hutchison AL, Han TH, Aranda K, Moose DL, White KP, Dinner AR, Lear BC, Ren D, et al. A Conserved Bicycle Model for Circadian Clock Control of Membrane Excitability. *Cell.* 2015;162(4):836-48.

8. Lutas A, Lahmann C, Soumillon M, and Yellen G. The leak channel NALCN controls tonic firing and glycolytic sensitivity of substantia nigra pars reticulata neurons. *Elife.* 2016;5(13):e15271.

9. Gao S, Xie L, Kawano T, Po MD, Guan S, Zhen M, Pirri JK, and Alkema MJ. The NCA sodium leak channel is required for persistent motor circuit activity that sustains locomotion. *Nat Commun.* 2015;6(6323).

10. Yeh E, Ng S, Zhang M, Bouhours M, Wang Y, Wang M, Hung W, Aoyagi K, Melnik-Martinez K, Li M, et al. A putative cation channel, NCA-1, and a novel protein, UNC-80, transmit neuronal activity in C. elegans. *PLoS Biol.* 2008;6(3):e55.

11. Kim BJ, Chang IY, Choi S, Jun JY, Jeon JH, Xu WX, Kwon YK, Ren D, and So I. Involvement of Na^+-leak channel in substance P-induced depolarization of pacemaking activity in interstitial cells of Cajal. *Cell Physiol Biochem.* 2012;29(3-4):501-10.

12. Lu B, Su Y, Das S, Wang H, Wang Y, Liu J, and Ren D. Peptide neurotransmitters activate a cation channel complex of NALCN and UNC-80. *Nature.* 2009;457(7230):741-4.

13. Lu B, Zhang Q, Wang H, Wang Y, Nakayama M, and Ren D. Extracellular calcium controls background current and neuronal excitability via an UNC79-UNC80-NALCN cation channel complex. *Neuron.* 2010;68(3):488-99.

14. Swayne LA, Mezghrani A, Varrault A, Chemin J, Bertrand G, Dalle S, Bourinet E, Lory P, Miller RJ, Nargeot J, et al. The NALCN ion channel is activated by M3 muscarinic receptors in a pancreatic beta-cell line. *EMBO Rep.* 2009;10(8):873-80.

15. Vatish M, Steer PJ, Blanks AM, Hon M, and Thornton S. Diurnal variation is lost in preterm deliveries before 28 weeks of gestation. *BJOG : an international journal of obstetrics and gynaecology.* 2010;117(6):765-7.

16. Lindow SW, Jha RR, and Thompson JW. 24 hour rhythm to the onset of preterm labour. *BJOG : an international journal of obstetrics and gynaecology.* 2000;107(9):1145-8.

17. Izzo F, Mercogliano F, Venturutti L, Tkach M, Inurrigarro G, Schillaci R, Cerchietti L, Elizalde PV, and Proietti CJ. Progesterone receptor activation downregulates GATA3 by transcriptional repression and increased protein turnover promoting breast tumor growth. *Breast Cancer Res.* 2014;16(6):491.

18. Tan H, Yi L, Rote NS, Hurd WW, and Mesiano S. Progesterone receptor-A and -B have opposite effects on proinflammatory gene expression in human myometrial cells: implications for progesterone actions in human pregnancy and parturition. *J Clin Endocrinol Metab.* 2012;97(5):E719-30.

19. Thomson AJ, Telfer JF, Young A, Campbell S, Stewart CJ, Cameron IT, Greer IA, and Norman JE. Leukocytes infiltrate the myometrium during human parturition: further evidence that labour is an inflammatory process. *Hum Reprod.* 1999;14(1):229-36.

20. Bollapragada S, Youssef R, Jordan F, Greer I, Norman J, and Nelson S. Term labor is associated with a core inflammatory response in human fetal membranes, myometrium, and cervix. *Am J Obstet Gynecol.* 2009;200(1):104 e1-11.

21. Ramon C, Preissl H, Murphy P, Wilson JD, Lowery C, and Eswaran H. Synchronization analysis of the uterine magnetic activity during contractions. *Biomed Eng Online.* 2005;4(55.

22. Eswaran H, Govindan RB, Furdea A, Murphy P, Lowery CL, and Preissl HT. Extraction, quantification and characterization of uterine magnetomyographic activity--a proof of concept case study. *Eur J Obstet Gynecol Reprod Biol.* 2009;144 Suppl 1(S96-100.

23. Lammers WJ, Mirghani H, Stephen B, Dhanasekaran S, Wahab A, Al Sultan MA, and Abazer F. Patterns of electrical propagation in the intact pregnant guinea pig uterus. *Am J Physiol Regul Integr Comp Physiol.* 2008;294(3):R919-28.

24. Young RC, and Barendse P. Linking myometrial physiology to intrauterine pressure; how tissue-level contractions create uterine contractions of labor. *PLoS Comput Biol.* 2014;10(10):e1003850.

25. Govindan RB, Siegel E, McKelvey S, Murphy P, Lowery CL, and Eswaran H. Tracking the changes in synchrony of the electrophysiological activity as the uterus approaches labor using magnetomyographic technique. *Reprod Sci.* 2015;22(5):595-601.

26. Smith R, Imtiaz M, Banney D, Paul JW, and Young RC. Why the heart is like an orchestra and the uterus is like a soccer crowd. *Am J Obstet Gynecol.* 2015;213(2):181-5.

27. Pierce SL, Kutschke W, Cabeza R, and England SK. In vivo measurement of intrauterine pressure by telemetry: a new approach for studying parturition in mouse models. *Physiol Genomics.* 2010;42(2):310-6.

28. Rada CC, Pierce SL, Grotegut CA, and England SK. Intrauterine telemetry to measure mouse contractile pressure in vivo. *J Vis Exp.* 201598):e52541.

29. Rosenberg K, and Trevathan W. Birth, obstetrics and human evolution. *BJOG : an international journal of obstetrics and gynaecology.* 2002;109(11):1199-206.

30. Smith R. Parturition. *N Engl J Med.* 2007;356(3):271-83.

31. Hamilton BE, Martin JA, Osterman MJ, Curtin SC, and Matthews TJ. Births: Final Data for 2014. *Natl Vital Stat Rep.* 2015;64(12):1-64.

32. Simpson KR, and Knox GE. Oxytocin as a high-alert medication: implications for perinatal patient safety. *MCN Am J Matern Child Nurs.* 2009;34(1):8-15; quiz 6-7.

33. Ehrenthal DB, Jiang X, and Strobino DM. Labor induction and the risk of a cesarean delivery among nulliparous women at term. *Obstet Gynecol.* 2010;116(1):35-42.

34. Clark SL, Belfort MA, Dildy GA, Herbst MA, Meyers JA, and Hankins GD. Maternal death in the 21st century: causes, prevention, and relationship to cesarean delivery. *Am J Obstet Gynecol.* 2008;199(1):36 e1-5; discussion 91-2 e7-11.

35. Liu S, Liston RM, Joseph KS, Heaman M, Sauve R, Kramer MS, and Maternal Health Study Group of the Canadian Perinatal Surveillance S. Maternal mortality and severe morbidity associated with low-risk planned cesarean delivery versus planned vaginal delivery at term. *CMAJ.* 2007;176(4):455-60.